INTEGRATION OF ULTRASONIC CONSOLIDATION AND DIRECT-WRITE

TO FABRICATE A MINIATURE SYNTHETIC APERTURE RADAR (SAR)

PHASED ARRAY ANTENNA

by

Christopher J. Robinson

A thesis submitted in partial fulfillment
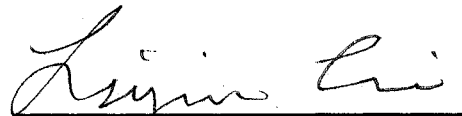of the requirements for the degree
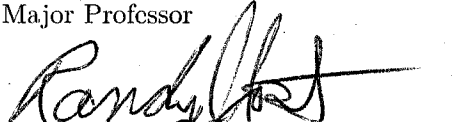
of

MASTER OF SCIENCE

in

Mechanical Engineering

Approved:

_____
Dr. Brent E. Stucker
Major Professor

_____
Dr. Leijun Li
Committee Member

_____
Dr. Randy J. Jost
Committee Member

_____
Dr. Byron R. Burnham
Dean of Graduate Studies

UTAH STATE UNIVERSITY
Logan, Utah

2007

Copyright © Christopher J. Robinson 2007

All Rights Reserved

Abstract

Integration of Ultrasonic Consolidation and Direct-write to Fabricate a Miniature

Synthetic Aperture Radar (SAR) Phased Array Antenna

by

Christopher J. Robinson, Master of Science

Utah State University, 2007

Major Professor: Dr. Brent E. Stucker
Department: Mechanical and Aerospace Engineering

A research project was undertaken to utilize Ultrasonic Consolidation (UC) and Direct-write (DW) to fabricate an advanced miniature synthetic aperture radar (SAR) antenna. This research necessitated fundamental research relating to the processes of UC and DW. The design of an enclosure for the SAR antenna was desired that could minimize the losses due to misalignment and other issues while decreasing the mass compared to current systems. In order to develop such a design there were numerous tests that needed to be performed for both DW and UC. The results from the testing as well as the general design of the SAR antenna formulate a base for design guidelines to be built upon in the future. The successful fabrication of a prototype SAR enclosure demonstrates the usefulness of UC and DW as well as the validity of the design parameters determined through testing.

(168 pages)

Acknowledgments

I cannot find words to express the gratitude that I have for all of those who have supported me in the research that has taken place in order to organize this thesis. The time, effort, and dedication that have been given by so many is truly a great show of the kindness and caring that is existent in the world today.

My thanks go, first and foremost, to Dr. Brent Stucker, without whom *none* of this would have been possible. I have been given numerous opportunities to further my education and my experience through the time and effort that Dr. Stucker has put into assisting me individually. The hours that he has spent on correcting my papers and helping me to understand how to be a more effective researcher will forever benefit me. I am especially grateful for the training in ethics that Dr. Stucker's example has given me. I would also like to thank Dr. Leijun Li and Dr. Randy Jost for being so willing to edit my thesis and give me feedback on very short notice. It is great to be around people who care about your success, thanks.

In doing the research that relates to this thesis I have been able to work and interact with a number of people from various organizations. I am very grateful to have been able to obtain friendships that will hopefully continue on with so many people. I would like to give special thanks to Jeremy Palmer at Sandia National Laboratories for providing me with beneficial research projects and assisting me in improving my engineering skills. The main portion of this thesis would not have been possible without the help and assistance of Bart Chavez at Sandia. Thank you very much for bailing me out of really tight situations over and over again. Thanks to all the others at Sandia whom I was able to work with such as: Karen, Berndie, Rob, Steve and everyone else. I would also like to thank Dr. Ryan Wicker at the University of Texas at El Paso (UTEP) for his assistance in research that was ongoing with UTEP, and especially for the moral support and encouragement. I truly enjoyed being able to work with people such as Amit Lopes, Frank Medina, Misael Navarrete, and Eric MacDonald at UTEP.

Thanks to all of the great friends and other students whom I have been able to get to know and who have helped me in so many ways, especially, Dan Swenson and Zac Humes for their continual support and encouragement.

I don't even know if there are words in the English language that can express my gratitude for my wonderful wife, Kayo, who has supported me mentally and emotionally without ever giving up on me. To my beautiful daughter Nami, who has shown me how to be kind and how to love, thank you so much for the hugs and kisses every time I came home. To my son Naoto, thank you for always being able to smile and relieving my stress by laughing so hard when tickled. To my family, I express the deepest love and greatest gratitude that the heart can imagine.

And finally to wonderful parents who have taught me how to work and that if I work hard then good things will happen. I can't imagine a better lesson. Thank you for the moral support and encouragement, as well as confidence that you have expressed in me throughout my life. Thank you also for the lessons in faith. If it were not for the support of a loving Heavenly Father, I would have never had the stability and endurance to make it to this point in my education.

I am truly grateful to have had the opportunity to perform this research and to learn essential skills for working in the engineering world. I know that I still have a wealth of knowledge to obtain, but I am grateful for the foundation that has been set through my associations with great people and the research and education that I have obtained.

Christopher J. Robinson

Contents

List of Tables

List of Figures

Acronyms

ABS	Acrylonitrile Butadiene Styrene
CAD	computer-aided drafting
CNC	computer numeric controlled
CT	computed tomography
CTE	coefficient of thermal expansion
DARPA	Defense Advanced Research Projects Agency
DW	Direct-write
ESA	electronically steerable array
FDM	Fused Deposition Modeling
FEM	finite element method
H/W	height to width ratio
LED	Light Emitting Diode
LENS	Laser Engineered Net Shaping
MAPLE	Matrix Assisted Pulsed laser Evaporation
M3D	Maskless Mesoscale Material Deposition
PHP	Pulsating Heat Pipe
RP	rapid prototype
SAR	synthetic aperture radar
SFF	Solid Freeform Fabrication
SL	Stereolithography
SLS	Selective Laser Sintering
SNL	Sandia National Laboratories
UAV	unmanned aerial vehicle
UC	ultrasonic consolidation
USU	Utah State University
UTEP	University of Texas at El Paso
UV	ultraviolet

Chapter 1

Introduction

Synthetic aperture radars (SARs) serve a very important role as a detection technique for many applications. The SAR program at Sandia National Laboratories has been fabricating SARs for decades and is amongst the leaders in the world. In order to remain competitive Sandia must be able to build a SAR that is smaller, has less mass and performs just as well if not better than previous versions. Through the use of additive manufacturing techniques a SAR can be assembled that minimizes losses that arise from misalignment issues, reduces the number of required parts, and greatly reduces the overall mass of the system.

There are a number of additive manufacturing techniques that can be used to produce the enclosure required for a SAR application. Stereolithography could be used to make a complex structure in very little time, but structural rigidity, strength and thermal conductivity pose problems. Laser Engineered Net Shaping (LENS) could be used to make a metal structure, but the cost and time are high and post processing is required, which can be complicated with multi-functional parts. The materials that are currently used for the antenna elements and arrays are not compatible with the extreme localized heating that occurs with a process such as LENS. There are a number of other rapid prototyping (RP) technologies that were considered, but ultrasonic consolidation (UC) was determined to be the best fit for this application.

UC has the capability of making parts that are at final dimensions when they are removed from the machine and substrate. The additive manner in which a UC structure is built facilitates the embedding of components and the ability to make a monolithic multi-functional structure. The temperature problems that arise with many other RP technologies are not present with UC because it does not create a high temperature gradient in the part

and does not require a high temperature substrate. This is particularly suitable for SAR fabrication. UC is also one of the few processes that use aluminum.

UC was chosen as the fabrication technique for the enclosure of an ultra-compact SAR antenna, but to fully utilize the capabilities of UC, Direct-write (DW) technologies were also incorporated to facilitate the fabrication of complex connections within the antenna array itself. DW is a process whereby conductive materials can be deposited on a three-dimensional surface in an additive manner. The type of DW selected for this project was a pressure nozzle deposition technique. By using DW, a connection from a coaxial transmission line to stripline could be created directly inside the UC fabricated enclosure. Ground connections could also be simplified by using DW conductive ink as the bonding material.

1.1 Synthetic Aperture Radar

There are many applications that require high resolution imaging from an airborne vehicle, such as environmental monitoring, earth resource mapping, and military applications. Some imagery systems work very well in the daytime with no obstructions in the sky, some work well in good weather and some work well at night, but it is essential that a system can collect imagery data day or night and even in inclement weather. Synthetic Aperture Radar (SAR) is one such system [1]. SAR has been researched for two decades and the advances that have been made are phenomenal. In 2005, Sandia National Laboratories developed a SAR weighing less than 30 pounds that has a four inch resolution from a 6.2 mile standoff distance. An image from this application can be seen in Figure 1.1. This is a major improvement over the 500 pound SARs available 15 years prior [2].

A 2-D image is generally obtained when using SAR. One dimension is the direction called range, which is what the SAR sees at any given time. The other dimension is the azimuth direction which is the direction that the SAR is traveling, as shown in Figure 1.2. For instance, if the SAR is being flown on an aircraft then the azimuth is in the flight direction. SAR provides a way to get a fine resolution in the azimuth direction which is one reason why it is very useful [1]. Generally to get a fine resolution in the azimuth direction
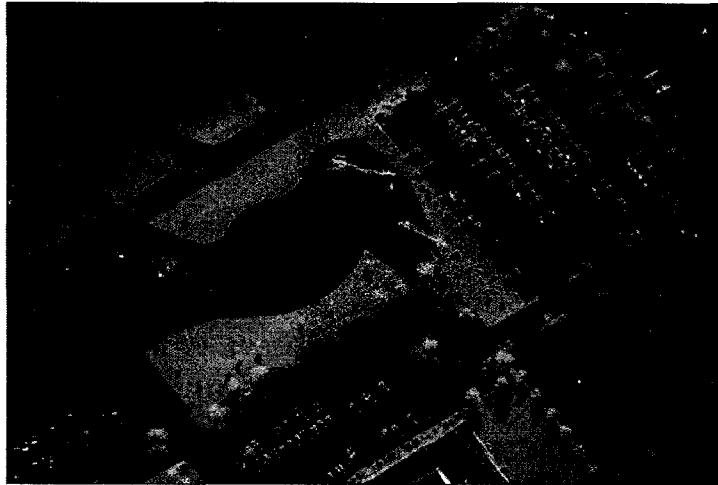
Fig. 1.1: Image produced using a SAR fabricated by Sandia National Laboratories.

a very large aperture is required, but SAR incorporates the movement of the vehicle that is transporting it to create a synthetic aperture. In the case of an aircraft, as it moves, the SAR collects data throughout the aperture path length and then and processes it using the Doppler frequencies of the echoes. This gives the effect of having a very large aperture, which results in the fine resolution desired.

Even though SAR uses a small aperture and collects data to simulate a large aperture, there are still difficulties in miniaturizing a SAR to make it easy to use in various applications. Two of the major difficulties are getting sufficient gain and bandwidth out of small antenna elements, and the other is the housing and gimbal system for the SAR.

In most antenna applications, excellent performance in a small package is desired. While simple patch antennas are easy to fabricate and fairly low cost the bandwidth is limited to a very narrow range. To improve upon this there are a number of options, such as stacked antennas or the use of quasi-Yagi antenna elements [3]. The quasi-Yagi elements have been proven to be able to provide a bandwidth of over 50 percent and they can be at least two orders lower in volume than a standard horn element for the same frequency [3]. For current SAR Fabrication, an array of quasi-Yagi elements is created and then advanced signal processing is used to output broad area images at high resolutions. Another major benefit to this type of antenna array is that the elements can be adjusted to any frequency
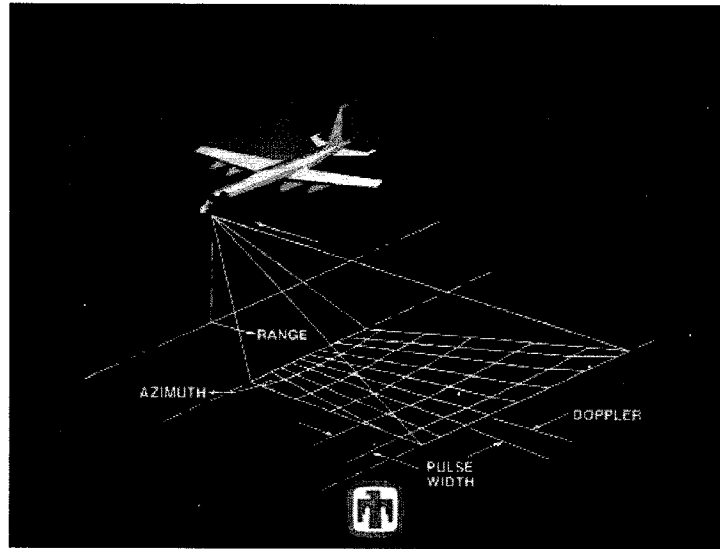
Fig. 1.2: Imaging concept of SAR.

and still maintain the wide bandwidth capabilities [3].

1.2 Additive Manufacturing

Although prototyping has been around for many centuries, Rapid Prototyping started over two decades ago when 3D systems, a company founded in 1986, released the first stereolithography (SL) apparatus in 1988 [4]. Since that time there have been numerous ways of producing parts in an additive manner for prototyping. Traditionally the RP technologies available have dealt with polymers such as UV curable epoxy and acrylic resins for SL, nylon materials for selective laser sintering (SLS) and ABS for fused deposition modeling (FDM). As these RP technologies evolved, there was a push toward going beyond prototyping to actual manufacturing with these techniques. As the philosophy on the use of these techniques has evolved so has the name, from rapid prototyping to additive manufacturing, which actually describes the processes.

Currently there are many designs being used that are facilitated by the use of additive manufacturing techniques. One such product is Invisalign, which is a corrective technique used by dentists and orthodontists, which won the 2001 Stereolithography Excellence Award [5]. This technique uses a computed tomography (CT) scanning technique to create custom

fit retainers for a person that corrects common tooth alignment problems. Other techniques have been developed that can additively fabricate metal structures. Some of these include LENS, metal powder SLS, and Ultrasonic Consolidation. Metal RP processes are of particular interest in many situations due to the need for increased strength and or stiffness, while maintaining the benefits of the additive manufacturing processes. Another group of rapid prototyping technologies are those used for depositing conductive, capacitive, and passive electronics, known as Direct-write (DW) technologies.

1.3 Ultrasonic Consolidation

Ultrasonic welding, which has been used for over 40 years [6], is a process whereby two pieces of metal can be joined with a true metallurgical bond by using acoustic vibrations [7], where a clamping force is used to press two pieces of material together, while the sonotrode and in some cases the anvil will rotate to feed the workpiece along the weld path. Typically, the welding horn is vibrated by the use of piezoelectrics to turn electric power into mechanical vibrations, which cause differential motion between the two pieces of material that are being welded together. This differential motion creates plastic-elastic deformation at the interface which breaks up and disperses surface oxides and other contaminates [6],[8], leaving a clean metal to metal contact surface. This contact allows a true metallurgical bond to form between the two workpieces and the applied pressure maintains contact that will not allow air to touch the clean surface, eliminating the formation of a new oxide layer. This clean atomic level bonding creates contact points. It has generally been shown that the more contact points there are, the better the weld strength [9].

UC is an additive manufacturing process that combines ultrasonic welding of metals with layer additive manufacturing techniques [10]. This is done by continuously welding "foil layers of previously deposited material during which the profile of each layer is created by contour milling" [8]. A schematic description of the process is shown in Figure 1.3. The UC process is a commercially available process that is incorporated into a unique machine, the Solidica Formation™ shown in Figure 1.4. The UC process is capable of producing features that are difficult or impossible to create by the use of other manufacturing techniques, with
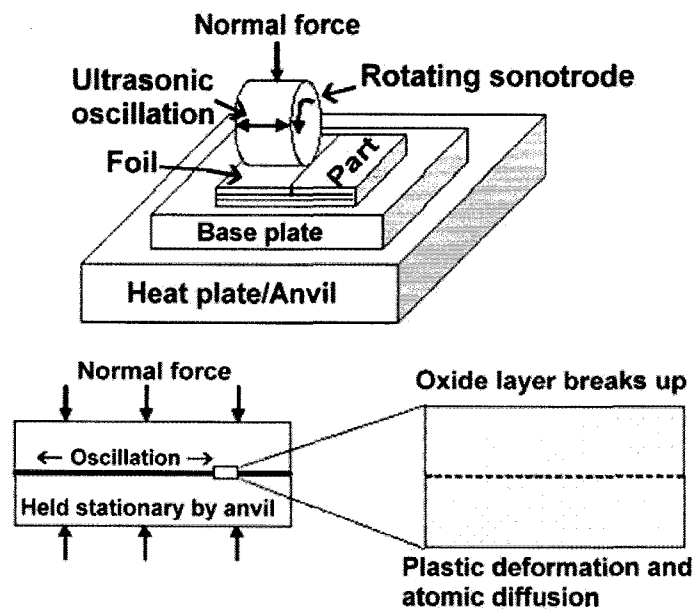
Fig. 1.3: Ultrasonic Consolidation process works by vibrating a foil material against a base substrate with a sonotrode layer by layer.

the added benefit of doing so in one machine in a single operation [7]. The UC process not only facilitates the design of advanced structures, but it can also be used to create multi-material components that are far superior to their homogenous counterparts, yet the melting, solidification and other issues that arise from welding materials are non-existent because this is a cold-working process and the molecular structure does not change because of elevated temperature.

Traditionally, embedding components in a metallic structure has been very difficult because metal RP processes generally use either high power lasers which will damage the embedded component or can only be performed on a very small scale. Additionally, most metal RP technologies create near net shape parts which require secondary machining processes that can damage embedded components. When embedding components such as sensors in a high temperature process, researchers at Stanford University found that there is generally delamination and other problems that arise due to stresses caused from the difference in the coefficient of thermal expansion (CTE) throughout the parts due to a large
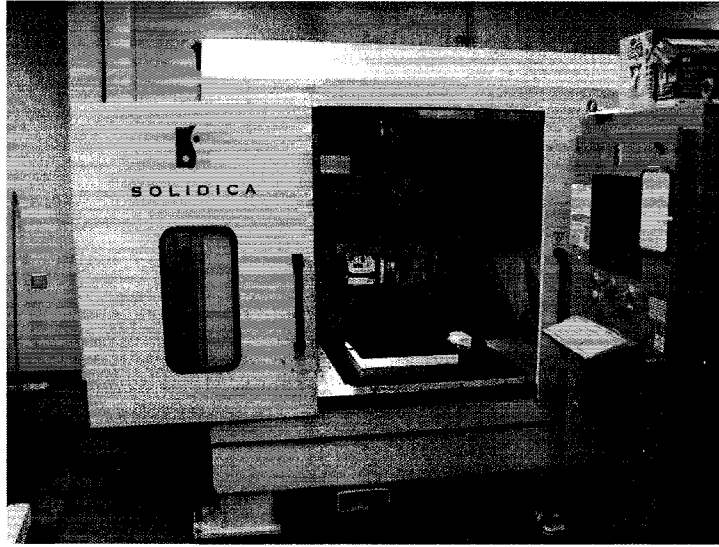
Fig. 1.4: Solidica Formation(TM) located at Utah State University.

thermal gradient [11]. UC is a process that produces metal parts at a temperature much less than the melting temperature of the materials and there are no major thermal gradients to cause induced stress from the mismatch of CTE. Another advantage to embedding within a UC structure is that much larger components can be embedded. The build size capabilities of a UC apparatus is 24"X 36"X 8" and yet the geometric tolerances are two thousandths of an inch because the geometry is created by the use of a CNC contour milling head. A very small or large component can be embedded as well as any connection leads or other driving devices so that an entire system can be created within a single structure.

1.4 Direct-write Technologies

Direct-write is the ability to write or print passive or active electronic components (conductors, insulators, batteries, capacitors, antennas, etc.) directly from a computer file without any tooling or masks. In this research, DW describes a mechatronic apparatus for dispensing conductive media in the liquid phase on three-dimensional contoured substrates at ambient temperature and pressure [12]. Three-dimensional features can be created by either following a curved substrate contour, or by building up DW material on top of previously deposited DW material in an additive fabrication fashion. Sprayforming can be

a very accurate and repeatable process to deposit conductive materials, but the temperature requirements are very high [13] and in a system with materials such as Teflon® it is necessary to maintain low temperature gradients. Ink jet deposition, by contrast, is a very effective low temperature way of making a deposit that can create three-dimensional features in limited space. For this research a DW system in which a pneumatic pump forces liquid conductive ink (conductive particles in a resin binder system) through a syringe was used. The syringe is attached to a 3-axis positioning system that is numerically controlled. This system is shown in Figure 1.5 [14].

Advanced DW systems can automatically control the start and stop pressures to give very precise deposition as well as optical sensors to determine the exact height of the path [12]. The flow rate can be controlled by pressure, orifice size, viscosity, and the size of filler particles. In this research, conductive inks are used, which are generally conductive particles in a polymer resin binder system. Once the ink has been deposited, any solvent must be driven off, which is generally done by the use of heat from methods such as thermal annealing or localized irradiation, and the polymer resin binder system dries to a hard coating. Conductivity varies with the ink formulation and cure temperature [15]. After the ink has been cured, it is a collection of particles bound in resin and is generally very brittle.
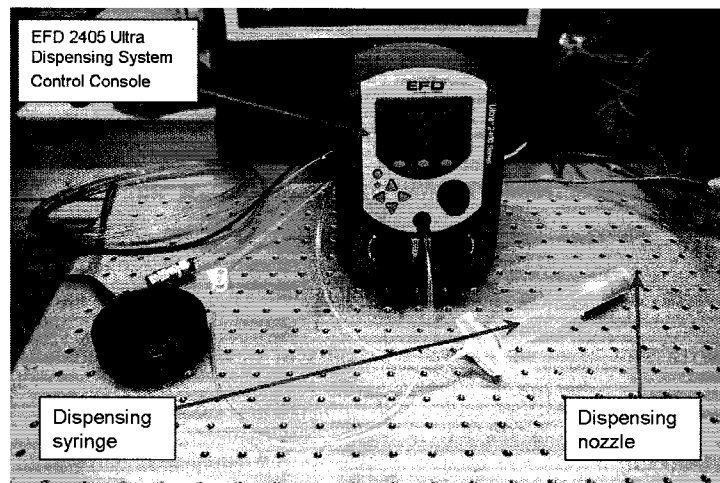
Fig. 1.5: DW dispensing mechanism used at the University of Texas at El Paso.

References

1. Kurt Sorensen, MiniSAR Radar Fact Sheet, http://www.sandia.gov/RADAR/images /SAND2005-3445PMiniSAR-fact-sheetp2-v4-redo.pdf, accessed December, 2006.

2. Laboratories, S. N., What is Synthetic Aperture Radar, http://www.sandia.gov/ RADAR/whatis.html, 2005, accessed December, 2006.

3. Sor, J., Deal, W. R., Qian, Y., and Itoh, H., A Broadband Quasi-Yagi Antenna Array, 29th European Microwave Conference, Munich, Germany, October 1999.

4. Chua, C. K., Leong, K. F., and Lim, C. S., Rapid Prototyping: Principles and Applications, World Scientific Publishing Co. Ptw. Ltd., Singapore, 2003.

5. About Align Technology, http://www.aligntech.com/generalapp/us/en/about/index. jsp, 2005, accessed December, 2006.

6. Daniels, H., Ultrasonic Welding, Ultrasonics, Vol. 3(4), 1960, pp. 190196.

7. Solidica, The New Future of Moldmaking, Moldmaking Technology, 2002.

8. Kong, C. Y., Soar, R. C., and Dickens, P. M., An Investigation of the Control Parameters for Aluminum 3003 under Ultrasonic Consolidation, Solid Freeform Fabrication Conference, Austin, TX, August 2002.

9. Kong, C. Y., Soar, R. C., and Dickens, P. M., A model for weld strength in ultrasonically consolidated components, Journal of Mechanical Engineering Science, Vol. 219, 2005, pp. 8391.

10. Kong, C. Y., Soar, R. C., and Dickens, P. M., Optimum process parameters for ultrasonic consolidation of 3003 aluminum, Journal of Materials Processing Technology, Vol. 146, 2004, pp. 181187.

11. Li, X. C., Golnas, A., and Prinz, F., Shape Deposition Manufacturing of smart metallic structures with embedded sensors, SPIE Smart Structures and Materials 2000 Conference, SPIE Paper 3986, 2000.

12. Church, K. H., Fore, C., and Feeley, T., Commercial Applications and Review for Direct Write Technologies, Material Developments for Direct Write Technologies, Vol. 624, 2000, pp. 38.

13. Sears, J. W., Sprayforming (Process Developments for Titanium Alloys), The Minerals, Metals, and Materials Society, Synthesis Processing of Lightweight Metallic Materials, 1995, pp. 331338.

14. Lopes, A., Navarrete, M., Medina, F., Palmer, J., MacDonald, E., and Wicker, R., Expanding Rapid Prototyping for Electronic Systems Integration of Arbitrary Form, Solid Freeform Fabrication Conference, Austin, TX, August 2006.

15. Palmer, J. A., Summers, J. L., Davis, D. W., Gallegos, P. L., Chavez, B. D., Yang, P., Medina, F., and Wicker, R., Realizing 3-D Interconnected Direct Write Electronics within Smart Stereolithography Structures, ASME International Mechanical Engineering Congress and Exposition, IMECE2005-79360, 2005.

Chapter 2

Thesis Statement

The research that is presented in and associated with this thesis is directed at being able to obtain a set of design guidelines to be used in fabricating advanced structures using UC integrated with DW. This research focuses specifically on the application of fabricating a SAR antenna, but the guidelines presented herein can be applied to various applications. UC is a very young process and therefore necessitated the fundamental testing of certain features that could be utilized in the fabrication of a SAR antenna. The answers to critical design questions are presented in the subsequent chapters of this thesis as the results of various testing and evaluation procedures.

Chapter 3 discusses the testing and results of a study to determine possible build heights of freestanding UC structures. Information contained in Appendix A presents the findings of mulit-material UC study. The results of integrating UC and DW into a single structure for the first time is presented in chapter 4. The information contained in chapter 5 is related to developing advanced thermal control devices that can be integrated into a UC structure. Chapter 6 describes the integration of the information contained in the previous chapters to fabricate a SAR phased array antenna. Throughout the entire testing and evaluation process of this research, various design guidelines were developed and are summarized in Appendix C.

Chapter 3

Maximum Height to Width Ratio of Freestanding Structures Built Using Ultrasonic Consolidation

1

This chapter is a conference paper published in the proceedings of the 17th Annual Solid Freeform Fabrication Symposium. All permissions to use this paper as a part of this thesis are contained in Appendix B.

Abstract

Ultrasonic consolidation (UC) is a process whereby metal foils can be metallurgically bonded at or near room temperature. The UC process works by inducing high-speed differential motion (20kHz) between a newly deposited layer and a substrate (which consists of a base plate and any previously deposited layers of material). This differential motion causes plastic deformation at the interface, which breaks up surface oxides and deforms surface asperities, bringing clean metal surfaces into intimate contact, where bonding occurs. If the substrate is not stiff enough to resist deflection during ultrasonic excitation of newly deposited layers, then it deflects along with the newly deposited layer, resulting in no differential motion and lack of bonding. Geometric issues which control substrate stiffness and deflection were investigated at Utah State University by building a number of free-standing rib structures with varying dimensions and orientations. Each structure was built to a height where lack of bonding between the previously deposited layers and the newly deposited layer caused the building process to fail, a height to width ratio (H/W) of approximately 1:1. The parts were then cut, polished, and viewed under a microscope. An ANSYS model was created to investigate analytically the cause of this failure. It appears

---

[1]Authors: C.J. Robinson, C. Zhang, G.D. Janaki Ram, E.J. Siggard, B. Stucker, and L. Li

build failure is due to excessive deflection of the ribs around a 1:1 H/W, resulting in insufficient differential motion and deformation to achieve bonding. Preliminary results show, when the H/W reaches 1:1, the von Mises stress is found to be tensile along portions of the bonding interface, which eliminates the compressive frictional forces necessary for plastic deformation and formation of a metallurgical bond. These tensile stresses are shown to be concentrated at regions near the edges of the newly deposited foil layer.

3.1   Introduction

Ultrasonic Consolidation (UC) is a novel additive manufacturing process developed by Solidica Inc., USA, utilizing the principles of ultrasonic welding [1]. The process builds up the rough part shape by ultrasonically welding or consolidating thin metal foils (typically 150 m thick). This ultrasonic addition is combined with 3-axis CNC milling to produce geometric details. The Solidica Formation^{TM} UC machine, commercially introduced by Solidica in 2000, is an integrated machine tool which incorporates an ultrasonic welding head, a foil feeding mechanism, a 3-axis milling machine, and software to automatically generate tool paths for material deposition and machining. Part fabrication takes place on a firmly bolted base plate (typically of the same material as the foil being deposited) on the top of a heat plate. The heat plate maintains the substrate at a set temperature allowing the deposition process to be carried out at temperatures ranging from ambient to 350 degrees Fahrenheit.

Figure 3.1 illustrates the basic UC additive manufacturing process. In this process a rotating ultrasonic sonotrode travels along the length of a thin metal foil placed over the substrate. The thin foil is held closely in contact with the substrate by applying a normal force via the rotating sonotrode. The sonotrode oscillates transversely to the direction of welding at a frequency of 20 kHz and at a user-set oscillation amplitude, while traveling over the metal foil. The combination of normal and oscillating shear forces results in generation of dynamic interfacial stresses at the interface between the two mating surfaces [1,2,3]. The stresses produce elastic-plastic deformation of surface asperities, which breaks up the oxide film, producing relatively clean metal surfaces under intimate contact, establishing
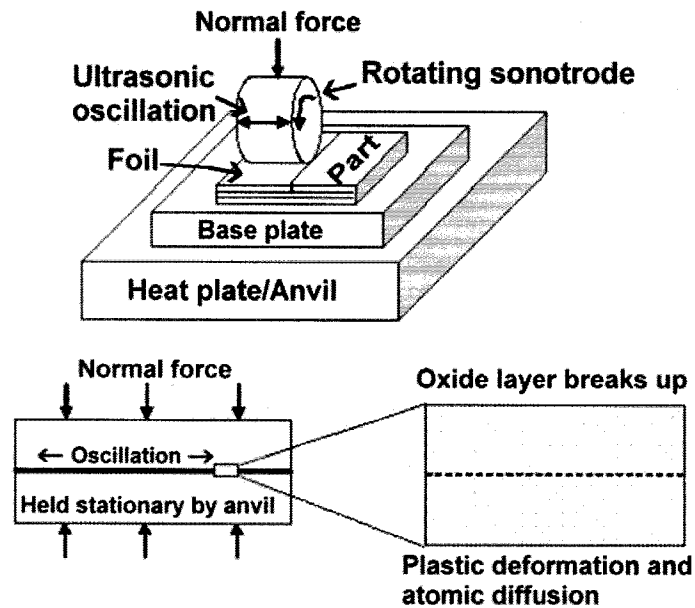
Fig. 3.1: Schematic of the ultrasonic consolidation process.

a metallurgical bond. Oxide films, broken up during the process, are displaced in the vicinity of the interface or along the weld zone. Local temperatures at the interface and the surrounding affected region (about 20 micrometers) can reach up to 50 percent of the melting point of the material being deposited [3]. After depositing a strip of foil, another foil is deposited adjacent to it. This process repeats until a complete layer is placed. After placing a layer, a computer controlled milling head shapes the layer to its slice contour. This milling can occur after each layer or, for certain geometries, after several layers have been deposited. Once the layer is shaped to its contour, the chips are blown away using compressed air and foil deposition starts for the next layer.

A closer examination of the UC process indicates that the process works, on a fundamental level, by inducing high-speed differential motion between the layer being deposited and the substrate (which consists of a base plate and any previously deposited layers of material). This differential motion is extremely important in producing interfacial stresses of adequate magnitude to cause oxide layer removal and plastic deformation at the interface, which are essential for bonding to occur. If the substrate is not stiff enough to resist

deflection during ultrasonic excitation of newly deposited layers, then it deflects along with the newly deposited layer, resulting in no differential motion. Under these conditions, the applied ultrasonic energy fails to generate high-enough stresses at the interface leading to lack of bonding. Since the substrate stiffness, for a given material, is dependent on its geometrical shape and dimensions, the UC process can be expected to be restricted to shapes and dimensions that would provide a stiff enough substrate for subsequent layer depositions.

While the above sounds quite plausible and is certainly a cause for concern, no published studies have been directed to examine the effect of substrate stiffness on bond formation during ultrasonic consolidation. A detailed understanding of this aspect is extremely important for successfully building parts, especially thin wall structures. Further, little is known about the effect of deposition orientation, which can provide a practical solution to the problem of substrate deflection, as the way ultrasonic oscillations are oriented with respect to substrate dimensions can significantly alter its resistance to deflection. In view of the above, the current work has been under taken to examine the role of substrate stiffness (in this case the H/W) and deposition orientation on bond formation during ultrasonic consolidation of Al alloy 3003. An attempt has also been made to gain greater insights into the subject through ANSYS modeling.

3.2 Experimental Work

In order to investigate the maximum H/W possible when creating free-standing ribs using UC, a series of ribs were created. These ribs were made with a constant length to width ratio of 10:1. Three different widths were chosen (0.25", 0.125", and 0.063") and the ribs were built to the maximum height possible. Each width was built in three orientations; longitudinal (the long axis of the rib is parallel to the tape direction), lateral (perpendicular to the tape direction) and 45 degrees (at a 45 degree angle to the tape direction) as shown in Figure 3.2. In order to create ribs that experienced the same trimming effects at each level, the excess material was trimmed from the rib after each deposition, rather than after every four depositions as is standard. The build parameters for each of the ribs were:
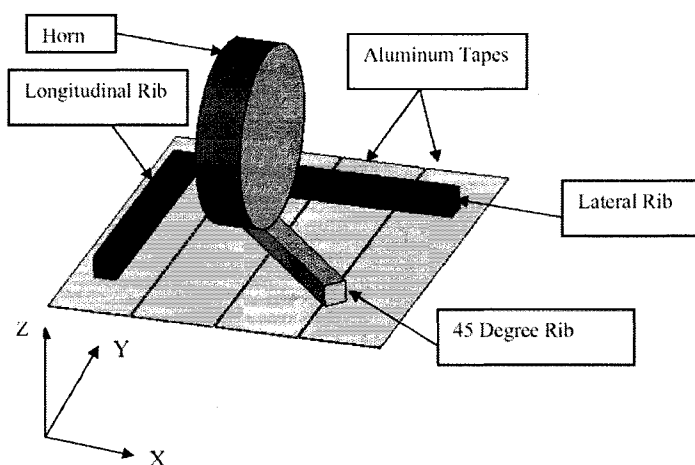
Fig. 3.2: Nomeclature for UC free-standing rib build orientation.

Amplitude = 16 m; Force = 1750 N; Feed Speed = 28 in/sec.

3.3 Experimental Results

As each rib was built, they were observed carefully to note the height when ribs failed to build properly. The build process was halted when the last deposited tape did not adhere to the previously deposited tape or when the last deposited tape "peeled up" during the trimming operation. The ribs were then cross-sectioned and observed under the microscope to ascertain the quality of the welds within the ribs. The results of each rib orientation follow.

3.3.1 Longitudinal Ribs

When building a rib along the direction of the tape the horn is vibrating perpendicular to the tape direction (across the width of the rib). This is the direction with the least resistance to vibration, which should lead to the worst linear weld density, a measure of weld quality in UC [4,5] as height increases. However, this direction of build allows the entire rib to be entirely created from a single tape, so issues that arise from having tapes laid next to each other, such as seams and the fact that they act as discontinuities during the trimming operation, are eliminated.

The appearance of the ribs built longitudinally was very good, as there were no seams due to adjacent placement of tapes. There was, however, noticeable lack of bonding along the edges of some ribs, as can be seen in Figure 3.3.

A summary of the results, including the height of the ribs and the H/W, are shown in Table 3.1 and a graphical representation of height to width is shown in Figure 3.4. In this build orientation the average H/W was 0.943. Two additional ribs were built in this direction of widths 0.50" and 0.93". The H/W of these ribs was 0.89 and 0.98, respectively. For each rib built in this orientation the mode of failure was detachment during the machining process. This would imply that the edges of each tape were not well bonded and there was excessive tape vibration during machining, which resulted in delamination due to insufficient bonding. When the ribs were polished and viewed under a microscope it appears that the weld density was very good in the center of the ribs, but the edges showed significant defects, Figure 3.5 shows these edge defects in the 0.93" rib. As the part height increased, there was little change in weld density, but the ribs with fewer defects were able to build to a greater H/W.

3.3.2 Lateral Ribs

When building a rib across the tape direction, the vibration is along the long axis of the rib, which is the stiffest direction. One difficulty in building across the tape direction is
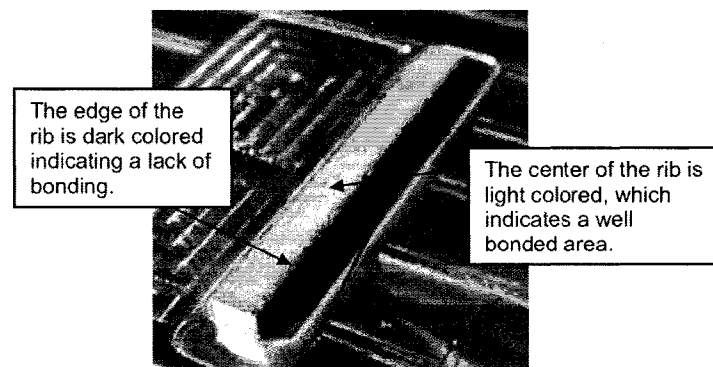
Fig. 3.3: Specimen with poor bonding at the edge (0.125" width).

Table 3.1: Results of longitudinal rib experiments

Width (in)	Orientation	Number of Layers	Height (in)	Ratio
0.25	long	40	0.244	0.976
0.125	long	16	0.0976	0.7808
0.0625	long	11	0.0671	1.0736
				Average Ratio = 0.943
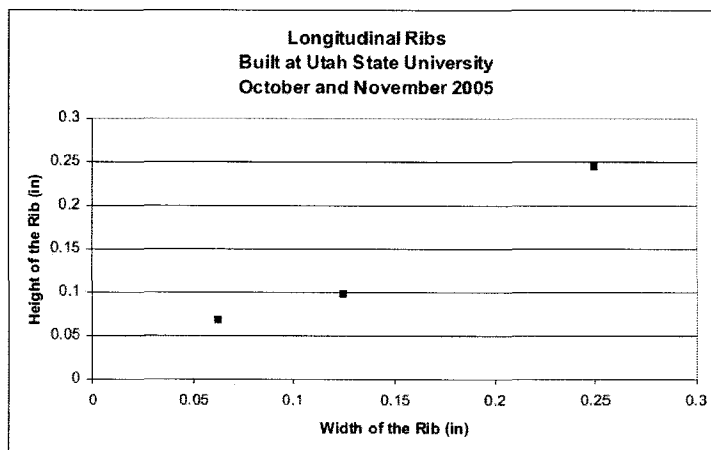
Fig. 3.4: Plot of height versus width of freestanding longitudinal ribs.

(a)   (b)   (c)
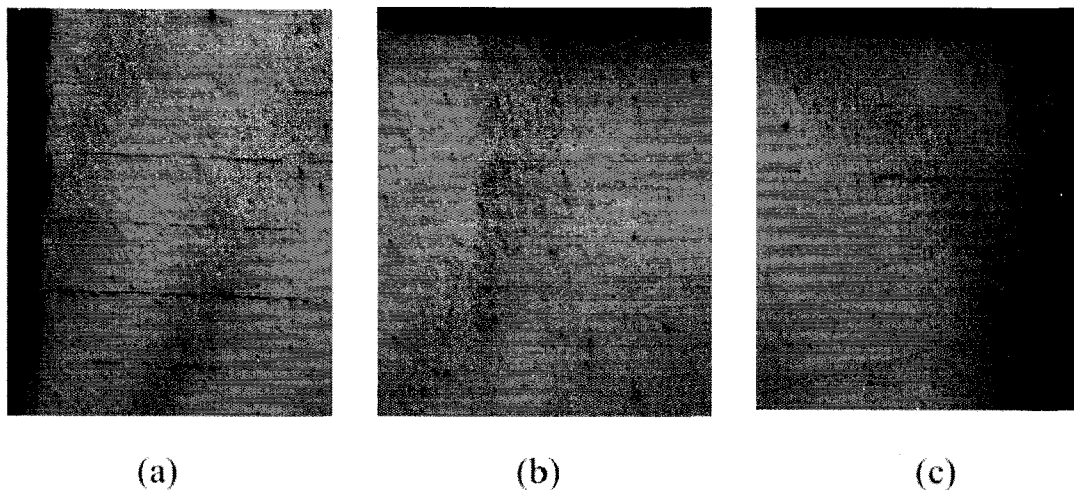
Fig. 3.5: Microstructures of 0.93" freestanding longitudinal rib: (a) Left edge, (b) Center, and (c) Right edge. Images are not continuous, but show that the center has a much higher weld density than the edges.

that there is such a small bonded area for each tape, particularly the thinnest ribs, that it becomes easy to peel the tapes off even with a weld density that would maintain integrity in one of the other orientations. Visibly the weld density did not appear as consistent as with the longitudinal ribs.

The results, including the height of the ribs and the H/W, are shown in Table 3.2 and a graphical representation of height to width is shown in Figure 3.6. The average H/W in this orientation was 0.943, which is coincidently the exact same as the longitudinal ribs. It is worth noting that the H/W varied greatly between specimens in the lateral direction. The mode of failure for each of the ribs built across the tape lay direction was a lack of bonding during deposition. Figure 3.7 shows the three ribs built across the tape direction. When viewed under a microscope at least some of these ribs show trends that would imply that as the build height increased the weld density decreased gradually until delamination occurred, this can be seen by observation of the 0.125" lateral rib, Figure 3.8.

3.3.3 45 Degree Ribs

For ribs built at a 45-degree orientation, the ribs are built along the direction of maximum shear, and there is a better tradeoff between resistance to vibration and area for each weld. One concern with this build is that it creates a point at the edge of each tape seam where there is almost no force applied during consolidation (since UC force is lowered proportional to deposit area). This sharp point also acts as a discontinuity during machining, which can cause the corners of each tape to peel. If a lower layer does not bond well, then subsequent layers do not bond well, as can be seen in Figure 3.9.

Visibly the weld density seems to be very good in the ribs built in this orientation,

Table 3.2: Results of lateral rib experiments

Width (in)	Orientation	Number of Layers	Height (in)	Ratio
0.25	across	30	0.183	0.732
0.125	across	17	0.104	0.830
0.0625	across	13	0.079	1.269
				Average Ratio = 0.943
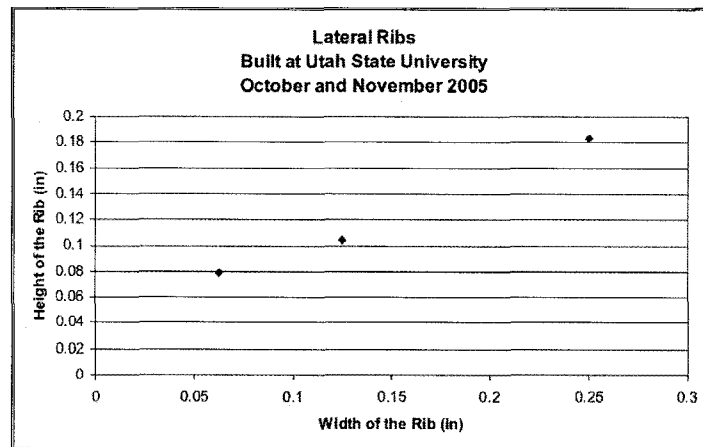
Fig. 3.6: Plot of height versus width of freestanding lateral ribs.
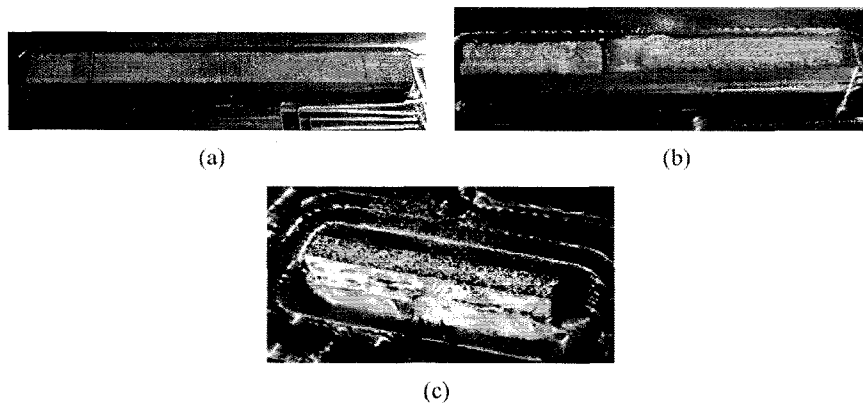
Fig. 3.7: Freestanding ribs built in the lateral direction: (a) 1/4", (b) 1/8", and (c) 1/16".
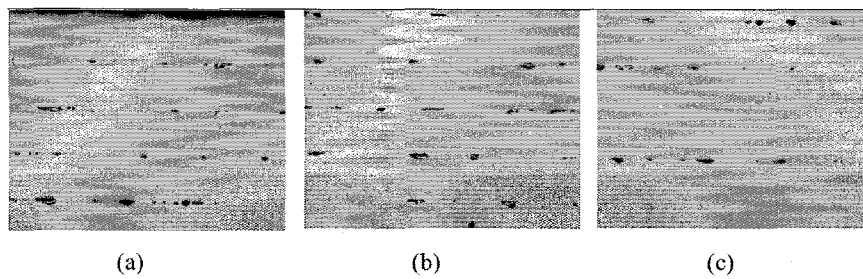
Fig. 3.8: Images of the 0.125" lateral free-standing rib where, from top (a), to middle (b), to bottom (c), it can be seen that the weld density decreases as height increases.
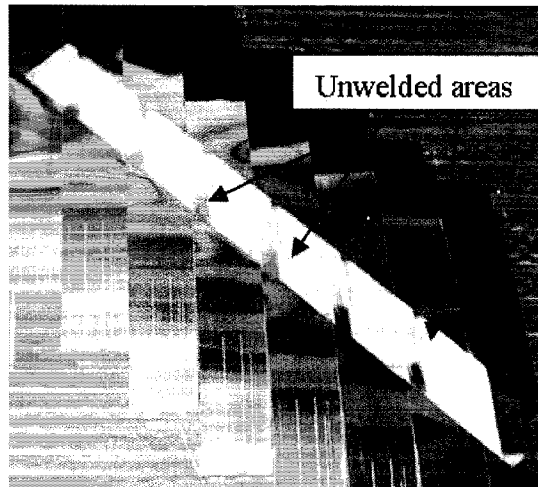
Fig. 3.9: 45° rib before excess tape has been trimmed. The unbonded areas (shiny metallic) are also noticeable inside the rib (dull, white). Shiny areas inside the rib show the areas where peeling occurred due to machining.

other than the issue with peeling along the corners of each tape. The results including the height of the ribs and the H/W are shown in Table 3.3 and a graphical representation of height to width is shown in Figure 3.10. The average H/W in this orientation was 1.017:1, which is significantly better than either of the other two orientations. The mode of failure was not consistent for the ribs built in this orientation, some failed due to machining and others because of a lack of deposition bonding strength. Figure 3.11 shows three ribs built at the 45 degree orientation. When viewed under a microscope these ribs show very good weld density even at the top of the ribs and along the edges, Figure 3.12. The 0.125" rib is the only one that showed significant defects, Figure 3.13, and the H/W of that rib was much lower than the other ribs built at 45 degrees. However, in some ribs built in this orientation it is possible to see where two tapes were not aligned perfectly next to each other, leaving

Table 3.3: Results of 45° rib experiments

Width (in)	Orientation	Number of Layers	Height (in)	Ratio
0.25	45 degree	41	0.250	1.000
0.125	45 degree	16	0.098	0.781
0.0625	45 degree	13	0.079	1.269
				Average Ratio = 1.017
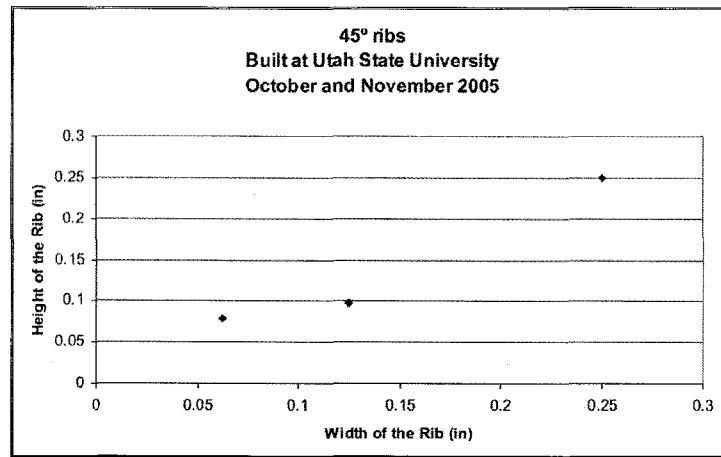
Fig. 3.10: Plot of width versus height of freestanding 45° ribs.

(a)

(b)

(c)
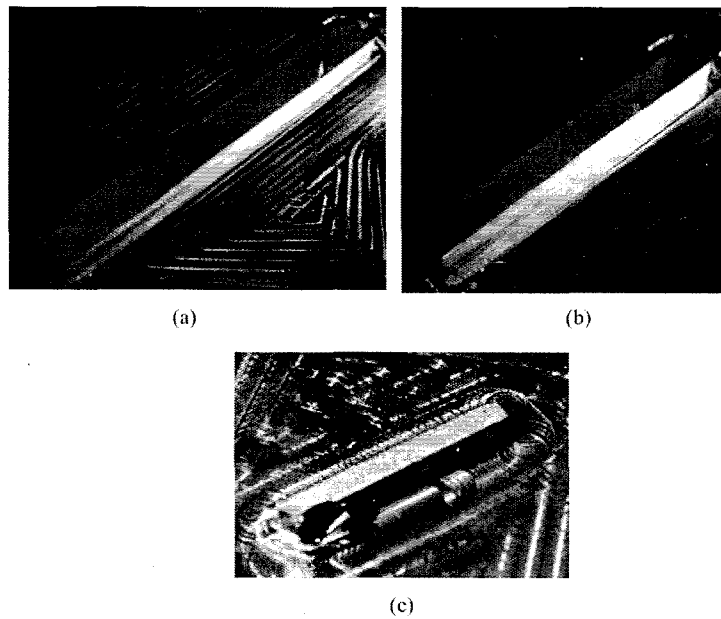
Fig. 3.11: Freestanding 45° ribs (a) 1/4", (b) 1/8", and (c) 1/16".
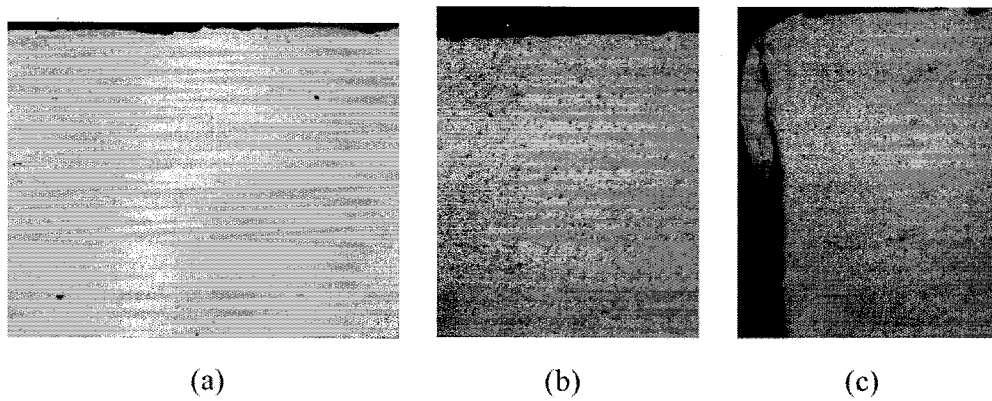
Fig. 3.12: Microscopic images of 45° rib structure weld density: (left) 0.063" rib top center, (center) 0.50" rib top center, and (right) 0.50" rib top left side.
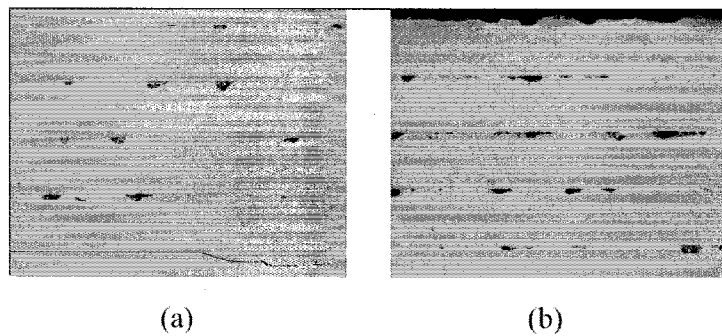
Fig. 3.13: Microstructures of 0.125" free-standing ribs structure: (a) Bottom of rib, (b) Top of rib.

a gap between tapes that are side by side, but this did not seem to cause adverse effects above that point in the build, as seen in Figure 3.14.

3.4 Experimental Discussion

The results show that under ideal conditions a H/W of 1:1 is achievable using UC. The orientation that produced the highest ratio and best weld density was the 45 orientation. However, on all 45 degree builds there was a significant portion of the edge that was not welded properly due to the tape peeling at adjacent sharp edge tape boundaries. Overall the 1/16" ribs built to the highest H/W value, as shown in Figure 3.15.

For build orientations that require laying of adjacent tapes, the seams presented major problems. These seams act as discontinuities during the milling/trimming operation, resulting in a peeling up of the tape at that location and a lack of bond in the area. As the build progresses, these areas of lack of bonding grow and sometimes result in build failure. This was particularly noticeable for the wider ribs, which needed a much larger number of layers to achieve the desired H/W. It is conceivable that a better milling feed and speed rate would result in less damage during trimming with parts with seams, which might eliminate this issue. In addition, it is possible that by trimming every fourth layer, as is customary during part building of large structures, that this problem would be reduced. However, at this point the presence of seams in free-standing ribs remains a major issue.

The 0.063" ribs achieved the highest overall H/W, which is likely due to the fact that the ribs were all built within a single tape width and that the total number of layers needed was small and thus reduced the likelihood of random trimming operation problems. Since the 0.125" ribs could not be entirely fabricated using one tape width and the surface that is bonded is small, the ribs failed premature as compared to the other ribs.

Through microscopic observation it appears that the longitudinal ribs have a very high weld density in the center, but have defects along the edges. The lateral ribs have a more consistent density across the ribs. The 45 degree ribs have near 100 percent weld density throughout the part, but they still fail at a H/W of about 1:1.

Fig. 3.14: Free-standing ribs built at a 45° orientation. Exposed gaps between adjacent strips of tape.
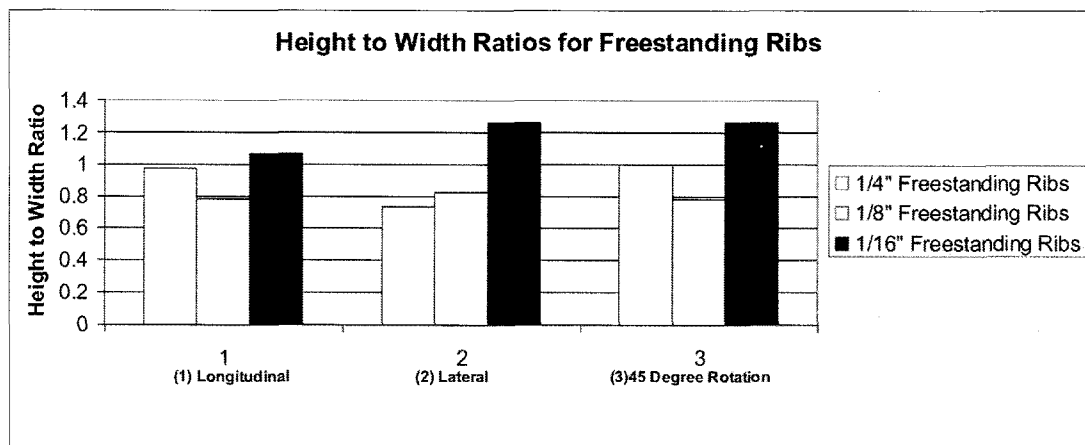
Fig. 3.15: A comparison of H/W for freestanding ribs.

3.5 Modeling

Failure in freestanding ribs at a 1:1 ratio was investigated analytically using an ANSYS model. The detailed model setup and analysis process are reported in another paper in this conference [6]. The vibrational behavior of the substrate and frictional behavior of the bond interface were simulated with a 2-D dynamic FEM model. Figure 3.16 shows the shear strain distributions at the 1500th vibration cycle in builds with various H/W. The shear strain measures the degree of elastic/plastic deformation, which measures the potential for bond formation. For build H/W less than 1:1, greater levels of shear strain exist near the bond interface. In addition, significant shear strain exists inside the builds. Such internal shear strain appears to be distributed in horizontal bands, apparently due to the interference of the traveling vibration waves. For build H/W greater than 1:1, the shear strain has a much lower level at the bond interface. At these build heights, the internal shear strain bands are no longer seen. This may be due in part to damping properties of aluminum which become important at H/W greater than 1:1.

Since bond formation is directly driven by the friction at the interface, the effect of H/W on friction stress was also analyzed. In Figure 3.17, it can be clearly seen that as the
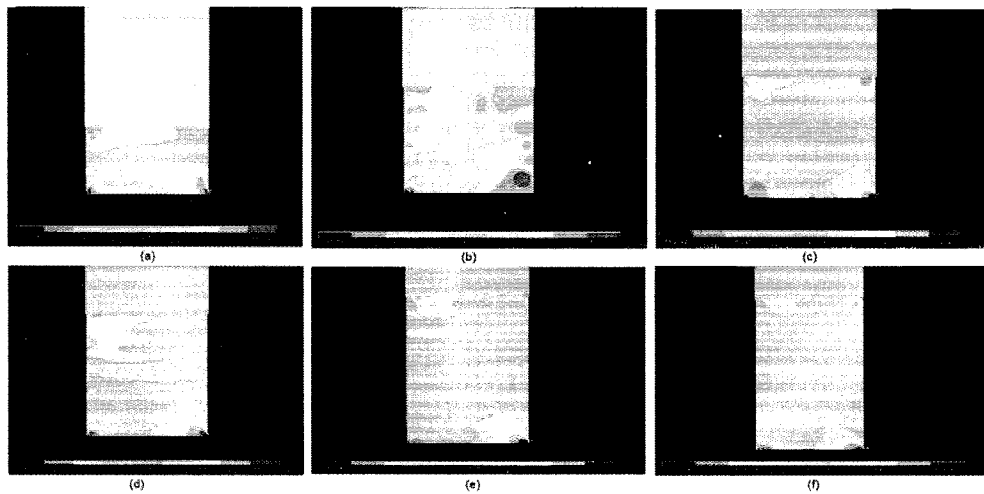
Fig. 3.16: Distribution of shear strain for the 1500th ultrasonic vibration cycle for different H/W, (a) H/W=0.25, (b) H/W=0.5, (c) H/W=0.75, (d) H/W=1.0, (e) H/W=1.5, and (f) H/W=2.0.
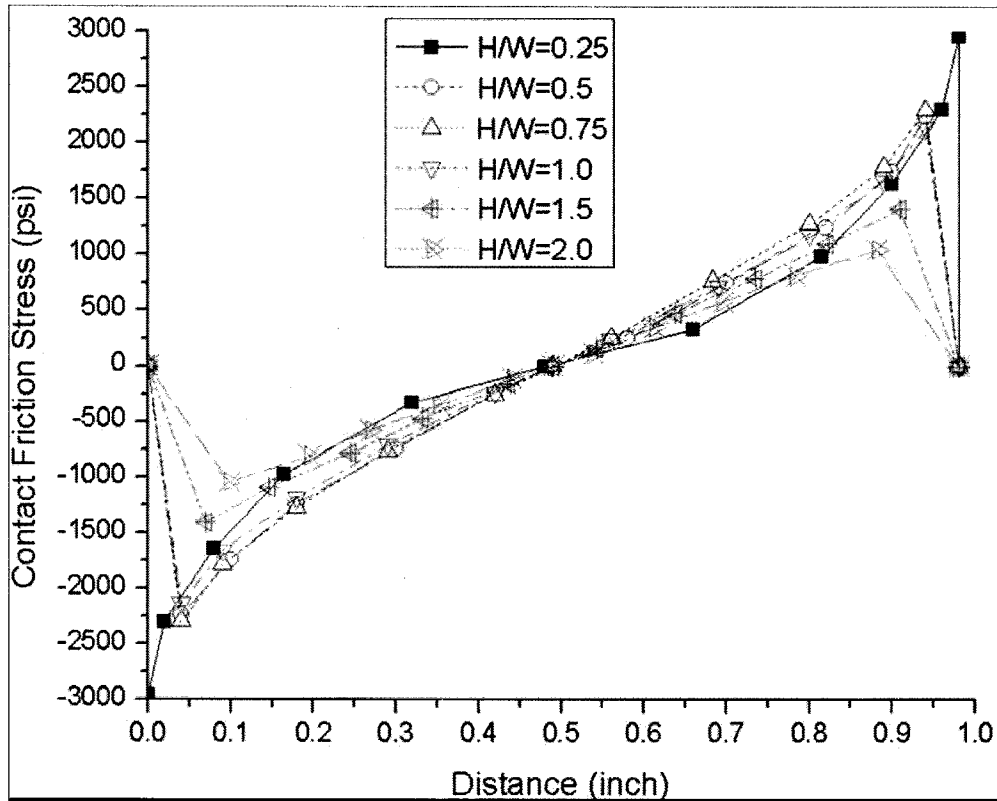
Fig. 3.17: Distribution of shear strain for the 1500th ultrasonic vibration cycle for different H/W, (a) H/W=0.25, (b) H/W=0.5, (c) H/W=0.75, (d) H/W=1.0, (e) H/W=1.5, and (f) H/W=2.0.

H/W increases, the peak friction stress decreases. For the H/W of 1:1, the peak friction stress is less than 1500 psi, while a minimum of 2000 psi friction stress is seen for H/W less than 1:1. Apparently, as the build height increases to H/W of 1:1, the frictional driving force for bonding has decreased to below a critical level.

3.6 Recommendations

To be able to obtain greater H/W, there are a number of suggestions based on this study.

- Free-standing, unsupported ribs should be avoided, if at all possible. Instead, patterns of ribs (such as a honeycomb pattern or intersecting ribs sections) or support

material should be used. Using a honeycomb pattern, H/W exceeding 100:1 have been demonstrated [7].

- Milling across seams in ribs presents a number of issues. Seams should be avoided when possible and more optimized milling parameters may help significantly.

- Ribs placed longitudinally will have the least resistance to vibration. When creating patterns of ribs, avoid designing members in the longitudinal direction.

- Tape laying patterns should be designed in such a way to maximize bonded area of the tapes on a rib.

- The H/W of 1:1 as the limit for the highest ribs seems to be associated with the elastic and damping properties of the aluminum material. With other building materials, this limit may increase or decrease.

3.7 Future Work

Although this study lends significantly to an understanding of free-standing ribs built using UC, a number of improvements to this study could be made.

- Optimized milling parameters should be studied to help alleviate the problem of tape peeling at seams.

- Microscopy of cross-sections at 0, 45, and 90 degree orientations should be observed for all tapes. This will provide an accurate comparison between the weld densities achievable in the different rib orientations, which is not possible using only microscopy on slices perpendicular to the long-axis of the rib.

- A more careful study of patterns of ribs and supporting materials for ribs should be performed.

- An investigation of the effect of changing UC parameters, particularly the amplitude of vibration, is merited.

- The validity of a 1:1 ratio for other materials should be investigated.

3.8 Conclusions

Freestanding ribs were built longitudinally, laterally and at a 45 degree orientation with respect to the tape direction of a UC machine. Each orientation presented a number of challenges for building free-standing ribs. The main parameters which seem to affect the ability to create free-standing ribs with a high aspect ratio are stiffness with respect to the sonotrode vibration direction, bonding area for tapes, the presence of seams in ribs, and the tape trimming operation. Careful control of these make possible ribs with a maximum H/W of approximately 1:1. The existence of this maximum height is associated with the vibrational and frictional behavior of the aluminum material under the given process conditions. When the H/W is greater than 1:1, both the shear strain and frictional stress at the bond interface are believed to have decreased to levels below the critical values for bond formation.

References

1. White D.R. "Ultrasonic consolidation of aluminium tooling." <u>Advanced Materials and Processes</u> vol. 161, 2003, pp. 64-65.

2. Daniels H.P.C. "Ultrasonic welding." <u>Ultrasonics</u>, 1965, pp. 190-196.

3. O'Brien R.L. "Welding Processes" in Welding Handbook (v2, 8th ed.), American Welding Society, Miami, 1991.

4. Kong C.Y., Soar R.C., Dickens P.M. "Optimum process parameters for ultrasonic consolidation of 3003 aluminium." <u>Journal of Materials Processing Technology</u> vol. 146, 2004, pp. 181-187.

5. Janaki Ram G.D., Yang Y., George J., Robinson C., Stucker B.E., "Improving linear weld density in ultrasonically consolidated parts." Solid Freeform Fabrication Symposium, Austin, TX, 2006.

6. Chunbo Zhang, Leijun Li, "A Study of Static and Dynamic Mechanical Behavior of Substrate in Ultrasonic Consolidation." Solid Freeform Fabrication Symposium, Austin, TX, 2006.

7. Clements J., George J., "Rapid Manufacturing of Satellite Structures and Heat Pipes using Ultrasonic Consolidation," American Institute of Aeronautics and Astronautics 2006, proceedings of the 20th Annual Conference on Small Satellites August 14-17, 2006.

Chapter 4

Integration of Direct-write and Ultrasonic Consolidation Technologies to Create Advanced Structures with Embedded Electrical Circuitry

1

This chapter is a conference paper published in the proceedings of the 17th Annual Solid Freeform Fabrication Symposium. All permissions to use this paper as a part of this thesis are contained in Appendix B.

Abstract

In many instances conductive traces are needed in small compact and enclosed areas. However, with traditional manufacturing techniques, embedded electrical traces or antenna arrays have not been a possibility. By integrating Direct Write and Ultrasonic Consolidation technologies, electronic circuitry, antennas and other devices can be manufactured directly into a solid metal structure and subsequently completely enclosed. This can achieve a significant reduction in mass and volume of a complex electronic system without compromising performance.

4.1 Introduction

A common design driver for many industries and applications is the push to make products more compact and integrated. Additive manufacturing techniques are being used to create complex, compact integrated structures, thereby reducing cost, size, and mass. Ultrasonic Consolidation (UC) and Direct-Write (DW) are two types of additive fabrication techniques used to create integrated structures.

---

[1]Authors: Christopher J. Robinson, Brent Stucker: Utah State University, Amit J. Lopes, Ryan Wicker: University of Texas at El Paso, and Jeremy A. Palmer: Sandia National Laboratories

One application requiring small, integrated structures is small satellites. This paper overviews a recent study by the authors to, for the first time, integrate the technologies of UC and DW to create multifunctional panels that are relevant to the types of systems needed in a small satellite. Two panels were created to represent possible structural panel sections of a small satellite. One panel demonstrates the ability to embed electrical circuitry, connectors, switches, DW electrical traces, and other components. The second panel demonstrates the ability to use DW to apply a patch antenna on the surface of a UC panel with an embedded honeycomb core created using UC.

4.2   Ultrasonic Consolidation (UC)

Ultrasonic Consolidation is an additive manufacturing process which deposits metallic foils using ultrasonic energy, followed by a milling operation to create the desired cross-section. UC works by creating differential vibration between the substrate or previously deposited layers and a newly deposited layer using a sonotrode. This differential vibration results in plastic deformation and metallurgical bonding between clean metallic surfaces [1]. UC is the only SFF technology which can create a solid metal part from engineering alloys at low temperatures, which enables the embedding of wiring, electronics, and other components without thermally destroying them. One important benefit of UC is that a build can be paused and left for essentially any amount of time and then restarted again with no adverse effects. In addition, the parts can be removed and set aside or used in another apparatus. This facilitates the combining of DW and UC without needing to integrate them into a single apparatus. However, for efficiency purposes, it would be possible to integrate a DW deposition head onto a UC apparatus for future work, which would eliminate the need to move the part between apparatuses.

The UC machine used for this work is a Solidica Formation$^{\text{TM}}$ beta machine located at Utah State University (USU). This is the same technology used to make the Solidica Chorus sensor that recently won the Gold Award at the 2006 Sensors Expo. This sensor measures temperature, vibration, and three-dimensional acceleration, adds GPS/dead reckoning location data, and then transmits the data wirelessly to any ZigBee-compliant or 802.15.4

platform, while all electronics are embedded within a solid piece of aluminum [2].

4.3 Direct-write (DW)

Direct-write is the ability to write or print passive or active electronic components (conductors, insulators, batteries, capacitors, antennas, etc.) directly from a computer file without any tooling or masks. Many different direct write technologies have been developed over the recent years, following funding by the Defense Advanced Research Projects Agency (DARPA) [3]. These DARPA-funded projects included Matrix Assisted Pulsed Laser Evaporation (MAPLE), nScrypt 3De, Maskless Mesoscale Materials Deposition (M3D) and Direct Write Thermal Spraying. nScrypt and MicroPen are two examples of technologies which use liquid inks to create DW traces. In addition, these inks can be extruded using simple extrusion devices. Ink is dispensed through a tip that is controlled by either a CNC head or other stage type controls; or it can also be dispensed by hand, depending on the apparatus. Many types of structures can be created using DW because traces can be drawn in three dimensions and vias can be created to step from one level to another in needed situations. Research in the area of new materials is ongoing, and as the number of useful materials increases so does the number of possibilities of this technology.

The DW apparatus used for this work is the 2405 Ultra Dispensing System (EFD Inc., East Providence, Rhode Island), shown in Figure 4.1, located at the University of Texas at El Paso (UTEP). The DW system consisted of an air pressure control console and a dispensing syringe and tip (with nozzle diameters down to 6 mils), which was connected to the console with a plastic hose. The console obtains an externally supplied inlet air pressure (up to 100 psi) and regulates the outlet pressure (from 0 - 5 psi), which was then supplied to the dispensing tip. The ink can be dispensed manually or controlled using LabVIEW and stages integrated at UTEP to draw given circuit profiles. It may be adapted to dispense a variety of fluids including conductive inks and virtually any other fluid [4].
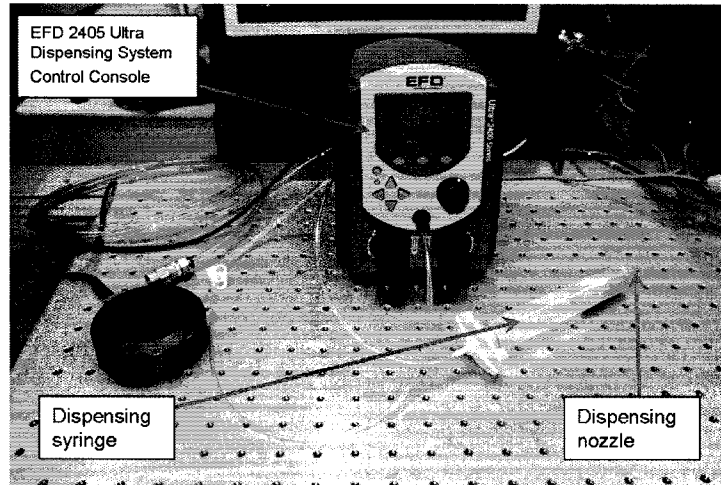
Fig. 4.1: The DW 2405 Ultra Dispensing System, located at the University of Texas at El Paso.

4.4 LED Panel Description

The first demonstration panel created using UC and DW is a 6" X 6" X 3/4" honeycomb panel with solid aluminum outer walls and face sheets, and a solid network of aluminum to support embedded circuitry. Embedded in the structure is a common 9-pin space connector, an LED and a mechanical on/off switch, all of which are connected with electrical traces drawn with conductive silver ink deposited using DW technology. A CAD model of this system is shown in Figure 4.2. While there are many different types of honeycomb structures and cores commercially available, a unique and custom honeycomb was created using UC, which has the added possibility of being able to embed components and circuitry directly into the honeycomb itself. As this demonstration panel had no specific structural constraints, the honeycomb was designed with an arbitrary wall thickness and height of 0.45 inches.

4.4.1 Build Process for the LED Panel

Based on previous experience with embedding electronics in UC structures, the following process plan was used to create the LED demonstration panel. Al 3003 H18 tape was ultrasonically consolidated to a solid Al 3003 H18 substrate. The integrated CNC mill
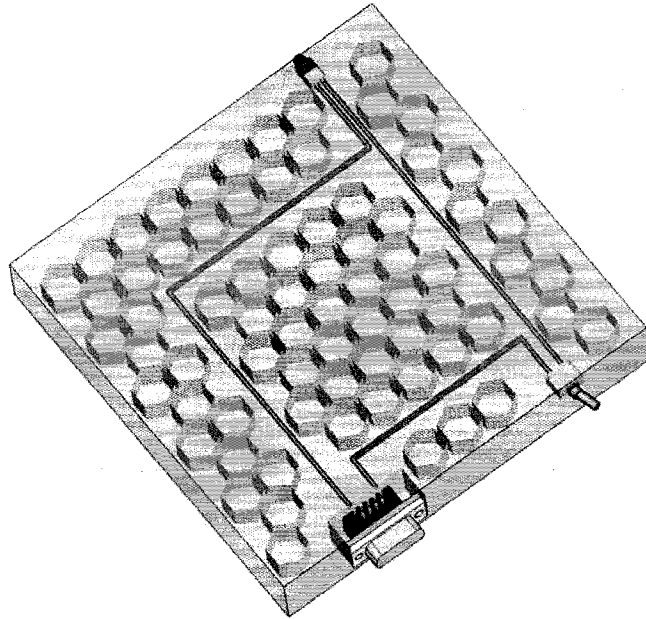
Fig. 4.2: CAD model of an integrated structure built using UC and DW, shown with upper facesheet removed to illustrate the honeycomb network and embedded electrical traces.

machined the geometry for the honeycomb, channels for the electrical traces, and pockets for embedding a space rated D-connector receptacle, a simple switch and an LED into the monolithic block that was formed from a combination of deposited Al and the Al substrate. The panel, attached to a larger substrate, after milling but prior to embedding of components is shown in Figure 4.3.

Following the creation of the basic panel structure, the various pre-manufactured components were potted into their respective pockets using Arctic Alumina thermal epoxy, which is both electrically non-conductive and non-capacitive. The demonstration panel and the connectors used were designed and selected so that all connections to pins and leads would be at the same height for easy accessibility for the DW tip. This was to minimize the number of times the panel had to be shipped between USU and UTEP. The channels for the conductive traces were then filled with the same epoxy and then the channels were again milled with a smaller end mill so that a channel with insulator on three sides was created. At this point, the components were all checked to ensure operability and the panel
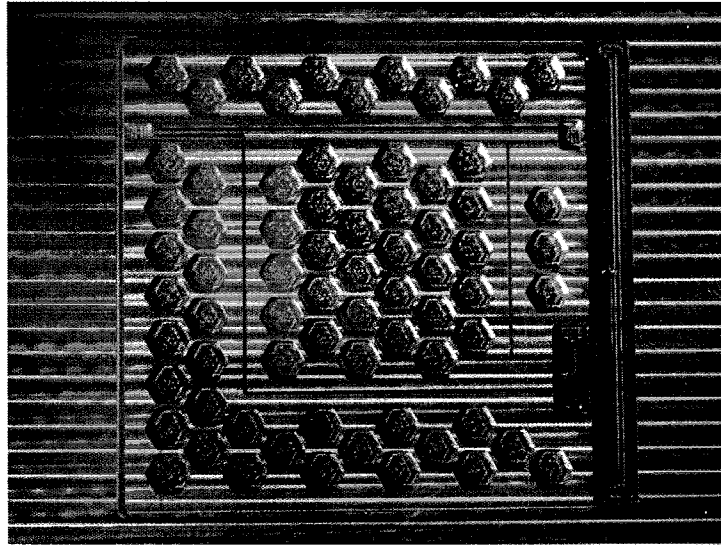
Fig. 4.3: The LED panel after UC, but prior to component embedding, showing the honeycomb structure, pockets for electronic components, and channels for DW traces.

was removed from the UC apparatus and taken to the DW apparatus.

At UTEP, DW traces were drawn to connect all parts of the system into one electrical circuit. The ink chosen for the traces was E1660-136 silver based ink. This ink was chosen for its properties of high conductivity, excellent wear resistance and very good flexibility.

In previous work at UTEP, an ink dispensing experiment was performed using several conductive inks on different substrates at a fixed dispensing pressure (4 psi), vertical gap (4 mils) and using a 6 mil dispensing tip. The parameters were chosen based on previous research done by Medina et al., and gave the most consistent interconnecting lines [4]. Figure 4.4 summarizes the results of the ink dispensing experiments. The results indicate that the E 1660 silver conductive ink gave the lowest average resistivity after thermal cure on all the substrates as compared to the other inks. Thus the E 1660 ink was selected for making the electrical interconnects for this research. Future research will include experimentation with smaller dispensing tips to get the narrowest consistent DW interconnect line.

The resulting circuit is powered through the connector by an external power source and controlled by the switch. A lit LED, when the switch is in the on position, indicates that the circuit is operating properly.

Comparison of average ink resistivitites using different substrates while oven curing
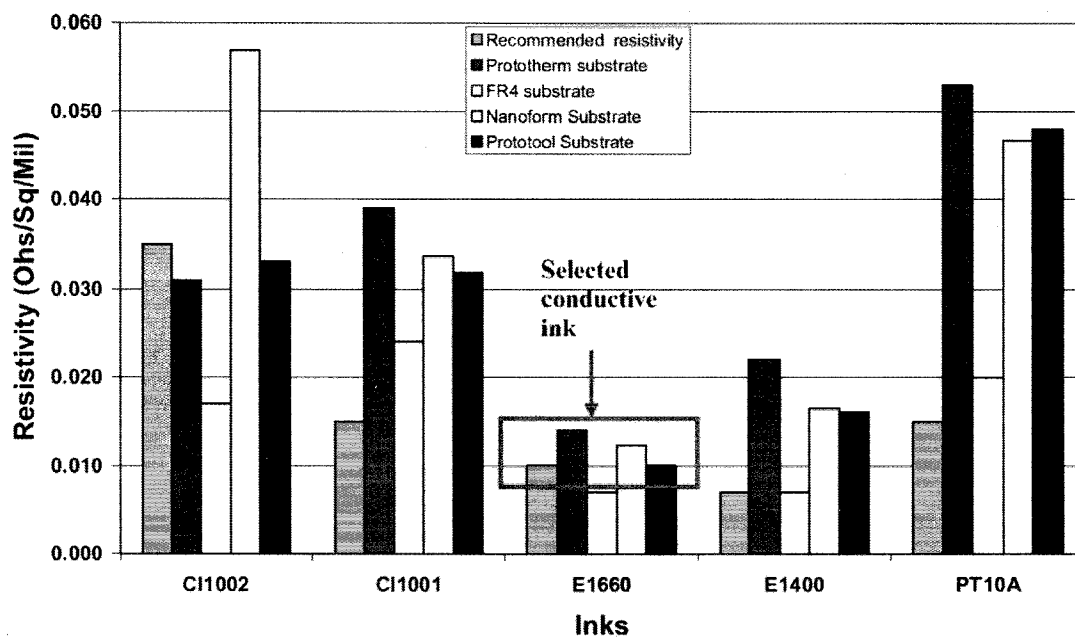
Fig. 4.4: Resistivity comparison of different inks on a variety of substrates.

At USU, the DW traces were then covered with more insulator material. The panel was placed back in the UC apparatus and milled flat before the face sheet was deposited using UC, completely embedding the system into a panel that is solid aluminum on the outside with a connector, switch and LED protruding from around the edges, as seen in Figure 4.5. This panel, while low in mass, is relatively stiff because of the honeycomb structure embedded within.

4.4.2   Testing of the DW Circuitry

Testing was performed throughout the entire LED panel build process. At every stage of the process, the LED responded properly, confirming that the circuit was functioning properly.

A parallel set of tests was performed on simple DW traces to ascertain the effects of the build process used on DW trace performance. For this test, there were no components
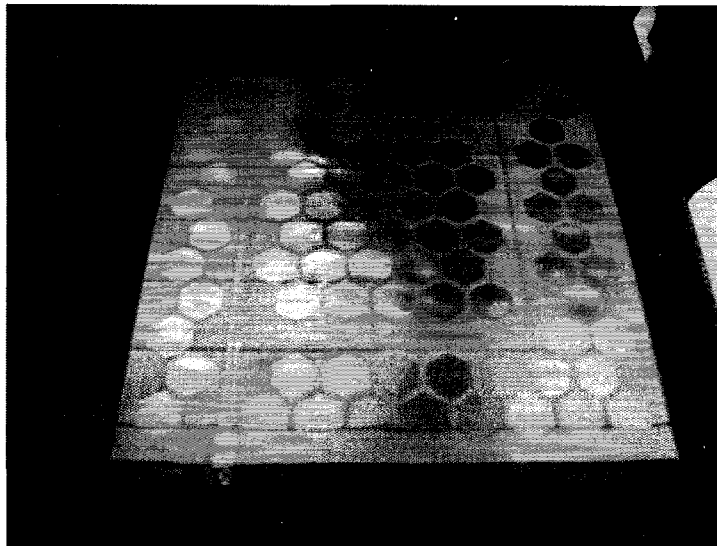
Fig. 4.5: The LED panel after completion.

for the traces to connect to; instead, simple DW pads were created external to a UC part so that electrical resistance could be checked, as shown in Figure 4.6. For this set of tests, the resistance of the traces was measured at different stages of the process and compared to see if there were any significant changes. Resistances of the straight and 90 degree bend DW traces prior to encapsulation by epoxy were 2.3Ω and 1.5Ω, respectively. The resistance after epoxy encapsulation but prior to UC encapsulation was 2.8Ω and 1.9Ω And the resistance after UC embedding was 2.3Ω and 1.6Ω. The decrease in resistance after UC embedding was likely due to additional curing of the ink traces and the epoxy from the elevated temperature (300 F) at which the UC deposition was performed; however, further studies would be necessary to ascertain whether ultrasonic vibration played any role in enhancing the conductance in addition to elevated temperature curing.

4.5 Patch Antenna Panel Description

The panel design for the surface drawn patch antenna demonstration was a 6" x 6" panel that was approximately 0.65" thick, also made of Al 3003 H18 material. A CAD representation of the part is shown in Figure 4.7. This panel was built to demonstrate that a structural panel created using UC can have an antenna drawn directly onto the surface
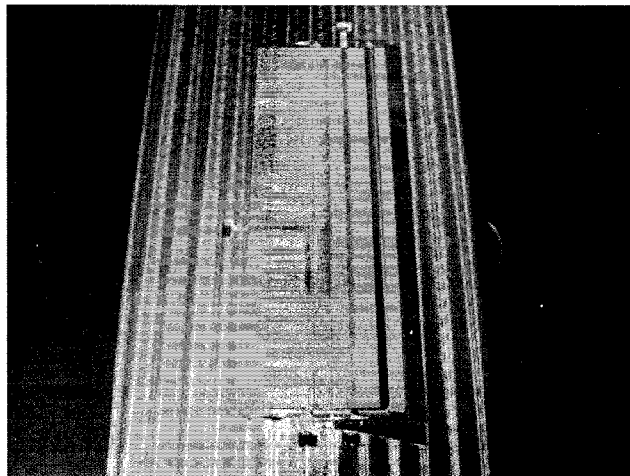
Fig. 4.6: Various DW traces encapsulated in Al 3003 using UC to test for performance degradation.

using DW technology. This antenna was designed to perform as a 10 GHz antenna, similar to one purchased from Labvolt. The antenna had critical dimensions in the width and length of the patch and microstrip as well as the trace thickness. The antenna also was attached to an SMA connector that was grounded to the backplane of the antenna, which in this case was the UC panel. A patch antenna works on the concept of capacitance so it was necessary to insert a dielectric material as the substrate for the antenna and to attach that to the backplane. The dielectric material chosen was 0.030" thick GML 1000. The ink chosen for the antenna was also E1660-136 silver based ink. A honeycomb structure with walls of 0.061" thickness was also used.

4.5.1 Build Process for the Patch Antenna

The process for building this panel was to start by directly using the CNC capabilities of the UC machine to create the honeycomb structure in the base substrate and then consolidating material on top of the substrate, thereby embedding the honeycomb. As aluminum face sheet material was added to the top, a lower area was created for attachment of the dielectric material using dielectric double-sided adhesive tape. Using this configuration, the antenna would not protrude above the surface of the overall aluminum structure, thus pro-
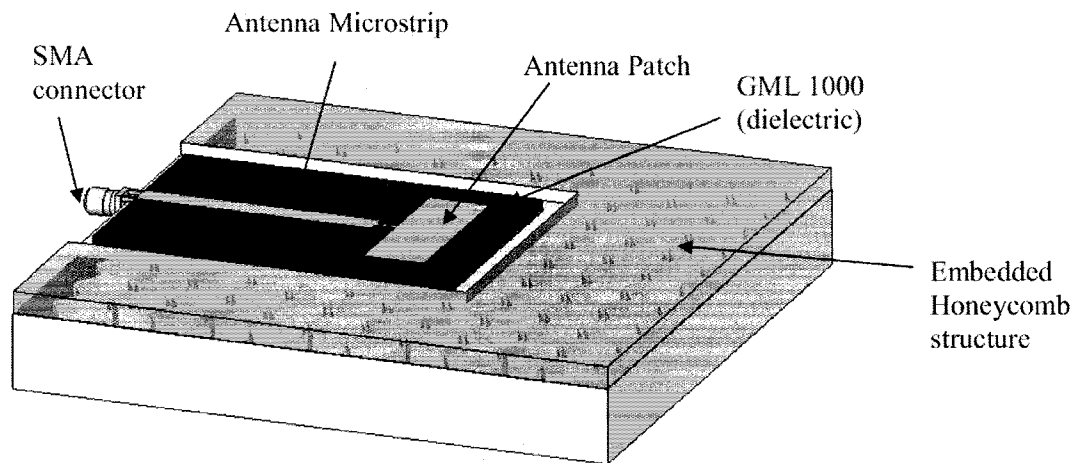
Fig. 4.7: CAD model of Patch Antenna panel where antenna is drawn using DW technology.

tecting it from damage. Slots for the SMA connector ground pins were cut into the panel and the connector was secured using arctic alumina epoxy. Care had to be taken to ensure that the ground pins of the connector were securely grounded to the panel. The antenna was then drawn onto the dielectric with the required dimensions starting from the end of the center connection pin of the SMA connector. Figure 4.8 shows the finished panel and antenna, with cylindrical testing attachment pins attached on two sides of the panel.

For future demonstrations, this panel could easily be integrated onto the surface of the LED panel, but for initial demonstration purposes these were built separately.

4.5.2   Testing of the Patch Antenna Panel

Because the antenna was designed to perform similarly to a Labvolt antenna, results were directly compared to the results from the commercial antenna. Testing was performed to measure the half power beam width. The first test performed was to expose the antenna to a signal at 10 GHz and record the output as the antenna was rotated 360 degrees. As can be seen in Figure 4.9, the pattern for the DW antenna is similar to the Labvolt antenna test results, but at a lower overall gain. The gain decrease is due to a number of factors, two of which are, that the dielectric substrates are not the same for the two antennas and the thickness of the patch was not accurately known. The half power beam width of the
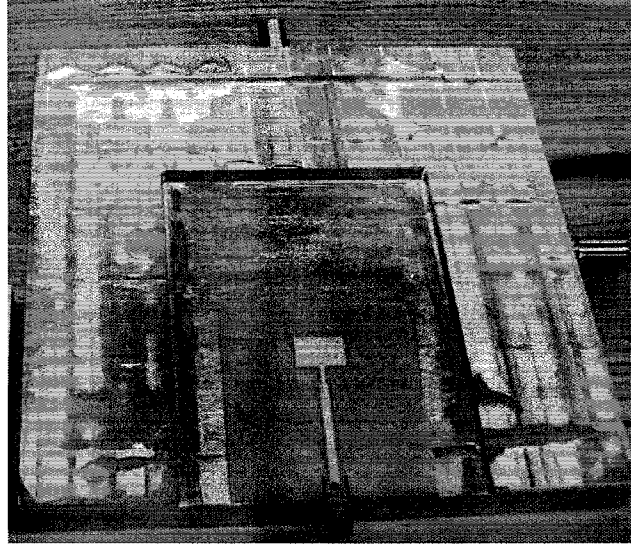
Fig. 4.8: Finished panel with embedded honeycomb and external patch antenna.

DW antenna was 62 degrees while the Labvolt was 74 degreees. The results of the test were promising and show that a working antenna can be directly written onto a structural UC panel.

4.6 Conclusions

Ultrasonic Consolidation and Direct-Write make the production of multifunctional satellite panels and other systems a possibility. By integrating these systems using simple process planning, it has been demonstrated that an integrated panel can have structural features, embedded circuitry and components, and serve as the backplane of an antenna that can easily be drawn on the surface using DW. The future integration of a DW apparatus onto the UC machine will make it simple to create multi-functional, integrated panels with embedded circuitry and components. For the case of small satellites, this should result in an overall decrease in the mass of the system, while increasing payload area and performance.
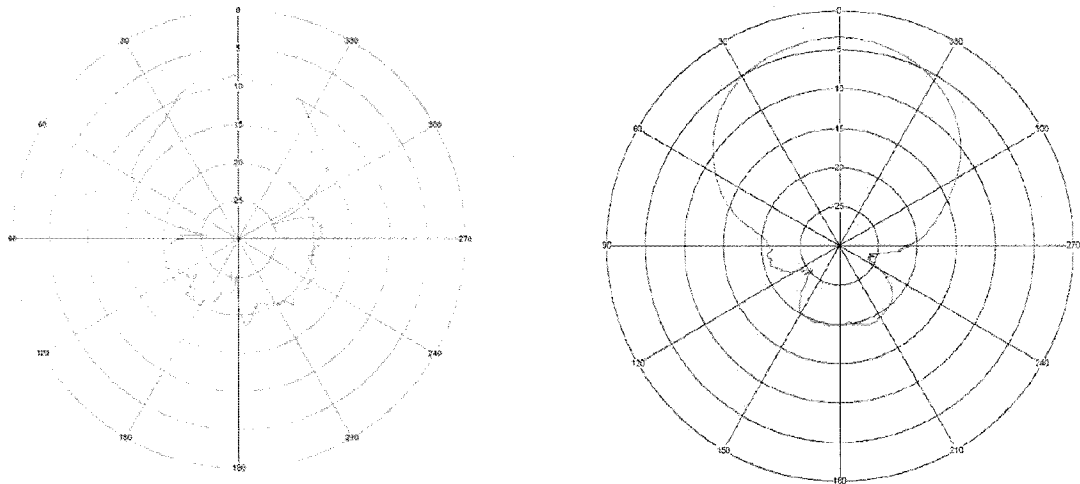
Fig. 4.9: Results from testing of the DW antenna tested at 10 GHz (left) and results from similar Labvolt patch antenna (right).

References

1. Janaki Ram G.D., Yang Y., George J., Robinson C., Stucker B.E., "Improving Linear Weld Density in Ultrasonically Consolidated Parts," Solid Freeform Fabrication Symposium Proceedings, Austin, TX, August, 2006.

2. Solidica (2006) http://solidica.com

3. Church K.H., Fore C., Feeley T., "Commercial Applications and Review for Direct Write Technologies," Materials Development for Direct Write Technologies, San Francisco, CA, April 24-26, vol. 624, pp. 3-8, 2000.

4. Medina F.R. , Lopes A., Inamdar A., Hennessey R., Palmer J., Chavez B., Davis D., Gallegos P., Wicker R., "Hybrid Manufacturing: Integrating Direct-write and Stereolithography," Solid Freeform Fabrication Symposium Proceedings, Austin, TX, August, 2005.

Chapter 5

Using Ultrasonic Consolidation to Rapidly Manufacture Advanced Structures with Embedded Thermal Management Devices

[1]

This chapter is a conference paper accepted for the International Conference on Manufacturing Automation (ICMA), 2007. All permissions to use this paper as a part of this thesis are contained in Appendix B.

Abstract

Rapid manufacturing of metal structures with embedded features using Ultrasonic Consolidation (UC) enables custom thermal control for a wide range of applications. UC allows for direct from CAD manufacturing of aluminum structures with enclosed cavities and embedded features. The Center for Advanced Satellite Manufacturing at Utah State University has been manufacturing and testing UC structures, including lightweight aluminum sandwich panels with honeycomb cores and embedded thermal sensors, thin film heaters, high conductivity materials, pulsating heat pipes, conformal cooling channels and heat pipe networks. The incorporation of these thermal control devices into structural panels gives thermal system designers the necessary tools to enable rapid manufacturing of reconfigurable thermal solutions for electronics packaging, aerospace, defense, and transportation industries.

[1]Authors: Christopher J. Robinson, Jared W. Clements, Erik J. Siggard, and Brent E. Stucker, Utah State University, Department of Mechanical and Aerospace Engineering, Logan, Utah, USA

5.1 Project Introduction

Thermal control is critical to many missions of space flight as well as other situations where there are heat sensitive electronics or materials involved. Space is a unique environment where there is no air to create convection to assist in heat transfer and therefore necessitates the use of advanced thermal control to maintain operating temperature. Some temperature control systems consist of materials that conduct heat well or heat carrying components which transport the heat to sinks where it can be irradiated to release the energy. The research discussed in this paper was performed to demonstrate the capabilities of rapid manufacturing to fabricate advanced thermal systems in an automated process. A series of coupon panels that simulate a portion of a satellite panel were developed that could be fabricated to serve as a proof of concept that the thermal distribution of a satellite can be improved by the use of Ultrasonic Consolidation.

5.2 Introduction to Ultrasonic Consolidation

Ultrasonic welding, which has been used for over 40 years, is a process whereby a metallurgical bond can be formed between two pieces of metal using acoustic vibration [1]. A sonotrode is used to provide both vibration and a clamping force to press two pieces of material together, which causes differential motion and plastic deformation between the two pieces of material. This plastic-elastic deformation at the interface breaks up and disperses surface oxides and other contaminates, leaving a clean metal to metal contact surface [1] [2]. This contact allows a metallurgical bond to form. In general, the more contact points generated between the materials, the better the bond strength [3].

UC is an additive manufacturing process that combines ultrasonic welding of metals with layer additive manufacturing techniques [4]. This is done by depositing layers of material by welding adjacent foils. After each layer of foil is welded, the profile of each layer is created by contour milling. A schematic description of the process is shown in Figure 5.1. The UC process is a commercially available process that is incorporated into a unique machine, the Solidica Formation shown in Figure 5.2. UC is capable of creating features within parts that are difficult or impossible to fabricate using other manufacturing
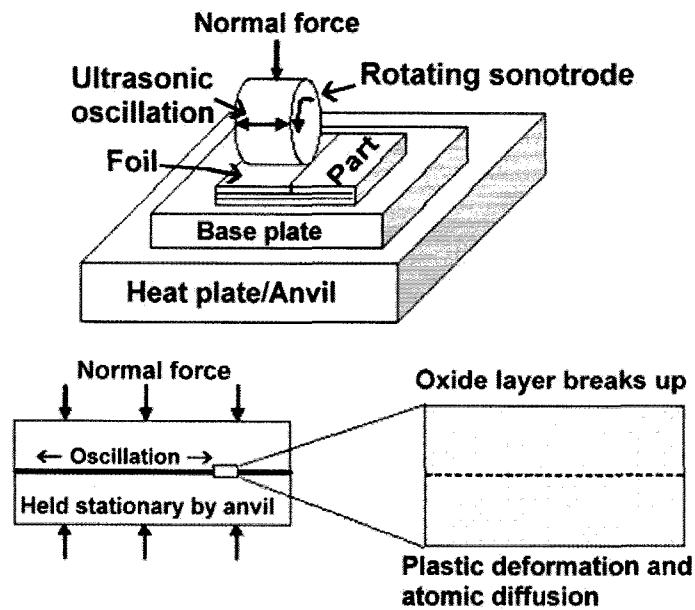
Fig. 5.1: Ultrasonic Consolidation process works by vibrating a foil material against a base substrate with a sonotrode layer by layer

techniques [5]. The UC process not only facilitates the design of advanced structures, but can also be used to create multi-material components that are far superior to their homogenous counterparts.

5.3 Embedded Components

Traditionally, when using RP processes, embedding components in a metal structure is problematic. This is due to the fact that metals are typically processed at elevated temperatures using high power energy sources which will thermally damage the embedded component or base material. Many metal RP processes create near net shape parts which require secondary finishing operations, which can also damage embedded components. When embedding components, such as sensors, in a high temperature process, there are commonly delamination and other problems that arise due to thermal stresses from a mismatch in the coefficient of thermal expansion (CTE) and the large thermal gradients present [6]. UC produces metal parts at a temperature much less than the melting temperature of the build
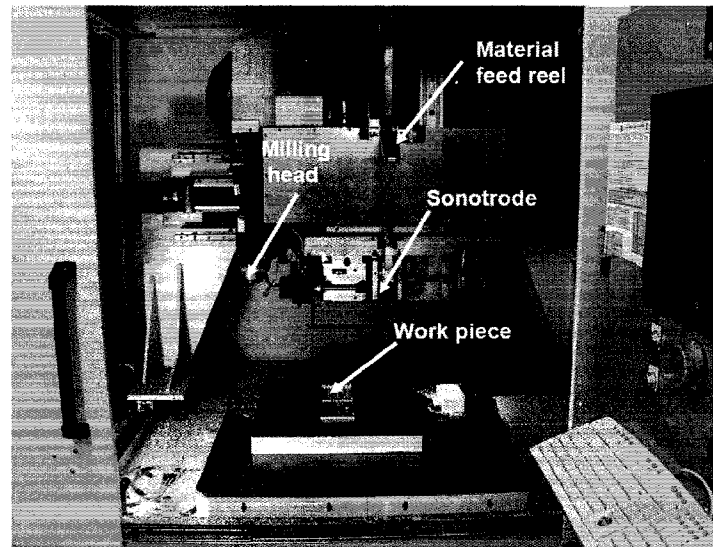
Fig. 5.2: Solidica Formation machine located at Utah State University

materials and only small thermal gradients are present, which help prevent induced stresses from CTE mismatchs. Another advantage to embedding within a UC structure is that a much larger component can be embedded. The maximum build size of a commercial UC apparatus is 24"x 36"x 6" with geometric tolerances of approximately two thousandths of an inch (the accuracy of the CNC milling gantry it is attached to). Both small and large components can be embedded as well as electrical connection leads or other devices so that an entire system can be created within a single structure.

When UC is used as the fabrication technique for structures such as satellite panels there are major benefits in that a single structure can incorporate numerous functionalities such as structural stability, harnessing, component housing, and thermal control. By integrating these functionalities into a single structure the size of the satellite can be greatly reduced and the mass and part count can be reduced through the reduction of fastening systems and additional housings. The research described in this paper was an investigation of the potential to use UC for the embedding of strip heaters, electrical harnessing, thermocouples, carbon fibers, and heat pipes to determine the benefits of different embedded thermal management approaches.

5.4 Design and Manufacturing of the Test Panels

A series of panels were designed and tested to investigate various approaches to thermal management in a panel. Each panel was designed to be of 5"x 11"x 1/2" in size.

5.4.1 Benchmark Panel

The first panel manufactured (benchmark) was designed to test the ability of UC to embed thermocouples, heaters, and the associated harnessing, but without any thermal enhancement devices, into an aluminium honeycomb structure. The CAD design is illustrated in Figure 5.3. A heater was placed in the lower left corner of the panel (the square object). A constant temperature impinging water jet was used as a heat sink and was located on the opposite corner of the panel during testing. Three equally spaced thermocouples were placed along the diagonal between the heater and the heat sink. Leads for the three thermocouples and the heater were designed to exit the panel at a single location in the middle of one long edge of the panel.

The initial step in the manufacturing process is to consolidate .084" of aluminum material to an aluminum substrate, providing material for the lower skin of the honeycomb structure as well as material for the embedded components. Cavities are then machined to a depth of 0.048" for the thermocouples, heater, and harnessing. The harnessing channels were designed such that all wires exit the panel at a common point and there are no channels perpendicular to the panel's long axis. One special design consideration for parts fabricated
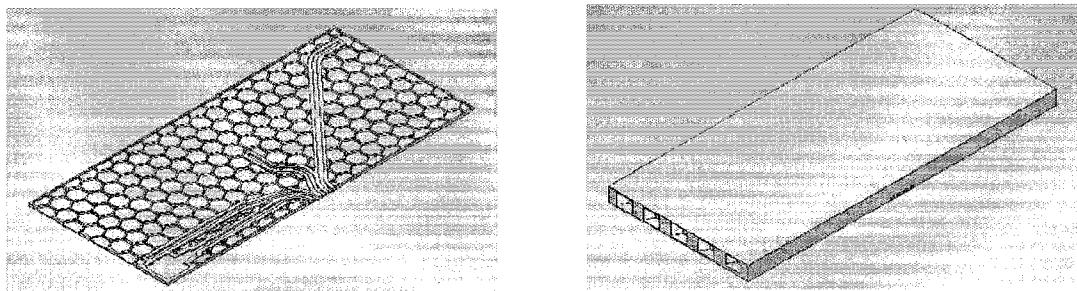
Fig. 5.3: CAD models of the benchmark panel, the left shows the harnessing layout and the right shows the panel completed with a skin included

using UC is that voids or channels larger than one tape width cannot be perpendicular to the sonotrode rolling direction, otherwise the sonotrode will "dip" into the cavity and create an unbonded area.

The thermocouples used were J-type iron-constantan (28) gauge solid wire, which is a relatively stiff wire. The stiffness of the wires accommodated the insertion of the thermocouple wires without the use of epoxy, as they would remain in place while additional layers of aluminium were consolidated above the channels to embed the wiring. However, the Kapton thin film heater, which was 0.8" square, was embedded using an alumina based thermal epoxy with a high stiffness to improve the bonding of the consolidated aluminium directly above the heater. Figure 5.4 shows the channels for the embedded components and the components after they have been inserted.

Subsequent to the insertion of the heater and thermocouples material is deposited until the height of the part is 0.464". This is the height of the honeycomb core before the skin is applied. At this point the honeycomb pattern is machined into the part. The honeycomb cavities extend all the way down to the bottom skin, with the exception that care is taken to avoid disturbing the heater, thermocouples and wires. These components are left embedded in solid aluminum while the material is removed above and in honeycomb areas around them.

The final fabrication step was to apply the upper surface skin to the panel. The skin is 6 layers of aluminium, a total 0.036". Because the total bonding area above the honeycomb is much smaller than that of a solid, flat plate the welding parameters were adjusted to compensate accordingly. In addition, it was found that leaving excess material around the exterior of the part facilitates welding along the edges of the panel. Edges of a part of often poor in UC due to the fact that the deposited foils often overhang the edge, reducing weld quality. Post processing of the part included removing the excess material from the rim of the panel and removing the panel from the substrate. This is accomplished primarily using the CNC machining capabilities of the Formation machine. Figure 5.5 shows the honeycomb before the skin is applied and a finished panel with the skin in place.
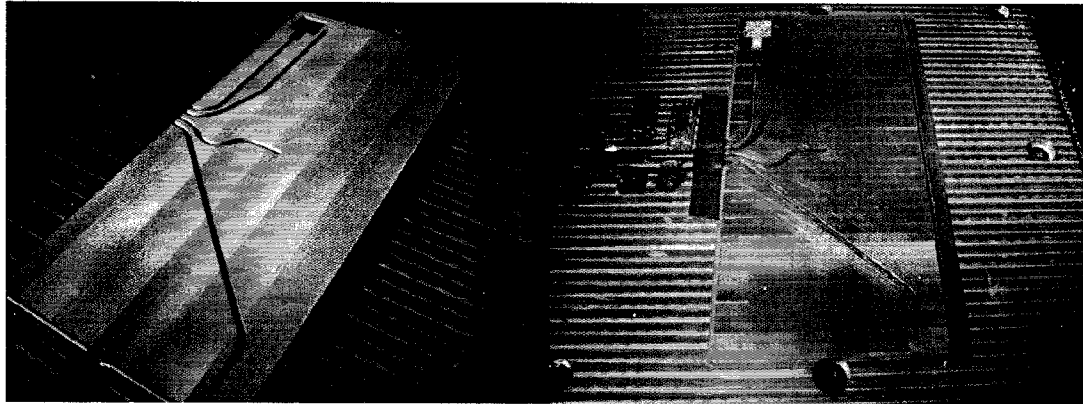
Fig. 5.4: Benchmark panel during fabrication showing the channels for the embedded components (left) and the components inserted and ready for embedding (right)
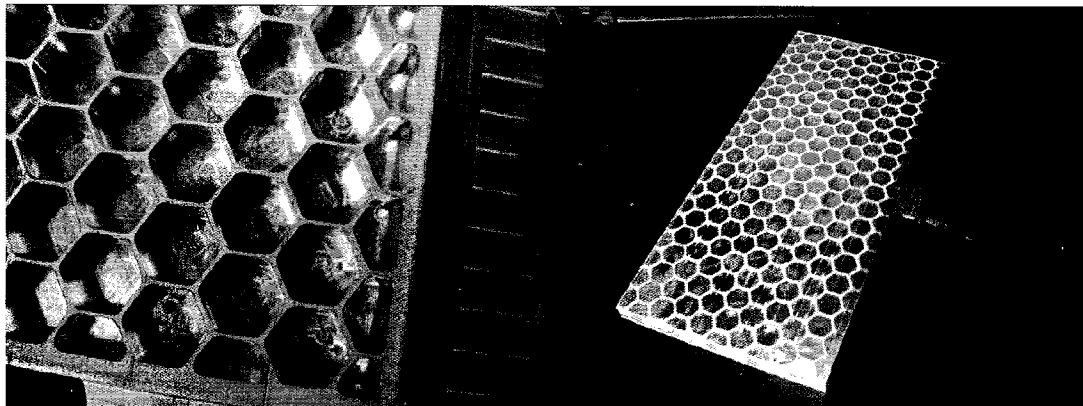
Fig. 5.5: Honeycomb core (left) and the finished panel with skin applied to the honeycomb core (right)

5.4.2 Thermal Doubler Panel

A panel was designed to investigate the ability to transfer heat using high modulus, high conductivity carbon fibers. In order to distribute heat uniformly, a weave pattern was desired rather than unidirectional fibers. Previous to this research the ability to embed metal fiber weaves and single carbon fibers within a UC structure had been demonstrated, so the possibility of directly embedding a carbon fiber weave seemed feasible. However, testing quickly demonstrated that brittle fibers in a weave configuration do not embed between aluminum layers during UC. Due to the brittleness of these fibers, when they were subjected to the vibratory and compressive loads involved in UC, the fibers break at their

overlapping/intersection points. It was determined that nickel coated carbon fibers could effectively be embedded, but due to the lower thermal conductivity and higher density of these fibers there thermal dissipation characteristics would not exceed that of the base aluminum material, and this panel was not completed.

5.4.3 Embedded Heat Pipes

A panel with embedded heat pipes was designed to investigate the ability to embed commercial off the shelf heat pipes. Heat pipes 10" long and 0.236" (6mm) in diameter with copper wicks and pure water as the working fluid were donated by Thermacore for this purpose. The CAD design for this panel is shown in Figure 5.6. Three heat pipes were laid diagonally between the heat source and the heat sink. Because the heat pipes were inserted at an offset angle the 1" wide sonotrode could easily span the cavities and weld the edges effectively.

Insertion of the heat pipes required one additional step in to the manufacturing process. After the thermocouples and heater were embedded, the deposition of new material proceeded for 0.25". At this height three 0.25" deep grooves were machined into the block of aluminium with a 0.25" ball end mill. The machining operation left a U-shaped groove slightly larger than the heat pipes. A small amount of thermal epoxy was applied into the bottom of the grooves and the heat pipes were pressed into place.

Deposition then resumed until the part reached the standard 0.464" height, and machining of the honeycomb core occurred. This machining left a solid block of material around the heat pipes, as designed and shown in Figure 5.6, similar to the material left around the thermocouples and heater. During the honeycomb machining process, a minor CNC programming error resulted in the milling tool broking through the aluminium skin surrounding one heat pipe, but without damaging the heat pipe itself. A photograph of the embedded heat pipe shown in Figure 5.7 thus serves as a good visual aid for understanding the design of the structure. Figure 5.8 shows this panel after the skin was applied but before post-processing.
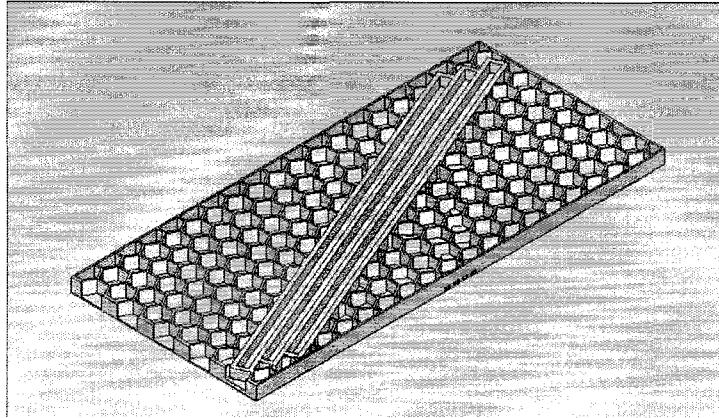
Fig. 5.6: CAD model of panel showing channels for embedding of pre-fabricated heat pipes
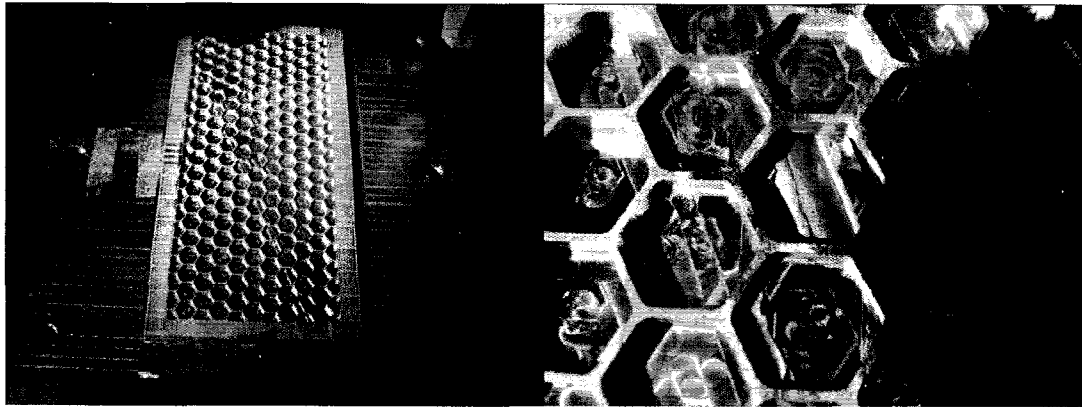
Fig. 5.7: Panel with embedded heat pipes where copper from the heat pipe can be seen

5.4.4 Integral Pulsating Heat Pipe

An integral pulsating heat pipe (PHP) panel was designed to investigate the ability to build and operate a PHP within a UC panel. Pulsating heat pipes are novel heat transfer devices that use multiple wraps of tubing to transport heat from the source to the sink. The innovative application here is that the PHP was machined directly into the structure instead of inserted as a pre-fabricated component. The PHPs in these panels were modelled after PHPs tested by Riehl [7].

Manufacture of the PHP required one step beyond that which was done for the benchmark panel. The UC process after embedding the thermocouples and heaters was interrupted in order to machine the channels. The process then continued and honeycomb was
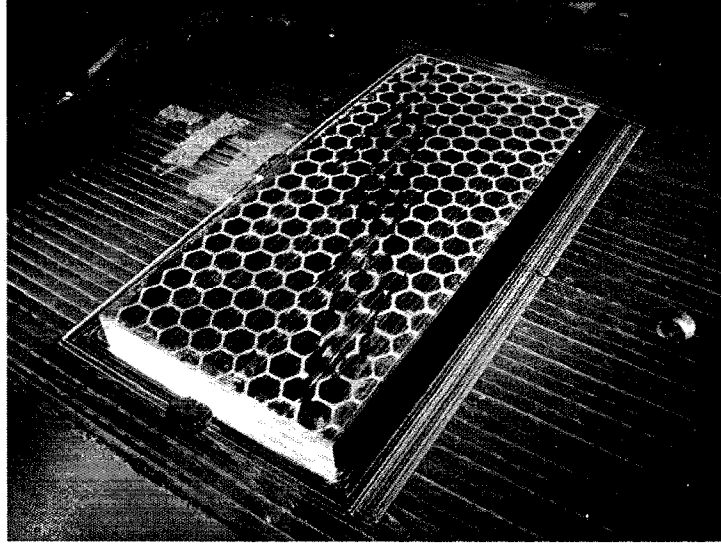
Fig. 5.8: Panel with embedded heat pipes completely built, but before removal from the substrate

machined, leaving a solid area of aluminium around the outside of the channels to act as walls for the channels.

Straight PHP Panel

The CAD design for the first version of the PHP panel can be seen in Figure 5.9. The PHP was designed to traverse the length of the panel 10 times with the bends occurring at the ends of the panel.

Diagonal PHP Panel

A second PHP was designed that ran at an angle from the heat source to the heat sink rather than along the length of the panel. This design consisted of only 3 traverse paths rather than 10.

5.5   Panel Testing Procedure

The panels discussed above were evaluated by experiments which measured temperature both internally, using the embedded thermocouples, and externally, using a thermal
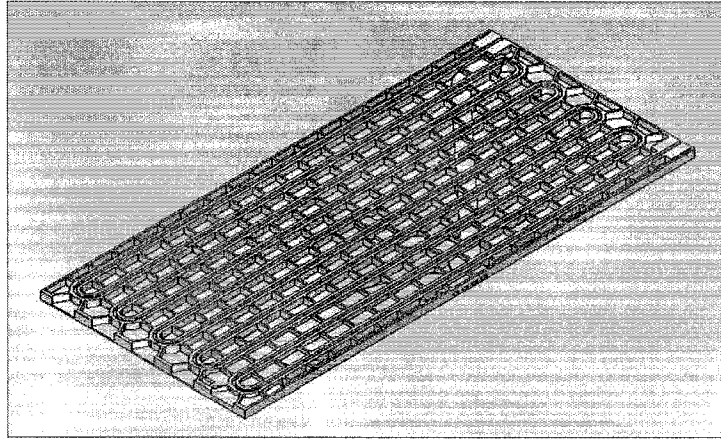
Fig. 5.9: CAD model showing the original PHP design layout with 10 bends

camera. To maintain consistency in the testing, an apparatus enclosure was designed to isolate the panels from air currents that could cause significant surface convection. An impinging jet of 30° C water, 3/4" in diameter, was placed so that it impinged at a set location on the corner furthest from the embedded heater. The embedded heater was set at a constant 20 W power level. Relevant surfaces of the panel and test fixturing were painted with flat black enamel paint to reduce heat reflection for thermal imaging. The embedded thermocouples were connected to a data acquisition board and the thermal camera was positioned and focused to obtain an image of the surface of the panel. A panel in the testing apparatus is shown in Figure 5.10.

For the case of the PHP panels, the channels required sealing with a commercial sealant to prevent leaking. The heat pipes were then filled to a 50 percent fill volume using several different fluids, as recommended by Riehl [7].

5.6   Results

5.6.1   Benchmark Panel Results

When the panel reached steady state the thermocouple readings and a thermal image were recorded. The thermocouple measurements give a final temperature difference of 40.45^{o} C. It can be seen from the thermal image in Figure 5.11 that this temperature difference is
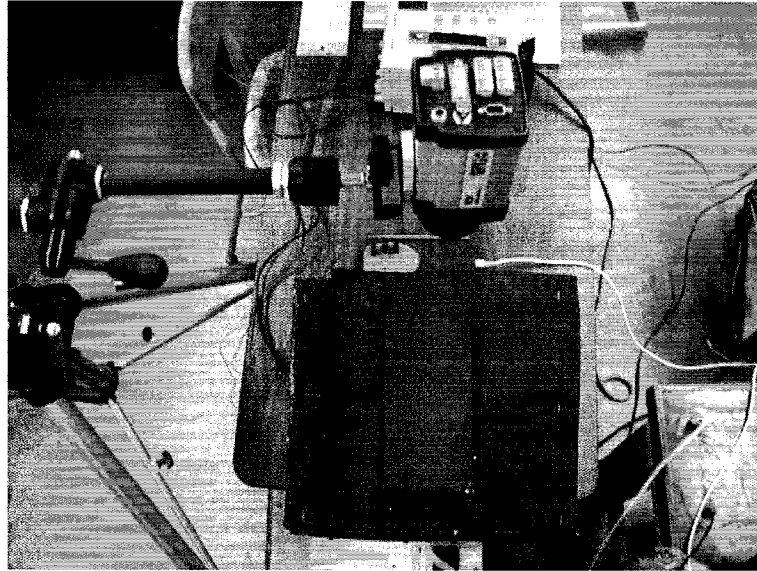
Fig. 5.10: Test set up without the box to shield the air currents

36.46℃   49.70℃   76.91℃
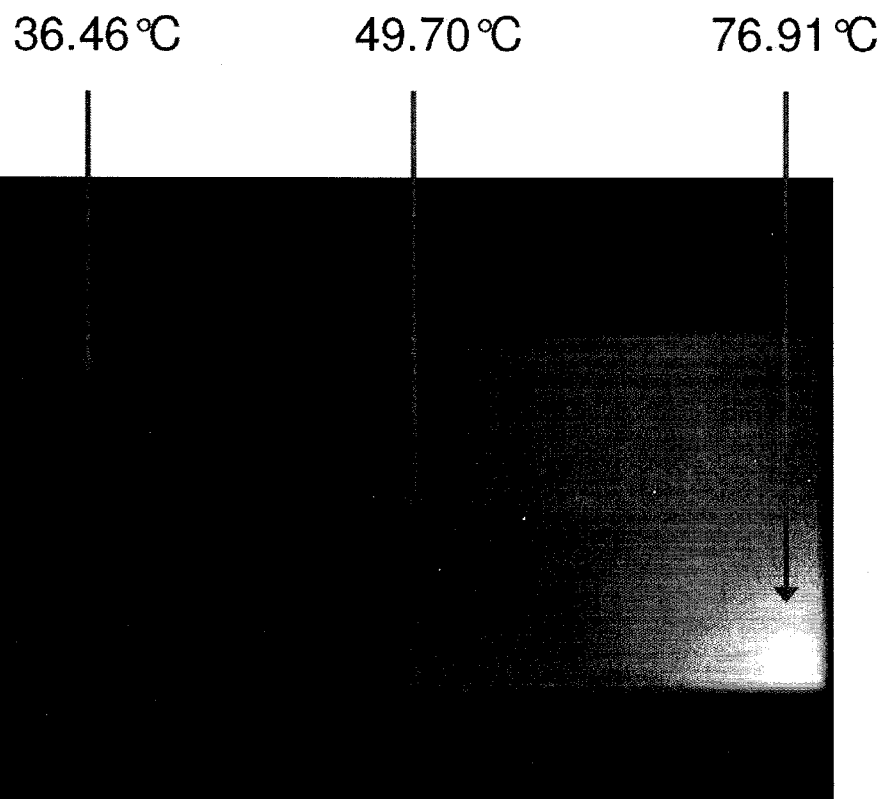
Fig. 5.11: Thermal camera image showing the temperature change across the surface of the benchmark panel, thermocouple readings are also listed in approximate locations

linear between the source and sink and is evenly distributed across the panel. It should be noted that the location of the hot thermocouple is not at the hottest location on the panel. Due to the desire to embed all the thermocouples and heaters in one operation they are all located on the same plane and thus cannot share the same location in space.

5.6.2 Embedded Heat Pipe Panel Results

The embedded heat pipe panel was prepared and tested in the same manner as the benchmark panel. The test results from the panel with embedded heat pipes are shown in Figure 5.12. It can be seen that the overall temperature difference was reduced from
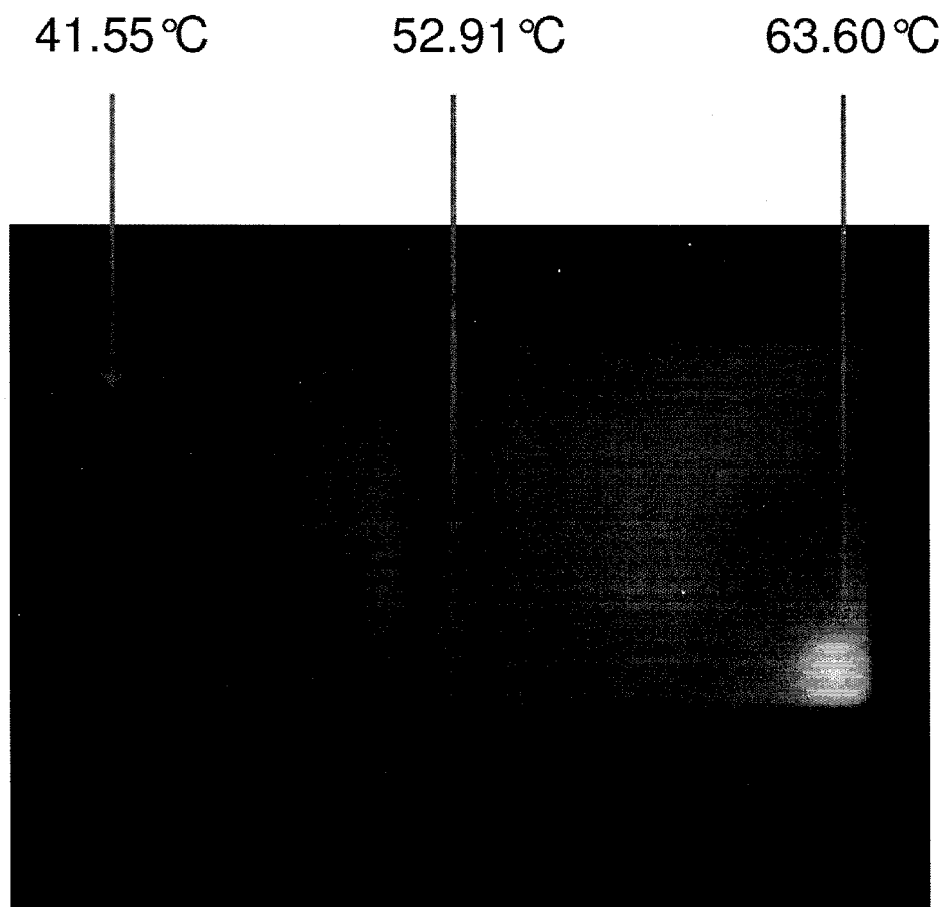
Fig. 5.12: Thermal camera image showing that the heat distribution is much more uniform when commercial heat pipes are embedded into the structure

40.45^o C to 22.05^o C. The infrared image shows that most of the temperature gradient is localized in the regions around the heater and the heat sink, whereas the bulk of the panel remained much more uniform in temperature than the benchmark. In addition, the highest temperature was reduced by over 13° C, even without the heat pipe directly overlapping the source location. These results show that it is possible to embed heat pipes using UC to significantly alter the temperature profile of a panel.

5.6.3   Integral Pulsating Heat Pipe Panel Results

Testing was performed on the PHPs as well. All tests showed no significant improvements over the benchmark panel. Even the second PHP panel, where the ends of the channels were placed very close to the heat source and sink, resulted in nearly the same temperature distribution as the benchmark panel, as can be seen in Figure 5.13. The pan-
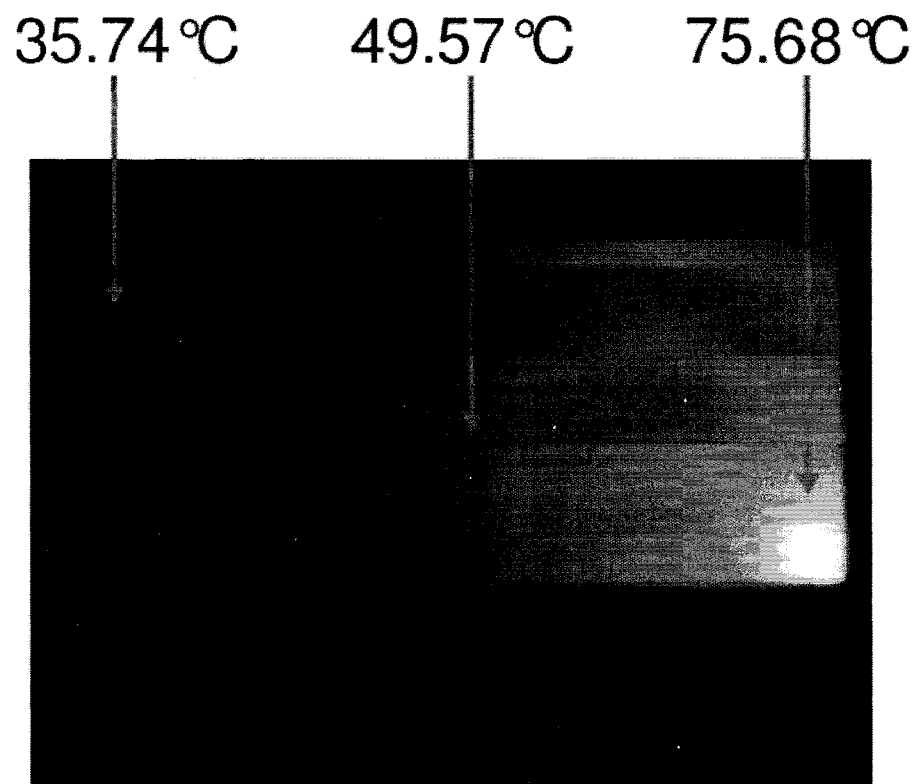
Fig. 5.13: Thermal camera image showing that the heat distribution is much more uniform when commercial heat pipes are embedded into the structure

els were tested numerous times with various fill volumes and working fluids, but it was determined that the PHPs in both panels were not working properly. The very slight improvement over the benchmark was likely due to the improved conduction path from the channels running between the heat source and sink.

5.7 Future Work

The failure of the carbon fiber thermal doubler and the PHP panels raise several areas for future work. It was found that coated carbon fibers could be embedded, but there needs to be significant research performed on selecting appropriate fibers and then testing to determine whether or not a sufficient mass fraction of fibers can be embedded to be thermally beneficial. Alternative PHP designs could also be investigated to determine whether different loop densities and geometries could result in effective PHP operation. Overall, however, the most promising future area is to continue to focus on optimizing the process for embedding commercial heat pipes into panels in order to provide more effective thermal management.

5.8 Conclusions

The effectiveness of using ultrasonic consolidation as an automated additive manufacturing process to fabricate integrated thermal monitoring and control devices within a structural aluminum honeycomb panel was investigated. A benchmark panel demonstrated the ability of UC to embed thermocouples, heaters and harnessing into an aluminium honeycomb structure. The benchmark panel served as a reference to determine the effectiveness of other thermal control components embedded into similar structures. Embedding carbon fiber weaves and directly creating pulsating heat pipes using UC both proved ineffective, but remain promising areas for future work. A panel with embedded water/copper prefabricated heat pipes showed that significant heat transfer improvements can be achieved. This work thus demonstrated the capabilities of UC to fabricate panels with embedded thermal control features.

References

1. **Daniels, H. P. C.**, Ultrasonic Welding, Ultrasonics, pp. 190-196, October-December 1965.

2. **Kong, C. Y., Soar, R. C.** and **Dickens, P. M.** , An Investigation of the control parameters for aluminum 3003 under ultrasonic consolidation, Solid Freeform Fabrication Proceedings, 2002.

3. **Kong, C. Y., Soar, R. C.,** and **Dickens, P. M.,** (2005) Ultrasonic consolidation for embedding SMA fibres within aluminium matrices, Composite Structures, 66, 421-427.

4. **Kong, C. Y., Soar, R. C.,** and **Dickens, P. M.,** (2004) Optimum process parameters for ultrasonic consolidation of 3003 aluminum, Journal of Materials Processing Technology, 146, 181-187.

5. **White, D. R.,**)2003)Ultrasonic Consolidation of Aluminum Tooling, Advanced Materials and Processes, pp. 64-65, January.

6. **Li, X., Golnas, A.,** and **Prinz, F.,** (2000) Shape deposition manufacturing of smart metallic structures with encapsulated sensors, Proc. SPIE, Vol. 3986, pp. 160-171.

7. **Riehl, R. R.,** (2004) Characteristics of an open loop pulsating heat pipe, International Conference On Environmental Systems, SAE Technical Paper number 2004-01-2509, July.

Chapter 6

Fabrication of a Mini-SAR Antenna Array Using Ultrasonic Consolidation and Direct-write

[1]

Misael Navarrete, Amit Lopes, Eric MacDonald, Francisco Medina and Ryan Wicker

University of Texas at El Paso, El Paso, TX, USA

This chapter is a conference paper accepted for the Rapid Manufacturing Conference (RM), 2007. All permissions to use this paper as a part of this thesis are contained in Appendix B.

Abstract

Ultrasonic consolidation (UC) and direct-write (DW) fabrication processes were combined to create a lightweight, monolithic, miniature synthetic aperture radar (mini-SAR) antenna array assembly. UC was used as a method for fabricating an enclosure designed to minimize tolerance stack up as well as to create a very low mass system with embedded components and enclosed features. DW was integrated to create 3-D RF connections, which alleviated misalignment issues as well as reduced the number of parts for stripline-to-coaxial transitions. By combining DW with UC, a number of design advantages arise, when compared to traditional machining techniques and conventional methods for integrating electronics into a volume and mass-limited structure. These design advantages, along with an overall assessment of the opportunities for using UC and DW for rapid manufacturing of integrated systems, are described.

---

[1]Christopher Robinson and Brent Stucker Mechanical and Aerospace Engineering, Utah State University, Logan, UT, USA, Karen Coperich Branch, Jeremy Palmer and Bernd Strassner Sandia National Laboratories, Albuquerque, NM, USA

6.1 Introduction

Imaging devices are used throughout the world in many applications. Research improvements to imaging systems are focused around increasing the performance of the imager and improving the versatility of devices to be used in varying platforms and under diverse conditions. This paper presents new research into the improvement of Synthetic Aperture Radar (SAR) imaging devices as a joint effort including manufacturing experts at Utah State University and the University of Texas at El Paso and SAR antenna and manufacturing experts at Sandia National Laboratories (SNL). A mini-SAR phased array antenna was fabricated through the marriage of two additive manufacturing techniques, namely ultrasonic consolidation (UC) and Direct-write (DW) material deposition. By using these additive techniques, an antenna was designed and fabricated that alleviated misalignment issues, while decreasing the mass of the system. New and innovative designs for RF connections were developed that can reduce the losses experienced during transmission.

6.2 Background

6.2.1 Synthetic Aperture Radar (SAR)

There are many applications that require high resolution imaging from an airborne vehicle. These include environmental monitoring, earth resource mapping, and military applications. An ideal imaging system should be capable of collecting imagery data day or night, even in inclement weather. Synthetic Aperture Radar (SAR) is one such system (http://www.sandia.gov/RADAR/whatis.html). SAR has been researched for more than two decades and the advances that have been made are phenomenal. A SAR antenna works by taking a line scan of an object, and then moving that line in order to create a 2-D image. In 2005, Sandia National Laboratories developed a SAR weighing less than 30 pounds that has a 10 cm resolution from a 10 km standoff distance. An image from this application can be seen in Figure 6.1. This is a major improvement over the 500 pound SAR's available 15 years prior (http://www.sandia.gov/RADAR/images/SAND2005-3445PMiniSAR-fact-sheetp2-v4-redo.pdf).

Fig. 6.1: Image produced using a SAR fabricated by Sandia National Laboratories

Sandia continually strives to miniaturize and improve the performance of its SAR systems. In order to miniaturize the antenna/gimbal assembly, an electronically steerable array (ESA) is required. Initial designs proved to be somewhat difficult because of mechanical misalignments, which caused signal losses in the antenna. In the redesign of this new ultra-compact system, the mass needed to be lowered in order to be practical for unmanned aerial vehicle (UAV) applications. Figure 6.2 shows the results of the original SAR redesign, utilizing traditional manufacturing technologies, prior to the onset of the research described in this paper.

6.2.2 Ultrasonic Consolidation (UC)

Ultrasonic welding, which has been used for over 40 years, is a process whereby a metallurgical bond can be formed between two pieces of metal using acoustic vibration (Daniels, 1965). A clamping force is used to press two pieces of material together, while a sonotrode is vibrated, typically using piezoelectrics, which cause differential motion between the two pieces of material. This differential motion creates plastic-elastic deformation at the interface which breaks up and disperses surface oxides and other contaminates, leaving a clean metal to metal contact surface (Daniels, 1965; Kong, 2002). This contact allows a metallurgical bond to form between the two workpieces. This clean atomic-level bonding
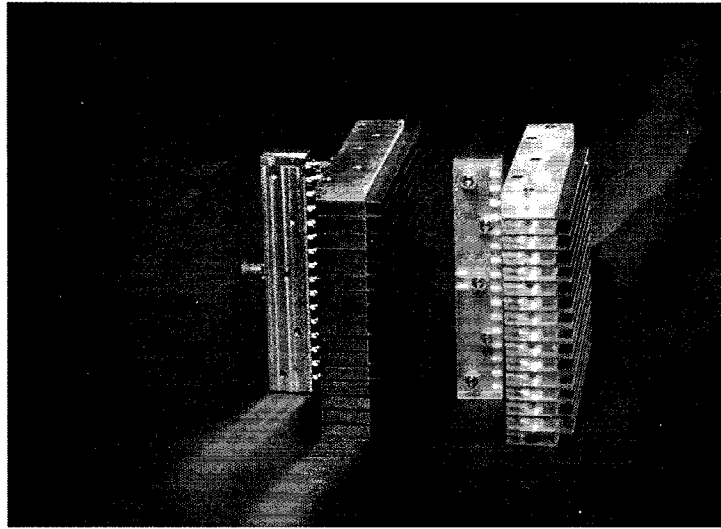
Fig. 6.2: Original design of an ultra-compact SAR antenna

creates contact points and it has generally been shown that the more contact points, the better the bond strength (Kong, 2005).

UC is an additive manufacturing process that combines ultrasonic welding of metals with layer additive manufacturing techniques (Kong, 2004). This is done by depositing layers of material by welding adjacent foils. After each layer of foil is welded, the profile of each layer is created by contour milling. A schematic description of the process is shown in Figure 6.3. The UC process is a commercially available process that is incorporated into a unique machine, the Solidica Formation shown in Figure 6.4. UC is capable of creating features within parts that are difficult or impossible to fabricate using other manufacturing techniques (White, 2003). The UC process not only facilitates the design of advanced structures, but can also be used to create multi-material components that are far superior to their homogenous counterparts. In addition, the issues that arise from hot welding materials are alleviated because UC is a cold-welding process and the molecular structure does not change due to elevated temperatures (Janaki Ram, 2006).

Traditionally, when using RP processes, embedding components in a metal structure is problematic. This is due to the fact that metals are typically processed at elevated temperatures using high power lasers, which will thermally damage the embedded component.
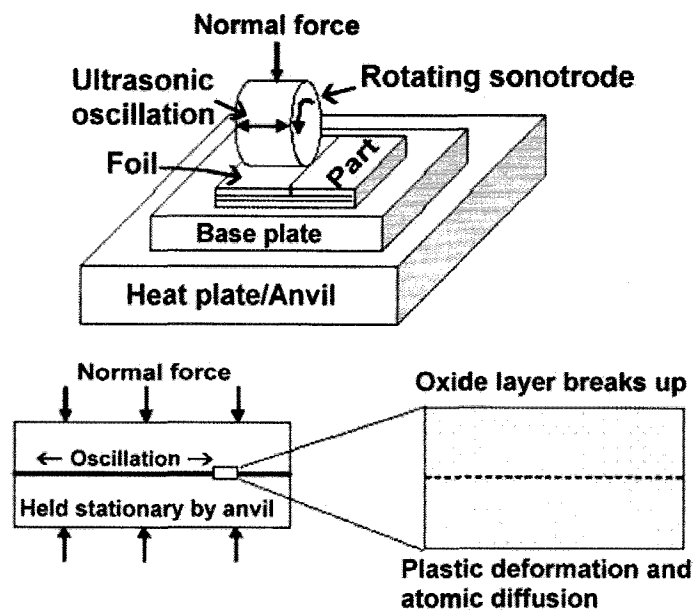
Fig. 6.3: Ultrasonic Consolidation process works by vibrating a foil material against a base substrate with a sonotrode layer by layer
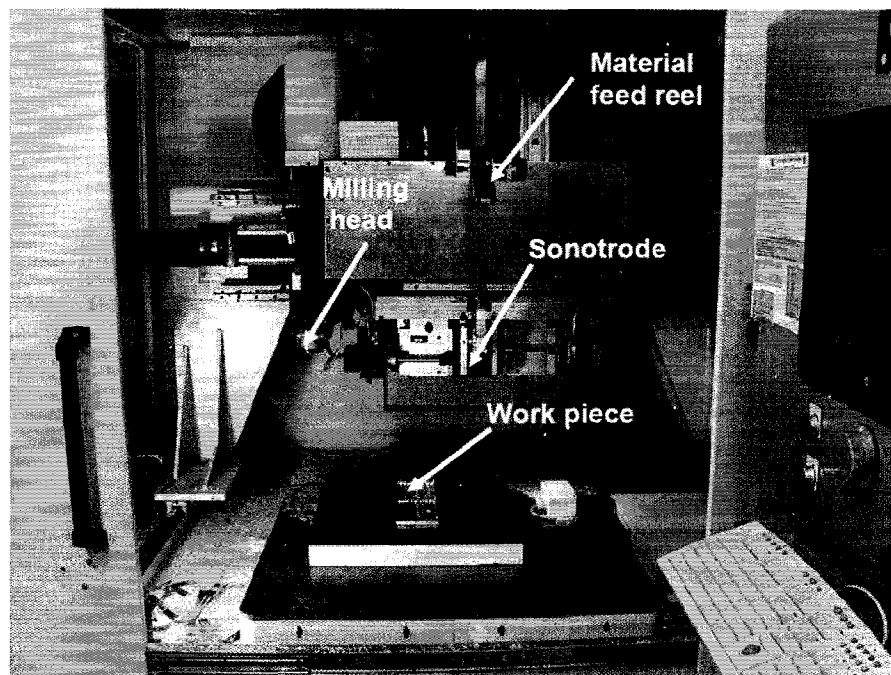
Fig. 6.4: Solidica Formation machine located at Utah State University

Other metal RP processes create near net shape parts which require secondary finishing operations, which can also damage embedded components. When embedding components, such as sensors, in a high temperature process, there are commonly delamination and other problems that arise due to thermal stresses from a mismatch in the coefficient of thermal expansion (CTE) and the large thermal gradients present (Li, 2000). UC produces metal parts at a temperature much less than the melting temperature of the build materials and only small thermal gradients are present, which help prevent induced stresses from CTE mismatches. Another advantage to embedding within a UC structure is that a much larger component can be embedded. The maximum envelope of a commercial UC apparatus is 24"x 36"x 6" (0.6mx0.9mx0.15m) with geometric tolerances of approximately $50 \mu m$ (the accuracy of the CNC milling gantry it is attached to). Both small and large components can be embedded as well as electrical connection leads or other devices so that an entire system can be created within a single structure.

6.2.3 Direct-Write (DW)

Direct-write is the ability to write or print passive or active electronic components (conductors, insulators, batteries, capacitors, antennas, etc.) directly from a computer file without any tooling or masks. In this research, DW describes a mechatronic apparatus for dispensing conductive media in the liquid phase on three-dimensional contoured substrates at ambient temperature and pressure (Church, 2000). Figure 6.5 illustrates a DW system in which a pneumatic pump forces liquid conductive ink (conductive particles in a resin binder system) through a syringe (Lopes, 2006). The syringe is attached to a 3-axis positioning system that is numerically controlled.

Advanced DW systems can automatically control the start and stop pressures to give very precise deposition as well as optical sensors to determine the exact height of the path (Church, 2000). The flow rate can be controlled by pressure, orifice size, viscosity, and the size of filler particles. In this research, conductive inks are used, which are generally conductive particles in a polymer resin binder system. Once the ink has been deposited, any solvent must be driven off, which is generally done by the use of heat from methods

EFD 2405 Ultra
Dispensing System
Control Console

Dispensing
syringe
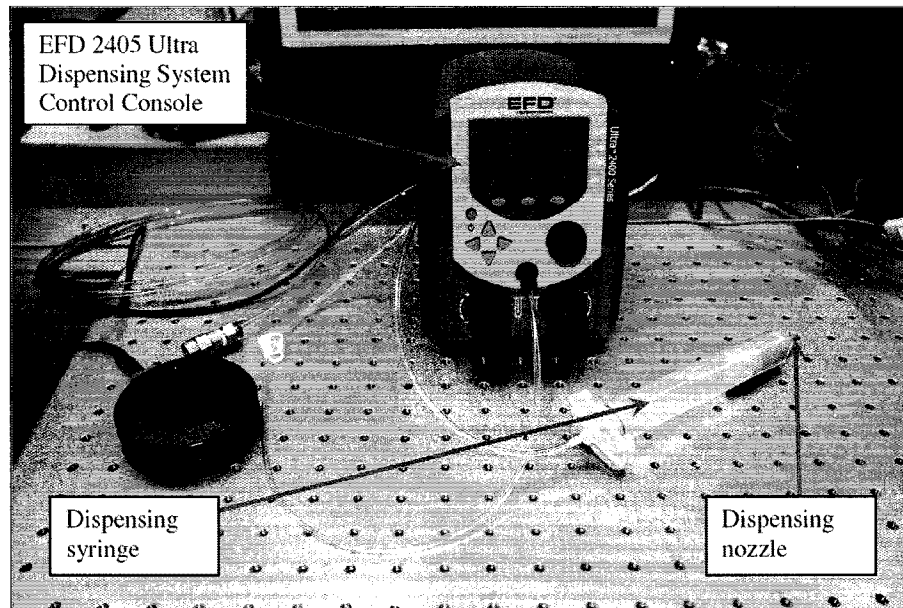
Dispensing
nozzle

Fig. 6.5: DW dispensing mechanism used at the University of Texas at El Paso

such as thermal annealing or localized irradiation, and the polymer resin binder system dries to a hard coating. Conductivity varies with the ink formulation and cure temperature (Palmer, 2005). After the ink has been cured, it is a collection of particles bound in resin and is generally very brittle.

6.3 Testing

As part of the new SAR design, one objective was to create an integrated structure rather than the "stack" of electronic cards and aluminum spacers shown in Figure 6.2. One important aspect of any design is to understand the design limitations inherent in the manufacturing processes that have been chosen. Although design and material constraints for many traditional processes, such as milling and injection molding, are well known, there are significantly different design benefits and drawbacks inherent in layered additive manufacturing processes. In particular, there is a significant lack of information on geometric and material performance constraints for both UC and DW. Thus an initial series of tests were required prior to finalizing the SAR design.

A common design feature utilized in many types of structures is a reinforcing rib. Due

to the fact that differential vibratory motion is necessary for bonding in UC, there exists an approximately 1:1 maximum height to width ratio (H/W) for an unsupported, freestanding rib. For supported structures (such as intersecting honeycombs or other patterns of ribs) H/W ratios can be greater than 10:1 (Robinson, 2006). For the SAR re-design, two types of rib-like structures were anticipated, overhanging tabs and hollow cylindrical supports. Thus, a series of experiments were performed to ascertain the ability of UC to create these features.

SAR redesign concepts included an embedded power divider card that has a copper coating on both the top and the bottom. It was unclear whether or not bonding would occur between the copper portion of the card and the aluminum consolidated on top of the card. To test the general capabilities of UC for multi-material bonding, a series of tests were performed and a detailed analysis of the results has been published elsewhere (Janaki Ram, 2006). An overview of this work as it relates to embedding the card used in this design is described below.

In addition to the design features mentioned above, a honeycomb-stiffened base was desired to maintain stiffness in the structure without a large mass penalty. The capability of UC to consolidate aluminum to the upper surface of honeycomb was also investigated and is published elsewhere (George, 2006).

The remainder of section 3 below overviews the specific tests that were performed in direct relation to this work on the ability of UC to create overhanging tabs, hollow cylindrical supports, and an embedded power divider in aluminum.

By using Direct-write technology to additively incorporate RF interconnects, advanced connections were envisaged to help alleviate misalignment issues that often occur in high frequency applications. The connections that needed to be made for the prototype design were the connection from the ground plane to each of the array cards, the connection between array cards and the power divider card and the connection between the output of the power divider card and the coaxial cable that transmits the signal outside of the enclosure. A number of tests on DW inks were performed and are explained below. These

tests included a determination of the electrical conductivity and mechanical properties of several candidate inks, as well as seep testing and an experiment to determine the ability of candidate inks to bridge structural gaps. All of this information was necessary to finalize the design of the SAR antenna array and its connections.

6.3.1 Overhanging Tabs

Overhanging features are features which have no support below them in the "z" direction (build direction) of a layered manufacturing process. UC can create limited overhangs, but they must be designed appropriately or they exhibit a lack of bonding. In early conceptual designs it was desired to have overhanging tabs to restrain array cards from moving or vibrating in the +z direction. Several methods for fabricating overhanging tabs were investigated. The first was to make a staircase-type support where each layer of UC material protruded slightly beyond the previous layer, with the longest tab being the portion that contacts the array cards and the shortest having very little overhang. Initial tests indicated that these tabs would not deflect, as desired for one potential design concept, but instead acted as a static support. Additional tests where the entire tab structure was made with all layers having the same cross-section proved to be more reliable for static supports. Figure 6.6

shows some of the tabs fabricated using both methods. It was observed that when fabricating the tab overhangs in UC, the protruding layers did not bond together to form a solid metal tab. This was due to the fact that previously deposited cantilevered layers were not constrained from vibrating during subsequent layer depositions. However, it was determined that the collection of cantilevered tabs was still sufficiently stiff to resist deflection when pressed against the array cards.

6.3.2 Hollow Cylinder Supports

A SAR antenna requires the antenna elements to be restrained accurately with respect to the other cards. As a restraint that would contact the face of each of the array cards, thin wall hollow cylinders were considered. The stability of such cylinders made using UC

Fig. 6.6: Tabs fabricated using a stairstep geometry (left) or a solid geometry (right)

was not known so testing was performed. Trials consisted of milling hollow cylinders with varying wall thickness from a thick section of consolidated material. The first attempt to create a cylinder with 0.25 mm wall thickness led to shear failure during machining in two of three cases. Other trials were performed using 0.5 and 1.0 mm wall thicknesses, which were both successful, Figure 6.7 shows some of the results of the testing.

One desirable design feature was to build these restraint cylinders on top of a honey-comb lattice. After forming the honeycomb, 6.35 mm of solid material was consolidated to the top surface of the honeycomb structure. The series of cylinders were then formed on the solid surface. The resulting specimens proved to be strong with good bonding between the cylinders and the facing, and between the facing and the surface of the honeycomb lattice, as shown in Figure 6.8.

6.3.3   Embedded Card

One major benefit when using UC is the ability to embed components. Early in the design stage it was determined that the power divider card could best be accommodated in the structure if it were embedded into the base of the structure. Testing of the embedded card consisted of making a pocket in an aluminum substrate, inserting the card so that the top of the card was slightly higher than the top of the pocket, and then consolidating aluminum to the base plate and across the top of the card. Welding parameters, including
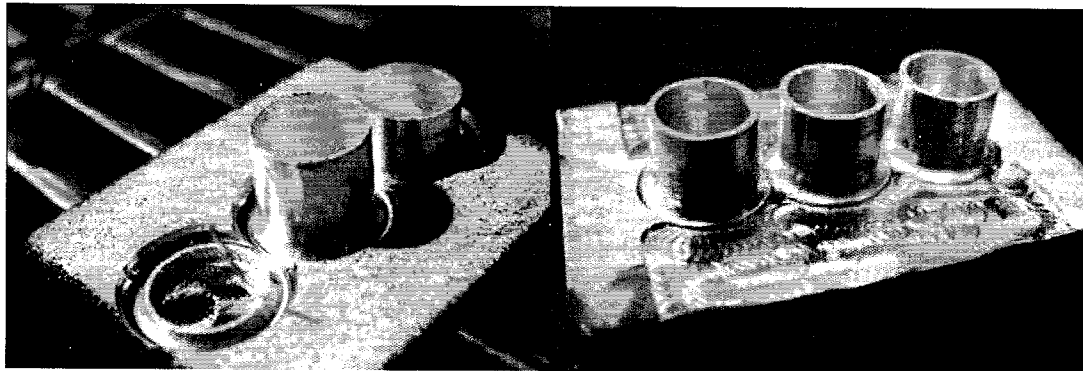
Fig. 6.7: 0.25mm cylinders (left) failed in shear while 0.5mm cylinders (right) were stable
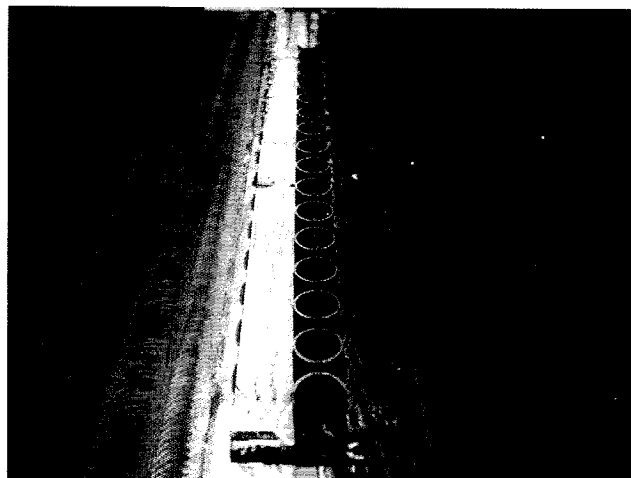
Fig. 6.8: Row of cylinders fabricated on top of a honeycomb lattice, with a thin facing in-between

speed, vibration amplitude, and the pocket depth, were adjusted in a series of tests. It was observed that typically the first five layers of aluminum above the card did not exhibit good bonding, but after the first 0.76 mm of aluminum, bonding began to occur over the top of the card.

In order to investigate the quality of the bond, the sample was cut perpendicular to the axis of the card. During cutting, the aluminum pulled away from the card, revealing that there was not a metallurgical bond between the structure and the copper coating on the card. The lack of bonding between copper and aluminum was attributed to the lack of stiffness in the power divider card, which is mostly Teflon®. Due to a large area of contact between the copper layer and the aluminum structure, however, the power divider card should be sufficiently electrically and thermally grounded. Figure 6.9 shows how the aluminum did not bond to the copper and some layers of aluminum did not bond together for certain conditions, even when the upper layers consolidated well.

6.3.4 DW Ink Conductivity Tests

A series of tests were performed at the University of Texas at El Paso to identify inks with suitable electrical conductivities for use in the SAR redesign. UTEP tested the inks
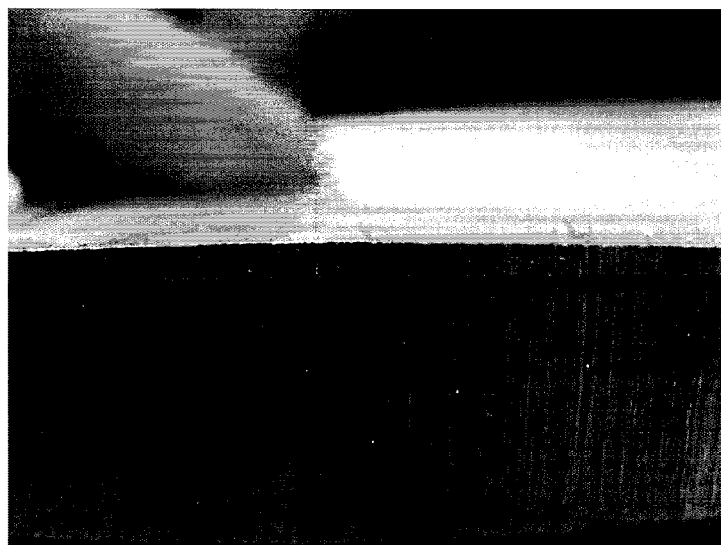
Fig. 6.9: This image shows an embedded card and some layers did not bond above the card

shown in Table 6.1. An ink dispensing experiment was carried out to select the ink with the minimum electrical resistivity and the best interconnection performance between the electronic components. The substrates used for this experiment consisted of a standard FR-4 board along with simple 3in x 3in x 0.25in (76mm x 76mm x 6.4mm) parts fabricated using stereolithography (SL) resin samples on the SL 250/50 machine. Isopropyl alcohol was used to clean the SL parts which were then post-cured in a UV oven prior to the DW process. A set of five 25 mm DW lines using a variety of inks were deposited on these substrates and cured at the recommended curing conditions (Lopes *et al.*, 2006).

There are many factors that can affect the conductivity of the ink, including the type of suspended particles, the type of polymer resin binding system, and the particle size. The substrates used for testing were a collection of UV curable resins. The results that were obtained are shown in Figure 6.10 (Lopes *et al.*, 2006). It was determined that the E 1660-136 silver ink was the best ink from amongst those tested. Parelec SDA 301 silver ink has a very low resistivity and has been used in various applications at Sandia, so this ink was also added after this for consideration in subsequent testing. Due to time and budget limitations, ink conductivity was not measured at RF/microwave frequencies. It is important to note that high conductivity/low resistivity at DC is not an indicator of high frequency performance.

6.3.5 Mechanical Strength of Interconnects

To connect the array cards to the power divider card, a special via connection was investigated. Fabrication of the via included inserting a pin into a pool of DW ink and then curing the ink to provide both a mechanical and electrical connection.

Table 6.1: Inks for the DW material performance study

Material Brand Name	Conductive Metal	Viscosity (CPS)	Cure Temperature
CI-1001 Silver conductive ink	silver	1200 cps @30 C	130 C for 10 min.
CI-1002 Silver conductive ink	silver	7500 cps @30 C	130 C for 10 min.
E1400 - 136	silver	15000 cps	138 C for 15 min.
E1660 - 136	silver	18750 cps	138 C for 15 min.
PT10-A	silver	12500 cps @30 C	110 C for 5 min.
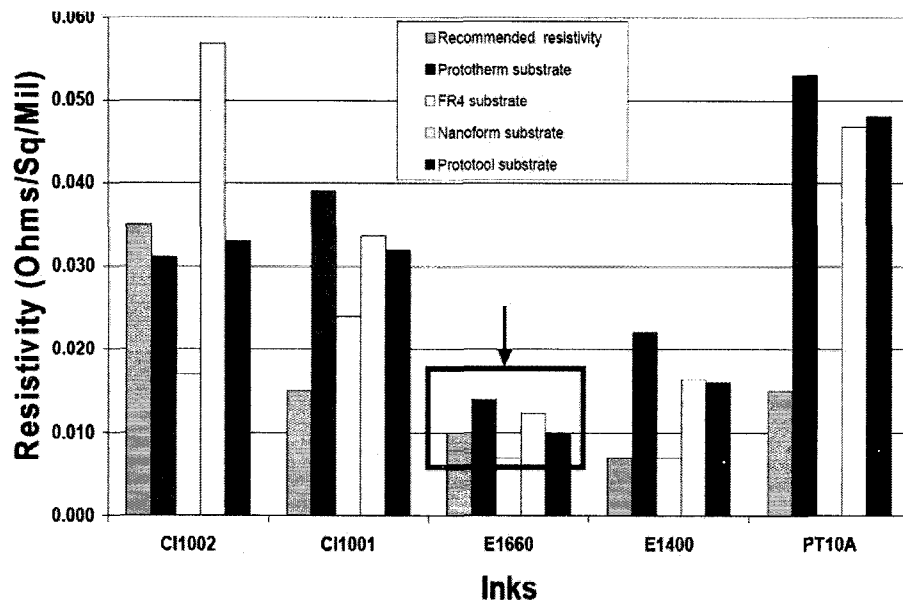
Fig. 6.10: Results of conductivity of DW ink testing performed at UTEP

The electrical signal would then pass from the pin, through the ink, and into the power divider card. More details on the design are discussed later in this paper. The primary benefit of this design was that it enabled assembly between a pin and cylinder under an acceptable degree of misalignment, as the ink could be used to fill the gaps. One concern with this design concept was the perceived brittleness of inks after curing. Tests were performed to test the strength of the bond between the inserted pin and the cured conductive ink. A test apparatus was designed in such a way that it could interface with a linear tensile test machine to grip the pin in one set of jaws and a platform containing the ink in the other set of jaws, as seen in Figure 6.11. Test specimens were fabricated using both the Parelec SDA 301 ink and the E1660-136 ink. The pull test results show that the E1660-136 outperformed the Parelec in regards to mechanical strength. To better assess the tensile strength of DW inks, a tensile strength comparison to the industry standard connection of solder Sn60/Pb40 was performed. Tensile test results for the solder connection clearly indicate a considerably stronger tensile strength (52 Lbf) as compared to any DW ink that
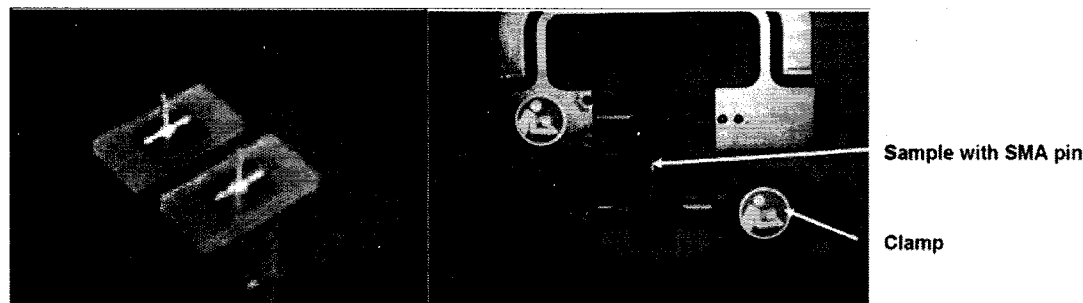
Fig. 6.11: (left) image showing the mounts for testing with pins inserted and (right) is a mount and pin in the testing apparatus

was tested (1.25 Lbf for SDA 301 and 2.6 Lbf for E1660 ink). These results are shown in Figure 6.12. Another concern was that the shrinkage of the ink during curing would cause holes in the ink, thus impeding signal flow. To investigate the shrinkage of the inks after curing, some specimens were viewed under a microscope and it was revealed that the Parelec material had a much greater shrinkage effect than the E1660-136 ink, as shown in Figure 6.13.

6.3.6   Seep Testing

Each of the array cards must be connected to a reflector plane at precisely the correct location. To do this, a slot for each card was designed into a housing which acts as the antenna reflector. In order to assemble the cards into the slots there must be some clearance. However, a gap after assembly would degrade performance. Therefore, this gap must be spanned by the DW ink. A series of tests were performed to ascertain if a gap within the UC machine tolerance could be spanned effectively with DW ink. Gaps of ranging in width from 0.05 to 0.09 mm were used for testing. To perform these tests, two plates were aligned next to each other and fastened into place using a thickness gauge and fasteners, shown in Figure 6.14. Ink was then dispensed over the gap and viewed under a microscope both before and after curing, see Figure 6.15 and Figure 6.16. The plates were then removed from the mounts and separated so that a cross-sectional view could be observed to determine the seepage depth. These tests were performed using both of the candidate inks. Again, the
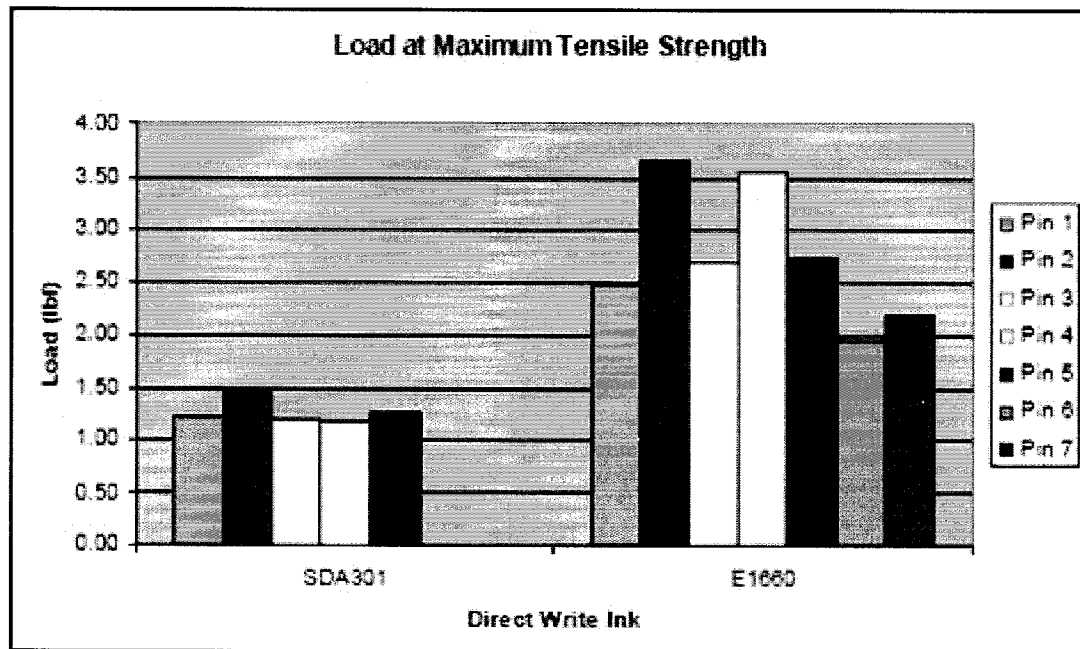
Fig. 6.12: Tensile test results for two DW inks
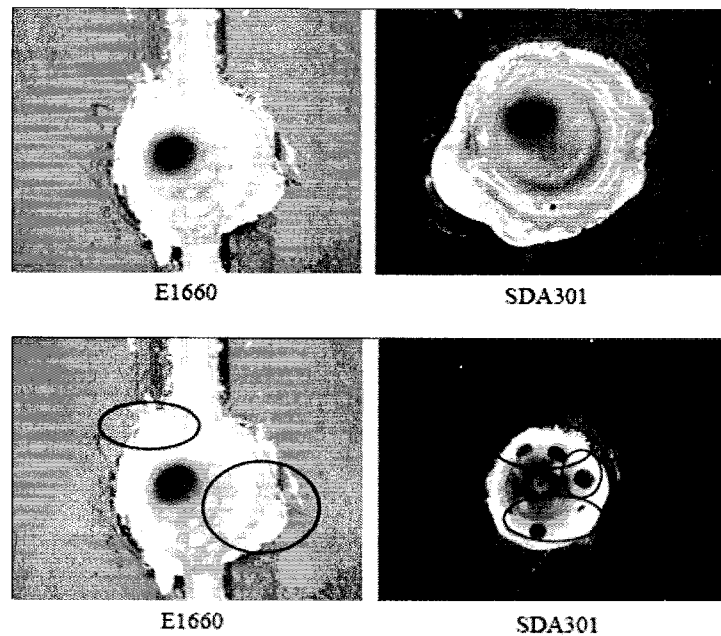
Fig. 6.13: Images showing gaps in material around a pin before (top) and after (bottom) curing
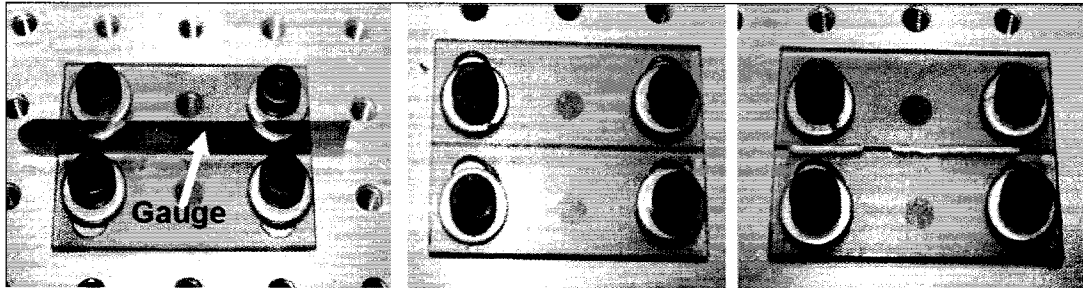
Fig. 6.14: Test setup for seep testing of DW inks

Top down image before curing

Top down image after curing

| 1.5 mil gap | 2.0 mil gap | 2.6 mil gap |
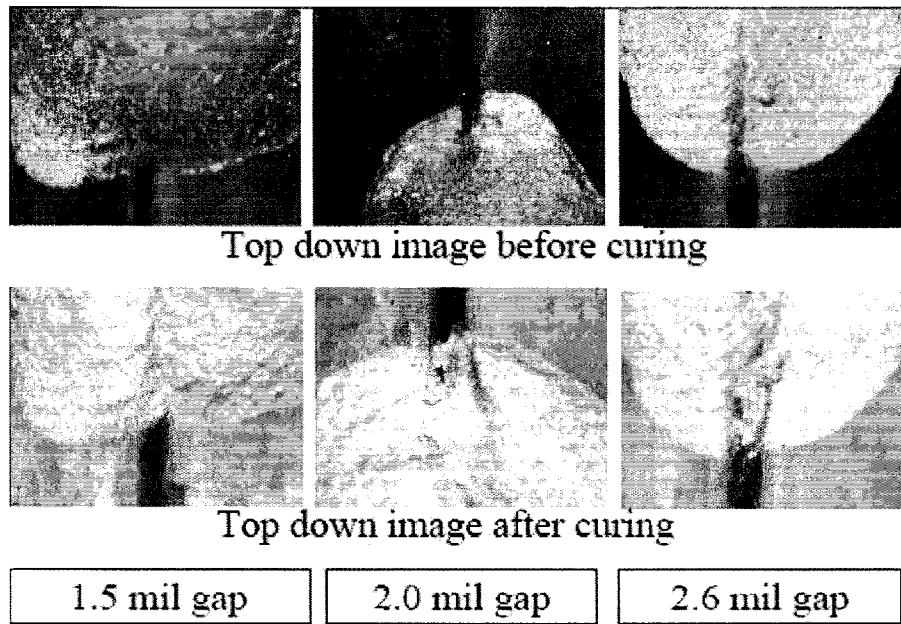
Fig. 6.15: E1660-136 ink deposited across gaps before (a) and after (b) curing (1 mil is equivalent to 25.4m)
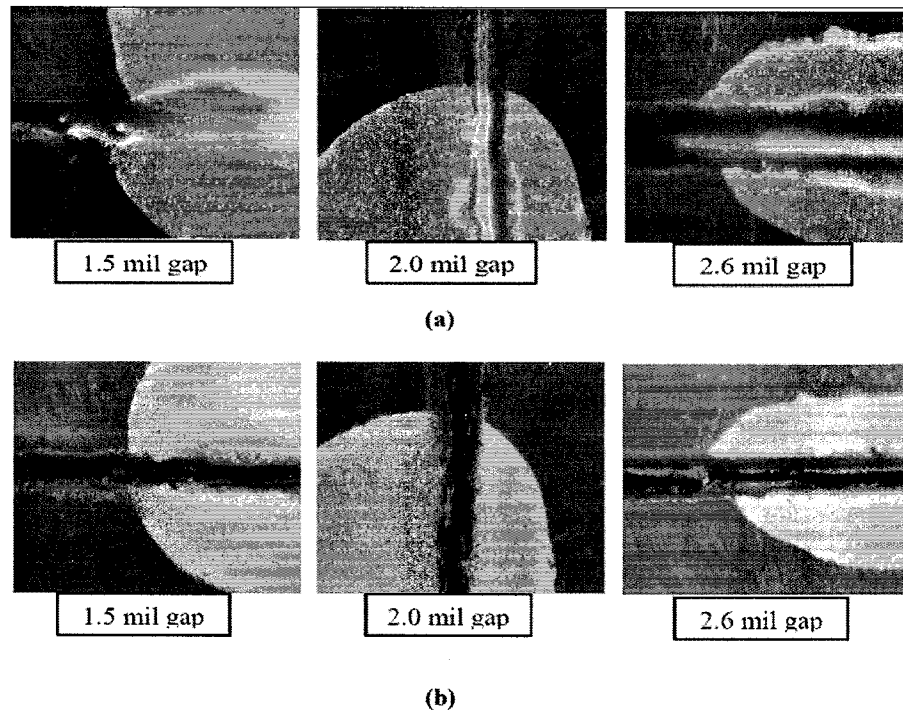
Fig. 6.16: Parelec SDA 301 ink deposited across gaps before (a) and after (b) curing (1 mil is equivalent to 25.4m)

E1660-136 ink showed more promise because it could span a wider gap with less seepage, as shown in Figure 6.17 and Figure 6.18. This is likely due to the size of suspended particles in the E1660-136 ink being much larger than those in the Parelec ink. For the connections that are required in this prototype design, it was determined that the E1660-136 ink would be the ink of choice.

6.4 Resulting Enclosure Design

The enclosure for the SAR antenna being considered in this research served a number of purposes. The first requirement was that it needed to hold 16 antenna cards and 1 power divider card rigidly in place. The enclosure also acts as a ground connection for each of the 17 cards, needs to house the RF interconnects, and provides the mounting mechanism for attachment to the main gimbals. In order to most efficiently meet all of the requirements of the enclosure, a structure that could incorporate as much functionality as possible into each
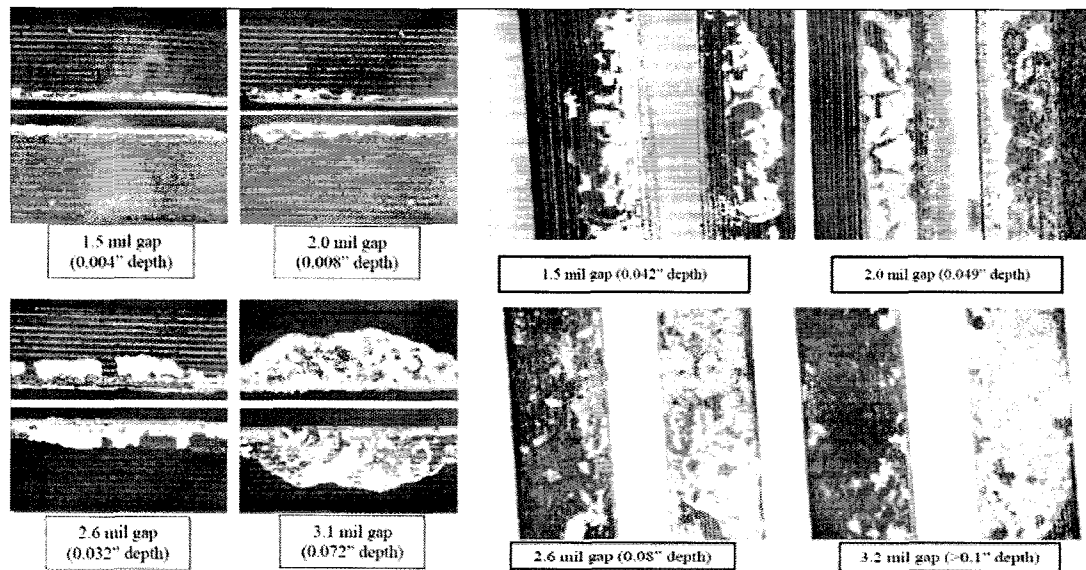
Fig. 6.17: Images showing seepage of E1660-136 (left) and SDA 301 (right) ink after curing (1 mil is equivalent to 25.4m)
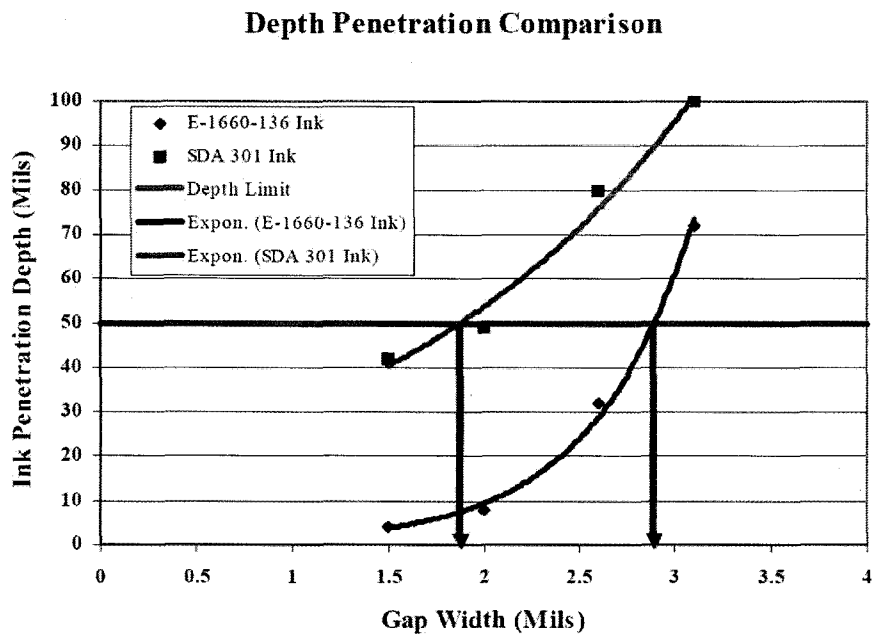
Fig. 6.18: Comparison of seep test results (1 mil is equivalent to 25.4m)

component was designed. A base portion was designed that would house and ground the power divider card, serve as partial support for all 16 array cards, house all interconnects, and provide a means for mounting to the gimbals. An upper portion of the box was designed to create the necessary ground connection for the 16 array cards, act as a reflector and fully support the array cards. A CAD model of the re-designed enclosure assembly is shown in Figure 6.19.

6.4.1 Honeycomb Base

The bottom of the base was designed so that fasteners could be used to mount the antenna to the gimbals. Sufficient depth was needed to house the interconnects between the array cards and the power divider card. In addition the base was designed to enable a connection between the output of the power divider card and other devices. This necessitated a bottom thickness greater than 3 mm. To reduce mass while meeting the stiffness requirements of the structure, a honeycomb base was designed with a cell pitch of 6.35 mm and wall thickness of 0.5 mm. The cell size was determined based on a tradeoff between fabrication time (due to milling tool size), mass and stiffness of the structure. The wall thickness was chosen as a value that could support the UC fabrication loads without buckling at the designed heights, but that would not create unnecessary mass penalties. This design can also be used to aid in heat transfer if the honeycomb structure is left open on both top and bottom, thereby creating a system of fins to convectively cool the structure. If the top and bottom are left open the stiffness of the structure is greatly reduced, but will still support the design loads. The base contains a slotted trench that acts as a guide location for the output coaxial cable. Figure 6.20 shows the CAD rendering and the UC fabricated honeycomb structure.

6.4.2 Truss Walls

The array card containment area is surrounded by a segmented wall with an internal truss structure for added stiffness. The innermost faces of the walls provide the material to be used as card restraints in three directions. The width of the wall was driven by the
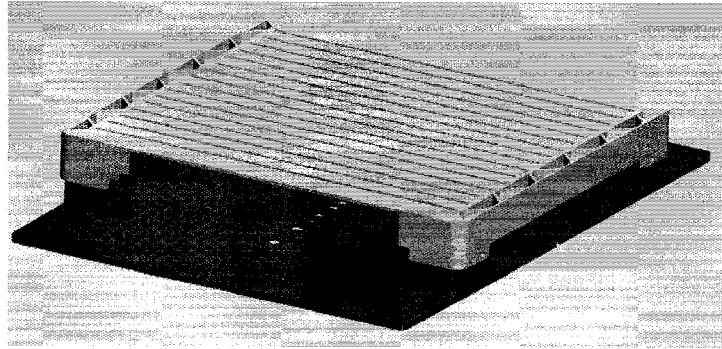
Fig. 6.19: CAD graphic of UC enclosure

Pocket for embedded
power divider card

Coaxial cable channel
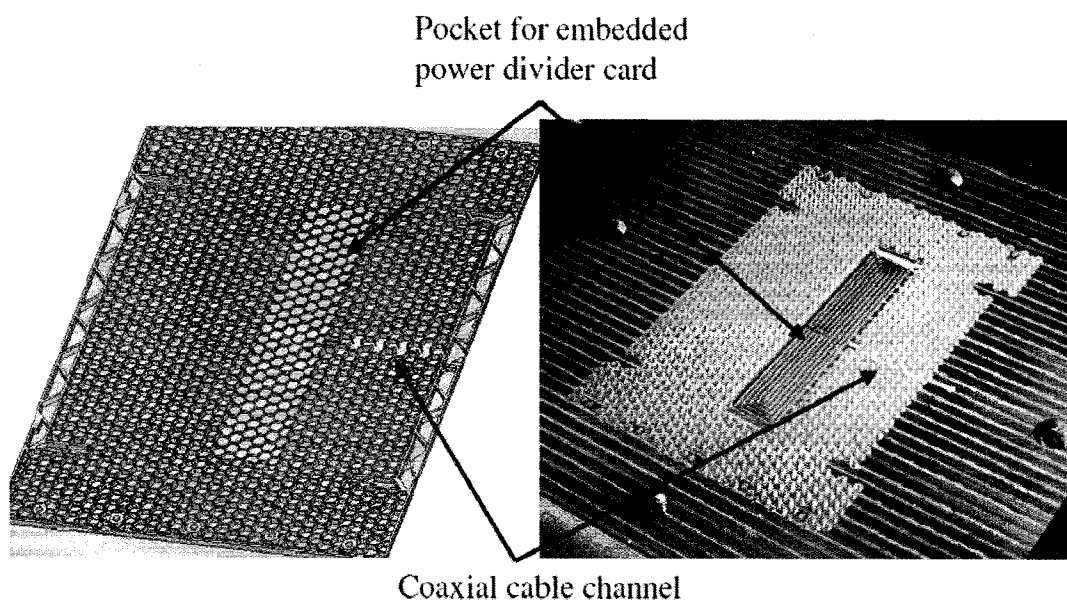
Fig. 6.20: (Left) CAD model of honeycomb base and (right) actual honeycomb base

need to provide strength for connector attachment, as well as the UC build capabilities for thin walls. A truss structure was chosen rather than a honeycomb structure because, for the chosen geometry, milling tool sizes and required stiffness, a truss structure resulted in a large mass benefit over honeycomb. The internal trusses saved space by eliminating the need for external ribs. Figure 6.21 shows a section of the truss walls as designed for this prototype.

6.4.3 Array Card Supports

The array cards must be supported and restrained from movement. Airy support theory was used to develop locations for the restraints that would minimize deflections in the cards. Minimizing deflections induced by assembly is a major design issue in high frequency RF applications as any deflection or misalignment will cause losses. To support the cards in the +x and -x directions, half cylinder supports were provided at the ends of the cards to create a line contact, as shown in Figure 6.22. Along the length of the cards there were two cylindrical supports to hold each card in the + y and two in the - y directions. These cylinders protruded 6.35 mm from the bottom of the structure and contact the face of the cards along a tangent line. These cylinders are separated by 0.538 times the length of the card L, as specified by Airy design. Each set of two cylinders contacts a card face on two sides. To restrain the cards in the - z direction there are two triangle supports located directly between the cylinder supports, which creates an effective point contact to minimize deflection, as shown in Figure 6.23. The restraint in the +z direction is incorporated into the upper portion of the box. Along the half cylinders, which act as x supports, there are overhanging tabs that contact ears on the antenna cards and cause an elastic deflection of 0.05 mm in the ear of the card to ensure a solid restraint. The ears on the cards were designed such that the ear will deflect 0.05 mm well before the entire card will have any deflection. This helps alleviate problems with tolerance errors in the fabrication process.
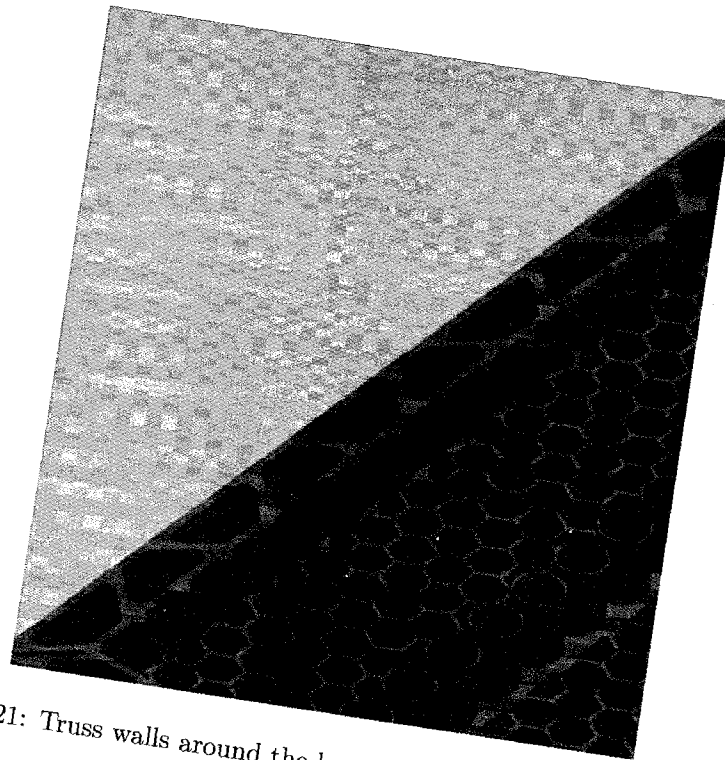
Fig. 6.21: Truss walls around the base and top of the UC enclosure

Half cylinders for support in +/- x

Hollow cylinders for support in +/- y

Embedded Power Divider card
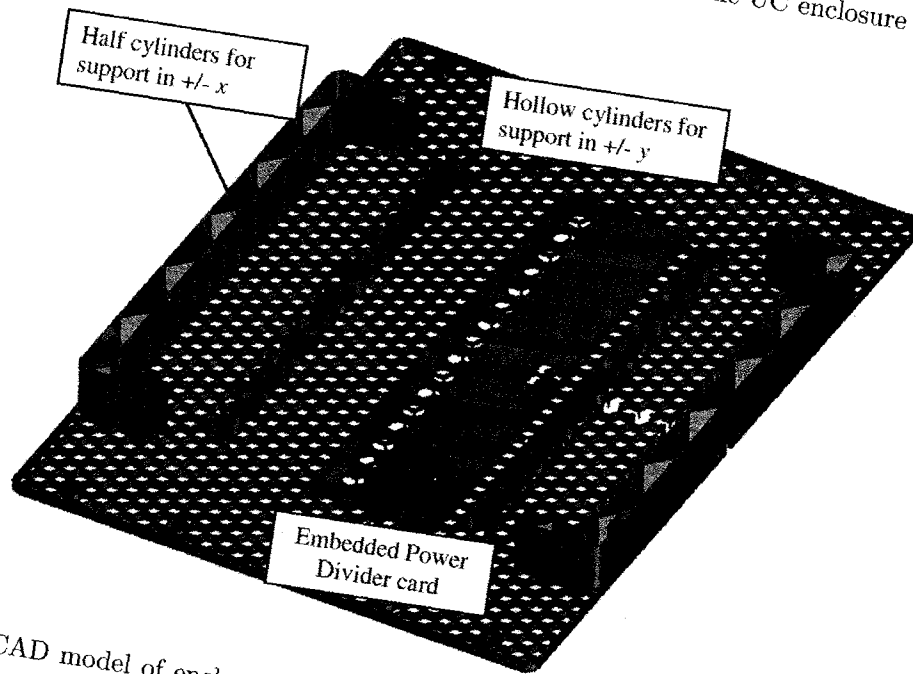
Fig. 6.22: CAD model of enclosure base showing restraints and material covering an embedded power divider card
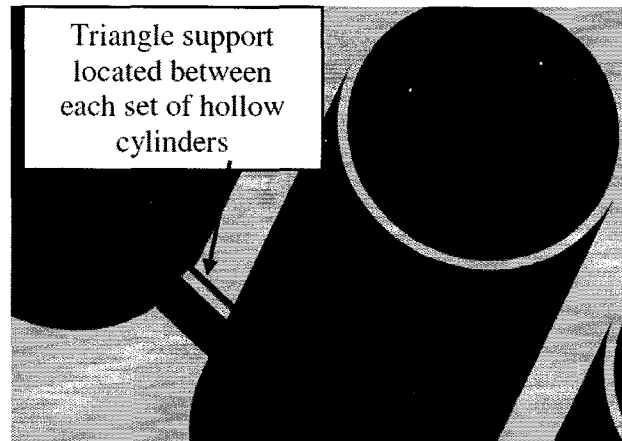
Fig. 6.23: Triangle supports are located between each set of hollow cylinders

6.4.4 Embedded Power Divider Card

One feature of the prototype design that utilized the unique benefits of additive manufacturing is the embedded power divider card. When receiving data this card takes the signals from each of the antenna cards and combines them. Some elements that had to be considered when embedding this card were that the card must not experience any induced deflection and both the top and the bottom of the card need to be well grounded to the structure to create the appropriate stripline connection. A pocket is incorporated in the honeycomb that is larger than the spine card; this can be seen in Figure 6.24. The general build temperature for UC is $300°$ F so the Teflon® in the card expands to fill the pocket, creating a very snug fit. The pocket for the card was designed slightly shallower than the thickness of the card to create an intimate connection between the aluminum and the ground plane of the power divider card. The build is continued by consolidating aluminum layers directly on top of the pocket and the embedded card. The overlying aluminum layers include sixteen ports or vias corresponding to holes in the upper portion of the card. The holes expose the ends of the 16 traces comprising the power dividing network, shown in Figure 6.25. The overlying UC layers are designed to be 1.78 mm high. Following encapsulation, small Teflon®spacers are pressed into the holes. This creates a receptacle for the DW ink and pins described previously.
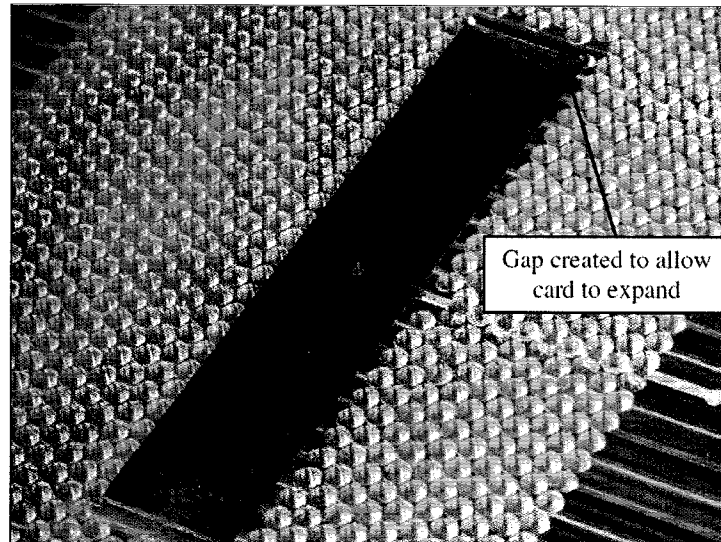
Fig. 6.24: Power divider card being embedded into UC fabricated base
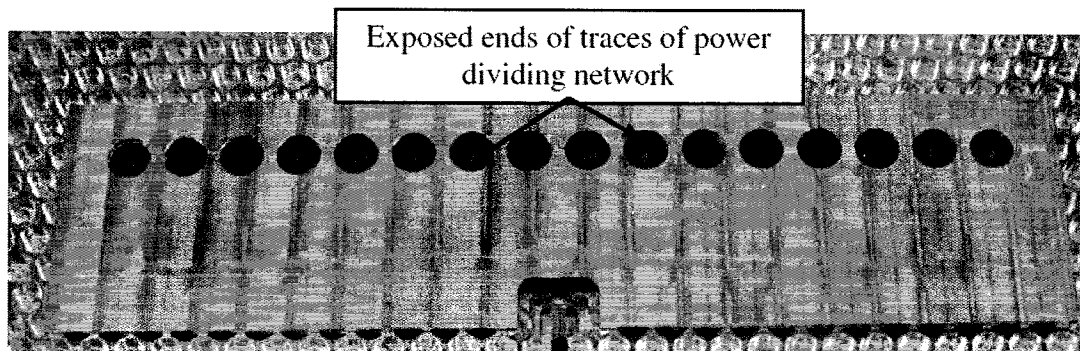
Fig. 6.25: After the card is embedded material is removed to reveal ends of traces that make up the power divider network

6.4.5 Slotted Reflector Plane

The final portion of the enclosure is the upper portion of the box that contains the reflector plane. This plane must be positioned such that each antenna element has no ground directly behind it, but that the ground connects right at the base of the element to create the stripline connection. To accomplish this, the reflector plane was designed with 16 slots which are held to very tight tolerances so that the cards slide in with very little play (Figure 6.26). This is necessary so that DW can be used to make a final connection, as discussed previously.

6.5 Connection Design

The connections that needed to be made for the prototype design were the connection from the ground plane to each of the array cards, the connection between array cards and the power divider card and the connection between the output of the power divider card and the coaxial cable that transmits the signal outside of the enclosure.

6.5.1 Ground Plane Reflector Connection

Each array card must be grounded to the enclosure with a line contact along the entire length of each card, due to the small wavelengths being transmitted. The height of the ground plane with respect to each of the individual antennas is very important and tight tolerances must be maintained. A slot in the UC ground plane (Figure 6.26) allows the cards to pass through with very little clearance. Once the antenna is assembled, DW inks are used to bond the ground plane to the array cards, maintaining accuracy in the height of the connection, and ensuring there is no conductive material directly behind the antenna elements, as shown in Figure 6.27.

6.5.2 Power Divider Card Connection

The connections between the antenna cards and the power divider is problematic, as there are two striplines that are twisted 90 degrees from each other that need to be connected. If you simply match the two striplines then you end up with a point contact,
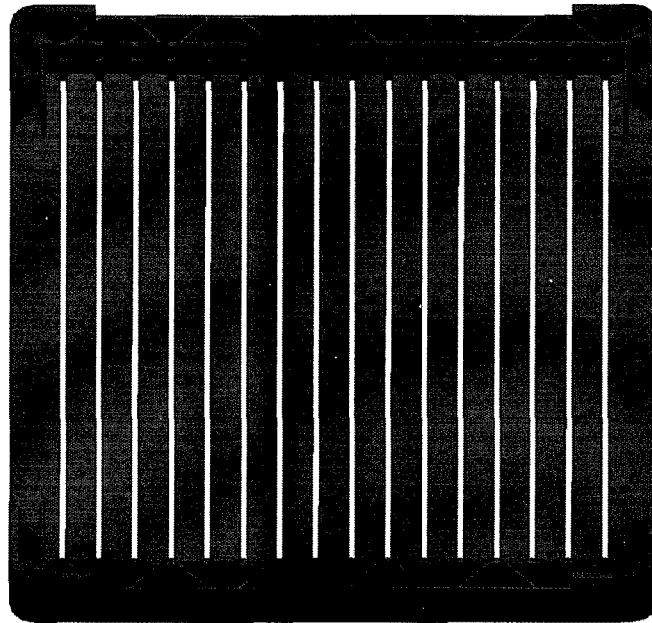
Fig. 6.26: Upper portion of the enclosure contains restraints and channels for array cards

DW ink is used to connect the array card and the reflector plane.
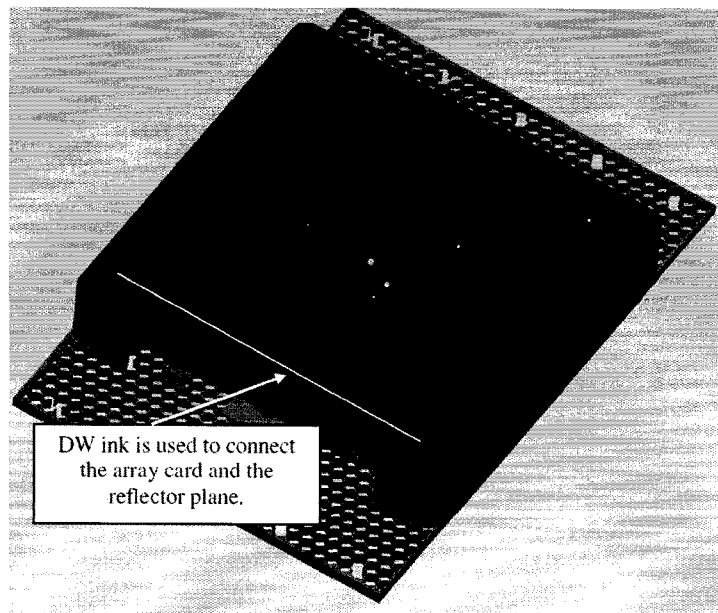
Fig. 6.27: Assembled antenna must have DW ink applied to the upper surface to complete the ground connections

which causes major radiation losses. The rotation must be made gradually so as to reduce signal loss. This requires the conductive portion of a bend to be thin so that the path length between the bottom and the top of the bend are not mismatched. For this prototype design a stripline to coax to stripline connection was chosen. This connection is made through the creative use of a pin and DW conductive ink. A pin was designed that can be directly applied to the stripline on the output of each of the antenna cards with a very thin tab being sandwiched into the array card. The pin gradually fans out into a cylinder so that the signal is able to travel directly through the middle of the pin and the transition is smooth from strip to cylinder. The pin has a head on the end opposite the tab to act as a mechanical support and a large area connection point to connect to the stripline in the power divider card. Directly outside of the pin there are holes or cavities filled with conductive ink that are lined with a Teflon® spacer that has the appropriate thickness to match the impedance of the stripline. The spacer is tightly pressed into the ultrasonically consolidated aluminum directly above the embedded power divider card. The aluminum structure provides the shielding, resulting in a coaxial connection fabricated using UC and DW. Due to the geometry of this connection losses have been greatly reduced.

Another source of losses is mechanical misalignment. In this design this is alleviated by positioning the pin into the DW conductive ink before the ink is cured so that even if there is some misalignment, there is little or no effect because the pin is in place before solidification occurs. Figure 6.28 depicts this connection.

6.5.3 Output Connections

The final connection required in this prototype design is that of the output from the power divider card to a coaxial cable to be used to exit the prototype. For this connection a piece of semi-rigid coaxial cable was chosen that has a conductor along the outside that will be grounded to the UC base. This semi-rigid cable is also connected to an SMA connector that is directly attached to the outer edge of the base. The connection to the power divider card is where DW ink is useful. This is a connection similar to a solder joint except that the tolerances are small and the DW ink can be applied in very thin layers to allow a matching
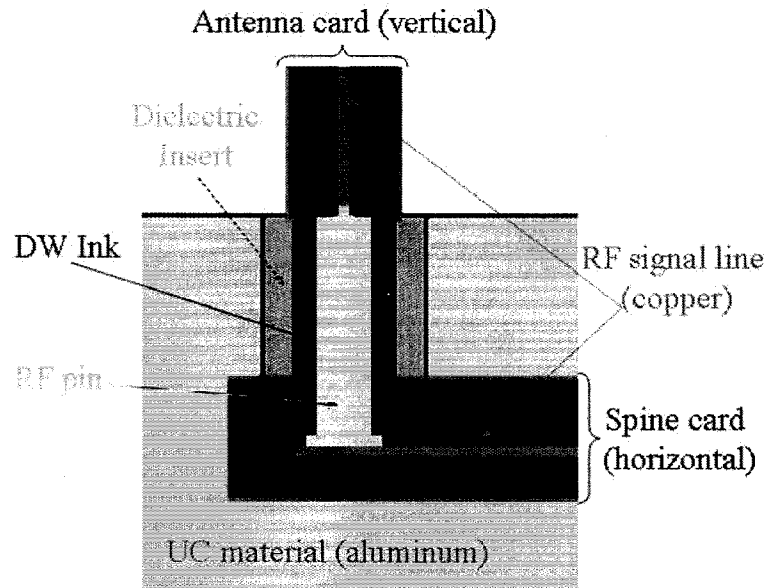
Fig. 6.28: This depicts the pin via to connect array cards to the power divider

of impedance at this point by applying an insulator and then another layer of conductor connected to ground.

6.6 Final Enclosure Fabrication

A prototype of the UC enclosure was fabricated to demonstrate the ability to rapidly manufacture the designed enclosure in an additive manner.

6.6.1 Upper Portion Fabrication

The upper portion of the enclosure, which includes the reflector plane, the channels for the cards to slide through and the tabs that act as + z restraints, was fabricated first. The channels for the array cards were machined directly into the base plate. The walls were built by depositing sufficient material to contain the walls of the structure (two solid walls that were each wide enough to contain the entire side wall within the deposition area). These were built up until the height of the tabs was reached. At this point, part of the geometry of the walls was milled (based on features that could not be milled after

89

completion of the wall). Then a subsequent set of solid layers were deposited above. Once the final wall height was reached, the complete wall geometry was milled, creating the half cylinder supports, the overhanging tabs and truss walls. Finally the build was removed from the UC machine and a separate milling machine was used to remove the enclosure from the substrate. Figure 6.29 shows the top portion of the enclosure.

6.6.2 Base Fabrication

The base of this structure integrates almost the entire functionality of the antenna, including the structure, fasteners and interconnects all into one monolithic part. The manufacturing began by milling a honeycomb pattern into the base plate of aluminum material. The pocket for the power divider card and a channel for the coaxial cable were milled into the honeycomb. The power divider card, which was at room temperature, was placed into the pocket, at 150° C, and the process was paused to allow sufficient time for the card to heat and expand. Aluminum was consolidated across the surface of the base and the card, as seen in Figure 6.30. Solid material was added to a height of 1.8mm, and then holes were machined for the interconnects between the array cards and the power divider card. These holes were machined to a very precise depth so as to expose the electrical connections on the power divider card without damaging it. A cutout was also created for the output from the power divider card to connect to the coaxial output cable. More material was then consolidated across the base, with the exception of the area directly above the power divider card. This was built up to 6.35mm and then the profiles of the cylinders were created and the cylinders were partially hollowed for mass reduction. Along the outer edges of the base, additional material was consolidated to reach the height necessary for creation of the half cylinder supports along the walls, which were then machined. The walls were also hollowed out to form the truss structure. This series of steps and the finished assembly are shown in Figures 6.31 through 6.34.
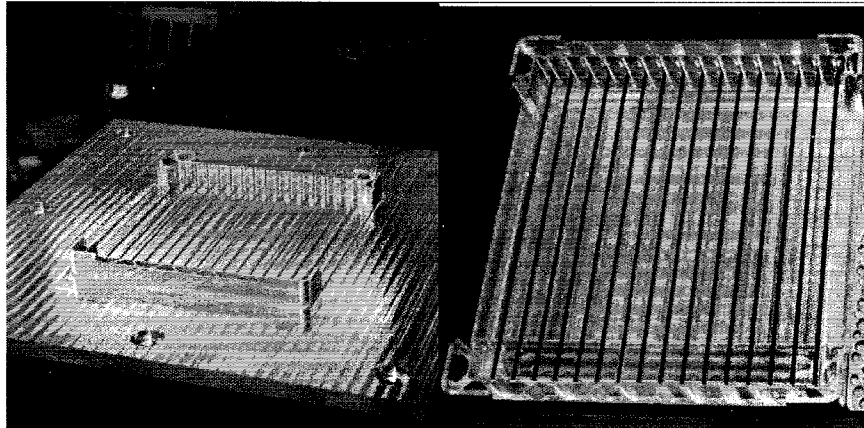
Fig. 6.29: Top portion of the UC fabricated enclosure before (left) and after (right) removal from the substrate
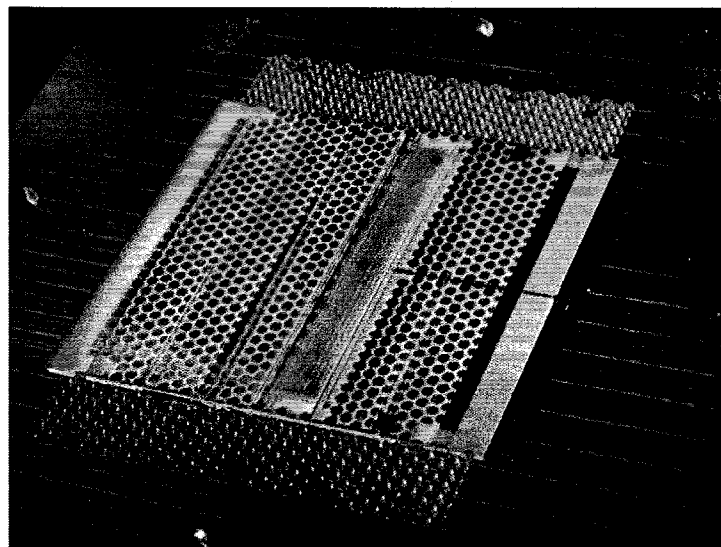
Fig. 6.30: Aluminum tapes have been consolidated across the honeycomb base and the embedded power divider card

6.7 Future Work

Although the structure has been successfully fabricated, a working SAR antenna has not been assembled. Array cards must be inserted and the DW connections must be made and tested to ascertain the performance of the design. It is expected that this design will perform comparably to or better than a traditionally manufactured antenna.
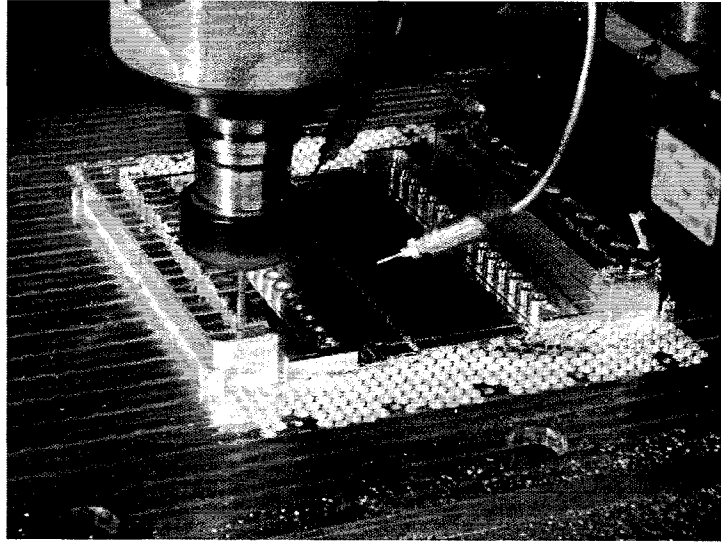
Fig. 6.31: A milling operation to create half cylinder supports in the base of the enclosure
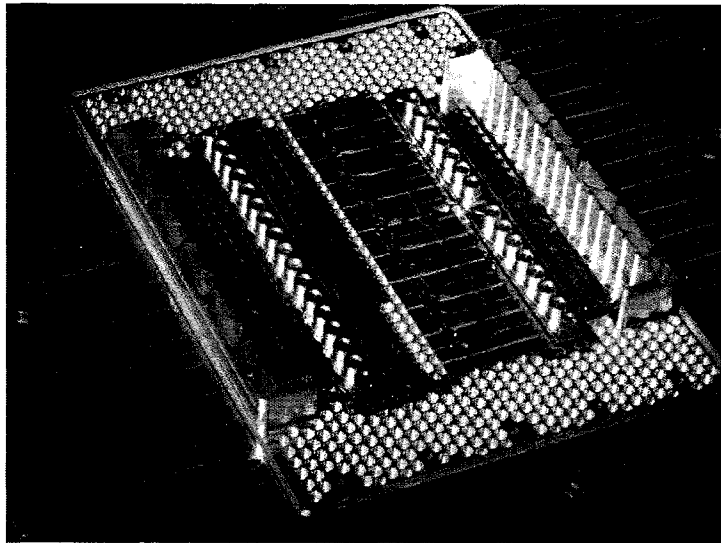
Fig. 6.32: Base of the UC enclosure before being removed from the substrate
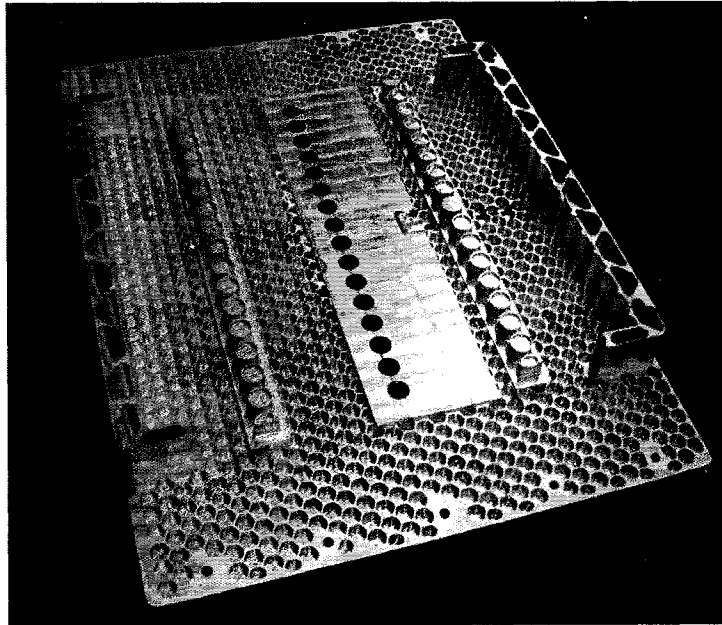
Fig. 6.33: Base of the UC enclosure after being removed from the substrate
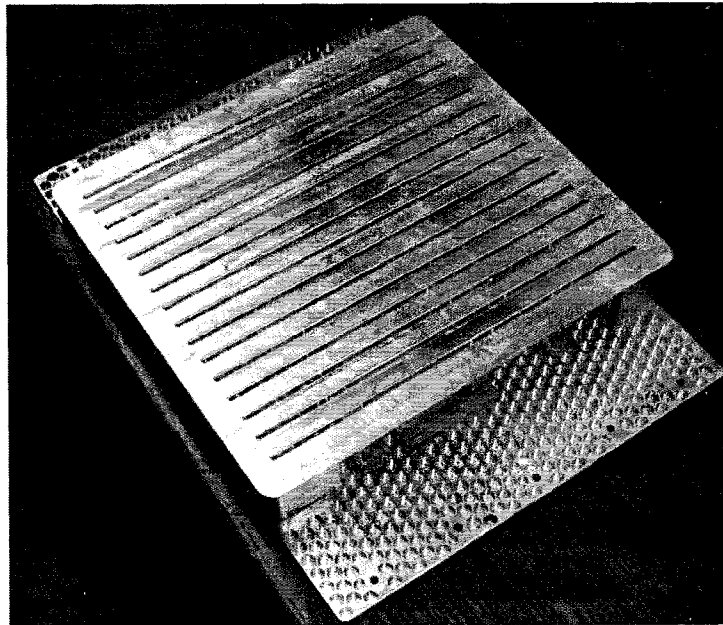
Fig. 6.34: Top and bottom portions of the enclosure assembled

Future research will investigate "plug and play" connections where cards can be inserted and removed as desired for modifications or replacement. This would be an entirely new approach to SAR design.

The development of a support material that can effectively be used in conjunction with UC would create the possibility of fabricating a structure that does not have a top and bottom portion, but that is created as a single structure. Although this would not work with the "plug and play" idea mentioned above, there may be other structural and alignment benefits of unitizing the structure.

Lastly, additional studies on DW inks should be performed to determine the performance of the identified inks at high frequencies.

6.8 Conclusions

By marrying the technologies of UC and DW, a prototype SAR antenna has been designed and fabricated. The enclosure is designed to be fabricated using UC and the enclosure acts as a housing for all interconnects, which are created using DW. The design includes many features which are difficult or impossible to manufacturing using traditional techniques, such as an embedded power divider card, internal honeycomb structures and channels, as well as overhanging tabs. The use of additive manufacturing facilitates the fabrication of interconnects that can reduce losses through proper shielding and grounding as well as making smooth transitions and eliminating misalignment issues. The structure has been fabricated and has demonstrated the capability of the UC process to fabricate complex multi-functional structures.

References

Church, K. H., Fore, C., and Feeley, T., "Commercial Applications and Review for Direct Write Technologies," Materials Development for Direct Write Technologies, **624**, pp. 3-8, 2000.

Daniels, H. P. C., "Ultrasonic Welding," Ultrasonics, pp. 190-196, October-December 1965.

George, J. L., and Stucker, B., "Fabrication of Lightweight Structural Panels through Ultrasonic Consolidation," Virtual and Physical Prototyping, 1 (4), pp. 227-241, 2006.

Janaki Ram, G. D., Robinson, C., and Stucker, B., "Multi-Material Ultrasonic Consolidation," Solid Freeform Fabrication Proceedings, 2006.

Kong, C. Y., Soar, R. C., and Dickens, P. M., "An Investigation of the Control Parameters for Aluminum 3003 under Ultrasonic Consolidation," Solid Freeform Fabrication Proceedings, 2002.

Kong, C. Y., Soar, R. C., and Dickens, P. M., "Optimum process parameters for ultrasonic consolidation of 3003 aluminium," Journal of Materials Processing Technology **146**, 2004, pp. 181-187.

Kong, C. Y., Soar, R. C., and Dickens, P. M., "Ultrasonic consolidation for embedding SMA fibres within aluminium matrices," Composite Structures, **66**, 2005, pp. 421-427.

Li, X., Golnas, A., and Prinz, F., "Shape deposition manufacturing of smart metallic structures with encapsulated sensors," Proceedings SPIE, **3986**, pp. 160-171, 2000.

Lopes, A., Navarrete, M., Medina, F., Palmer, J., MacDonald, E., and Wicker, R., "Expanding Rapid Prototyping for Electronic Systems Integration of Arbitrary Form", Solid Freeform Fabrication Proceedings, 2006.

Palmer, J. A., Summers, J. L., Davis, D. W., Gallegos, P. L., Chavez, B. D., Yang, P., Medina, F., and Wicker, R. B., "Realizing 3-D Interconnected Direct Write Electronics within Smart Stereolithography Structures," Proceedings of the 2005 ASME International Mechanical Engineering Congress and Exposition, IMECE2005-79360, 2005.

Robinson, C. J., Zhang, C., Janaki Ram, G. D., Siggard, E. J., Stucker, B., and Li, L., "Maximum Height to Width Ratio of Freestanding Structures Built Using Ultrasonic Consolidation," Solid Freeform Fabrication Proceedings, 2006.

Sandia National Laboratories Radar [online]. Available from http://www.sandia.gov/ RADAR/images/SAND2005-3445PMiniSAR-fact-sheetp2-v4-redo.pdf [accessed December, 2006]

Sandia National Laboratories Radar [online]. Available from http://www.sandia.gov/ RADAR/whatis.html [accessed December, 2006]

White, D. R., "Ultrasonic Consolidation of Aluminum Tooling," Advanced Materials and Processes, pp. 64-65, January, 2003.

Chapter 7

Conclusions and Future Work

7.1 Conclusions

Defense as well as other industries are interested in improving the functionality and feasibility of imaging devices such as SARs. To facilitate the use of a SAR in applications such as for an unmanned aerial vehicle (UAV), the size and mass of the SAR must be greatly reduced over the current designs. It has been demonstrated that great improvements can be made through the use of additive manufacturing techniques. Through the use of UC and DW a prototype SAR antenna array has been fabricated to demonstrate the enhanced capabilities of using additive manufacturing.

7.1.1 Tall Structures

Due to the newness of the UC process there was much testing and initial analysis that had to be performed in order to develop a set of guidelines that could be used to direct the design of the SAR prototype. Guidelines that have been developed for assistance in design and fabrication of integral structures is contained in Appendix C. The testing showed that in freestanding structures there is a height to width ratio (H/W) limit of 1:1 for UC structures. If this ratio is to be exceeded the structures must either be supported such as in a honeycomb configuration or else the fabrication process must take into account the design constraints and then the 'build up' and 'machining' operations must be ordered in a way to allow a H/W of greater than 1:1. Through modeling it appears that the 1:1 ratio is both material and parameter dependent, so variations in material or welding parameters would likely alter the maximum H/W. It was also shown that in general, ribs oriented at a 45 degree angle to the building direction will have a higher weld density and they have a higher maximum H/W than other orientations. In patterns such as honeycomb, a more

effective bond will be produced when the ribs are not oriented parallel to the direction that the tape is being laid.

7.1.2 Multi-material Fabrication

Other testing demonstrated that there is a possibility of welding various materials to aluminum, which could enhance the structural stiffness, strength and rigidity. The multi-material bonds could also be used to increase the connectivity for bonds between the ground plane of an antenna and the base structure.

7.1.3 DW-UC Integration

The additive manner in which parts are built as well as the ability to pause the UC process during fabrication, makes embedment of new features a straightforward process. In this work a design for a type of RF interconnect that can be built by integrating UC and DW together has been developed. These interconnects can alleviate some of the losses incurred when transmitting high frequency signals from one stripline conductor to another stripline conductor that are twisted 90 degrees from each other. For general applications it was observed that conductive traces can effectively be embedded into a UC structure and that the UC fabrication process did not produce adverse effects on the conductivity of the cured ink. DW was used to print a high frequency RF patch antenna, but it was determined that although the antenna operated appropriately, losses were incurred as compared to commercial antenna fabrication techniques and materials. DW ink was also tested and proved to be useful as a mechanical connection in some situations where a highly conductive connection is desired.

7.1.4 Advanced Thermal Control

It has also been demonstrated that thermal control devices such as a heat pipes could be integrated directly into the structure of the SAR to assist in heat transfer and allow the SAR to operate for greater lengths of time and under adverse conditions. Attempts were made to fabricate a working pulsating heat pipe directly into the structure, but success

was not achieved. However, the embedment of prefabricated heat pipes was quite easily achieved.

7.1.5 SAR Design

Based on results from experiments related to building tall structures, multi-material bonding, embedding components, embedding circuitry, integration of DW and UC, integral functionality, thermal control, and complex geometry, a final design was prepared for the fabrication of the enclosure of a MiniSAR antenna. This enclosure featured the use of UC and DW to create a very lightweight structure that could effectively house the antenna elements while providing the necessary ground and restraint system for the antenna. Features included a honeycomb base, truss reinforced walls, an Airy type minimum deflection restraint system, overhanging restraint tabs, embedded circuitry and embedded components. The UC enclosure was fabricated and prepared for integration into the entire antenna array system. Fabrication of this multi-functional metal prototype provided sufficient evidence that UC can be used to manufacture a SAR enclosure.

7.2 Future Work

The work presented in this thesis has provided considerable information related to UC and DW manufacturing limitations in general and SAR design in particular. However, there is still a considerable amount of work that could be done to fully characterize these processes and this application. Some suggestions for future work follow.

7.2.1 H/W of UC Structures

The study conductive on maximum H/W of freestanding structures involved the general parameters for UC fabrication, but did not focus on specific aspects of the process. Milling parameters should be optimized to reduce the effect of machining-related defects on rib failure, so that welding-related effects could be studied more carefully. Ribs could also be built with no machining beyond the first level so that the machining effects are eliminated within most of the rib. Additional ribs should be fabricated and cross-sections of each rib

should be taken at 0, 45, and 90 degrees from the axis of the rib. Ribs could also be built at more orientations to develop additional information. Identical ribs should be built with varied parameters to determine the effects of welding parameters, especially the amplitude of vibration. The validity of the 1:1 ratio with various materials should be explored both experimentally and analytically. A more in-depth exploration of patterns of ribs such as honeycomb and the effects of filler materials should also be performed.

7.2.2 Multi-material UC

The work contained in Appendix A, constitutes additional work in the area of multi-material part fabrication. This work did attempt to optimize parameters, but attempted to determine which materials could be consolidated with the optimal parameters for aluminum. Further work should be commenced to optimize the welding parameters, along with testing on a much larger number of sample materials. Further work looking into the microstructural and microchemical properties of the bonded regions is also advised. More effective methods of second material deposition could be researched and integrated to create a more complete study of multi-material bonding.

7.2.3 DW Ink

There are many variations of conductive inks that can be used in a DW technique and even more can be developed. A careful study of various DW inks should be performed in which the inks are tested with high frequency RF signals. A more in depth look at the material properties and curing of the DW inks is also advisable. The connections that were designed for the SAR antenna should be tested and compared with other connection techniques that could be utilized. More effective methods to deposit the insulator material surrounded electrical traces should be explored. The development of an integrated machine should be pursued.

7.2.4 Thermal Control

In this work, the main objective was to find a method of integrating a thermal control

device into a structure. However, a more detailed study on embedding pre-fabricated heat pipes and optimal orientations and sizes should be pursued. The fabrication of integral heat pipes is an area for additional work that could greatly impact the usefulness of UC. A method for embedding items that can work to improve the thermal conductivity of a part should be further investigated.

7.2.5 SAR Antenna Design

Initially, additional work needs to be performed on this particular design to assemble and test the entire antenna as a complete array. This will verify the usefulness of integrating UC and DW for RF connections in an array. Also connections and restraints that would allow a plug and play system need to be further researched. Support material for large voids needs to be performed so that a single monolithic structure can be fabricated. Additional work on the bonding of face sheets to honeycomb structures would assist in reducing the mass due to support areas to facilitate bonding. There is still significant work that needs to be performed to answer all the design questions relating to such a new technique as UC, but this work has laid a foundation whereupon additional work can be added to develop a complete set of design guidelines for advanced UC structures that have integral capabilities facilitated by other processes such as DW.

Appendices

Appendix A

Use of Ultrasonic Consolidation for Fabrication of

Multi-material Structures

G.D. Janaki Ram, C. Robinson, Y. Yang, and B.E. Stucker Department of Mechanical and Aerospace Engineering, Utah State University Logan, UT 84322-4130, USA

This appendix is a paper submitted as a journal article to the Rapid Prototyping Journal. All permissions to use this paper as a part of this thesis are contained in Appendix B.

Abstract

Purpose - Ultrasonic consolidation (UC) is a novel additive manufacturing process developed for fabrication of metallic parts from foils. While the process has been well-demonstrated for part fabrication in Al alloy 3003, some of the potential strengths of the process have not been fully explored. One of them is its suitability for fabrication of parts in multi-materials. This work aims to examine this aspect.

Methodology/approach - Multi-material UC experiments were conducted using Al alloy 3003 foils as the bulk part material together with a number of engineering materials (foils of Al-Cu alloy 2024, Ni-base alloy Inconel 600 , AISI 347 stainless steel, and others). Deposit microstructures were studied to evaluate bonding between various materials.

Findings - It was found that most of the materials investigated can be successfully bonded to alloy Al 3003 and vice versa. SiC fibers and stainless wire meshes were successfully embedded in an Al 3003 matrix. The results suggest that the UC process is quite suitable for fabrication of multi-material structures, including fiber-reinforced metal matrix composites.

Originality/value - This work systematically examines the multi-material capability of the UC process. The findings of this work lay a strong foundation for a wider and more efficient commercial utilization of the process.

Key words: Additive manufacturing, Ultrasonic consolidation, Ultrasonic welding, Multi-material structures, Fiber-reinforced metal matrix composites.

Paper type: Research paper

A.1 Introduction

Ultrasonic Consolidation (UC) is a novel additive manufacturing process developed for fabrication of metallic parts from foils. The process uses a high frequency ultrasonic energy source to induce combined static and oscillating shear forces within metal foils to produce solid-state bonds and build up a near-net shape part, which is then machined to its final dimensions using an integrated, 3-axis CNC milling machine (White, 2003). UC combines the advantages of additive and subtractive fabrication approaches allowing complex parts to be formed with high dimensional accuracy and surface finish, including objects with complex internal passageways, objects made up of multiple materials, and objects integrated with wiring, fiber optics, sensors, and instruments. Because the process does not involve melting, one need not worry about dimensional errors due to shrinkage, residual stresses and distortion in the finished parts. This will also help in dealing with metallurgically incompatible dissimilar material combinations.

One unique aspect of UC is that highly localized plastic flow around embedded structures is possible, resulting in sound physical/mechanical bonding between the embedded material and matrix material, although the exact mechanism by which it is made possible is not yet fully understood (Doumanidis and Gao, 2004; Kong et al., 2005). This ability can be utilized in a number of ways, including manufacture of fiber-reinforced metal matrix composites with structural fibers for localized stiffening, optical fibers for communication and sensing, shape memory fibers for actuation, or wire meshes for planar or area stiffening (Yang et al., 2006). It is possible to simply insert pre-fabricated components (such as thermal management devices, sensors, computational devices, etc.) into machined cavities of the part under construction prior to encapsulation by subsequent material addition (Siggard et al., 2006).

While, in principle, the UC process can be utilized for manufacturing of multi-material structures (White, 2003; Wohlers, 2003; Hu et al., 2006), the capabilities of the process are yet to be fully explored. Practically no published information is available on multi-material UC, with most of the work being carried out on Al alloy 3003 (Kong et al., 2004).

Successful extension of the process to widely used engineering materials like Fe, Ni, and Cu, and to dissimilar combinations like Al/brass, Al/stainless steel, and Al/Ni, will significantly expand commercial opportunities for ultrasonic consolidation.

In view of the above, in the current work an attempt has been made to explore multi-material UC. A number of engineering materials in the form of foils (hereafter referred to as dissimilar or second materials) were tried in combination with Al alloy 3003 foils (as the bulk part material). In addition, the possibility of embedding SiC fibers and a stainless steel wire mesh in an alloy 3003 matrix were examined. Multi-material UC deposit microstructures were examined to evaluate bonding or embedding characteristics between various second materials and Al alloy 3003. The main aim of this study is to broadly assess the UC process for fabrication of multi-material structures, including fiber-reinforced metal matrix composites.

A.2 Experimental work

A.2.1 Materials

Al-Mn alloy 3003 (nominal composition by wt.%: Al-1.2Mn-0.12Cu) foil (150 m thick and 25 mm wide) obtained from Solidica, Inc., USA, was used as the bulk part material for all experiments. Deposition experiments were conducted on an Al 3003 base plate (dimensions: 355x355x12 mm) firmly bolted to the heat plate of the Solidica Form-ation UC machine. The materials used for multi-material UC experiments are listed in Table A.1 . All these second materials were in the form of foil (except SiC (fiber) and stainless steel 304 (wire mesh)). Since the machine does not facilitate automatic feeding of multiple foil materials simultaneously, the second materials used in this study were not fed through the machine's foil feeding mechanism, but were manually placed, while the bulk part material Al alloy 3003 foil was automatically fed by the machine in the usual manner.

A.2.2 Deposition experiments

Deposition experiments were conducted in such a way that they facilitate study of

Table A.1: Materials used for multi-material UC and their forms.

Material	Nominal Composition (Wt%)/Thickness
Al alloy 3003 (Al 3003)	Al-1.2Mn-0.12Cu, 150 μm thick foil
Al alloy 2024 (Al 2024)	Al-4.5Cu-1.5Mg, 225 μm thick foil
SiC fiber	100 μm diameter
MetPreg*	Al203 short fiber reinforced Al matrix composite tape, 325 μm thick
Inconel 600** (IN 600)	Ni-15Cr-8Fe-0.15C, 200 μm thick foil
Brass	Cu-30Zn, 75 μm thick foil
Stainless steel AISI 347 (SS 347)	Fe-18Cr-11Ni-1Nb-0.08C, 150 μm thick foil
Stainless steel AISI 304 wire mess (SS mesh)	Fe-18Cr-8Ni-0.08C, 25 μm diameter wire
*MetPreg is the registered trademark of the Touchstone Research Laboratory, Ltd., USA. ** Inconel 600 is the registered trademark of the International Nickel Company, Canada.	

bonding between Al 3003 and a second material, and vice versa, following one or both of the following methods:

Method 1 (direct welding): Method 1 deposition procedure consisted of depositing a few layers of Al alloy 3003 (on an Al alloy 3003 base plate) and then placing a layer of a given second material on the Al 3003 deposit, and running the ultrasonic head directly over the second material layer. After depositing the second layer, a layer of Al 3003 was deposited on the second material in some cases. This method was used to bond a single layer of second material or as many as three layers of second material, with each layer individually being welded to the previous layer.

Method 2 (indirect welding): Method 2 deposition procedure consisted of depositing a few layers of Al alloy 3003 foil (on an Al alloy 3003 base plate) and then placing a given second material layer on top of the previously deposited layer, and then using the automatic tape feeder to lay Al 3003 over the second material while running the ultrasonic head over the layers, thus simultaneously bonding the top Al 3003 layer to the second material, as well as the second material layer to the Al 3003 substrate in one pass.

In the case of SiC fibers, the experimental procedure consisted of: i) depositing a layer of Al 3003 on top of an Al alloy 3003 base plate, ii) placing a SiC fiber on the top of the deposited Al 3003 layer and holding it in place using a custom-designed fixture, and iii) depositing a layer of Al alloy 3003 on the pre-placed fiber. More details on fiber embedment experiments are presented elsewhere (Yang et al., 2006).

The process parameters used for all the deposition experiments are listed in Table A.2. These parameters were found to ensure good bonding between Al alloy 3003 foils (Janaki Ram et al., 2006). However, no attempts were made in this study to optimize process parameters for maximizing bond quality between Al 3003 and any of the second materials, except in the case of SiC. For SiC fiber embedment, a comprehensive process parameter optimization exercise was undertaken using statistically designed experiments involving use of oscillation amplitude, normal force, welding speed, fiber orientation, and substrate temperature at five different levels. Deposits produced using various process parameter combinations were evaluated for fiber/matrix bond strength using "push-out" testing, based on which optimum process parameters were identified (shown in Table A.2.)More details on this process parameter optimization exercise are presented elsewhere (Yang et al., 2006).

A.2.3 Metallography

All the deposits were metallographically examined to assess bonding or embedding characteristics between various second materials and Al alloy 3003. Samples corresponding to longitudinal and/or transverse sections were extracted from each of the deposits and were prepared for microstructural study following standard metallographic practices. Microstructural observations were conducted on as-polished samples using optical and scanning

Table A.2: Process parameters used for multi-material UC experiments.

Material combination	Amplitude (μm)	Speed (mm/s)	Force (N)	Temperature (F)
All combinations except Al 3003/SiC fiber	16	28	1750	300
SiC fiber*	20	34	1700	300
*Fiber was oriented at 45 to the welding direction.				

electron microscopes.

A.3 Results and discussion

A.3.1 Mechanism of bond formation

Before discussing multi-material UC deposits, a brief explanation of the dominant bonding mechanisms in ultrasonic welding, which are still a matter of considerable debate, is in order. As in the case of any other solid state welding process, two conditions must be fulfilled for bond formation during ultrasonic welding: i) generation of atomically clean surfaces, and ii) intimate contact between clean metal surfaces. The bonding process in ultrasonic welding can be looked at as repeated and successive occurrence of two distinct stages: i) generation of contact points (Contact Stage), and ii) formation of bonds across the contact points (Bond Stage). These stages are discussed below.

The situation at the mating surfaces at the beginning of ultrasonic welding can be visualized as shown in Figure A.1. All surfaces are characterized by some surface roughness at the microscopic level. The hills and valleys pattern on the mating surfaces does not allow 100% surface contact at the interface; instead, the mating surfaces contact only at surface asperities. Thus, in a way, the first Contact Stage is immediately accomplished as the mating surfaces are brought into contact under the influence of applied normal force. It is at these oxide-covered contact points that bonding initially occurs in the next stage of the process, as described below.
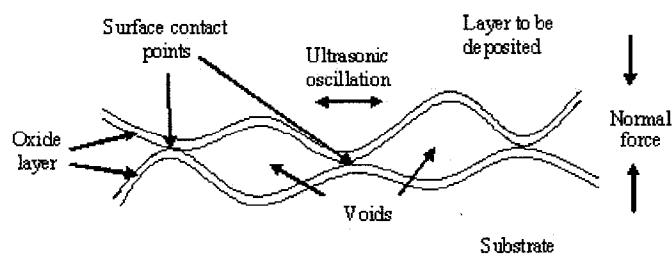
Fig. A.1: Schematic of the mating surfaces at the beginning of ultrasonic welding.

As the sonotrode travels over the layer to be deposited, simultaneous application of normal and oscillating shear forces results in generation of dynamic interfacial stresses between the two mating surfaces at the contact points. The stresses produce cracks in the surface oxide layers (oxides are usually brittle) as well as induce plastic deformation in a thin layer of metal (up to 20 microns) just beneath the oxide layer (plastic deformation can itself cause further cracking in the oxide layer). As this happens, nascent metal from beneath extrudes through the cracks in the oxide layer causing disintegration of oxide layers into smaller pieces, which are dispersed in the vicinity of the bond zone by metal flow. This process generates atomically clean metal surfaces and brings them into intimate contact, establishing a metallurgical bond. This completes the first Bond Stage of the overall process. After the first Bond Stage, there may be numerous "no-bond" regions (corresponding to the original "no-contact or void" regions) along the interface, still covered with oxide layer.

As the process progresses, the bonded regions (formed in the first Bond Stage) grow in size, aided by plastic deformation and diffusion. Plastic deformation at the bonded regions results in squeezing of metal into the voids and the mating surfaces across the void regions approach. As this happens, new points come into contact. This marks the completion of the second Contact Stage of the process. Continued application of ultrasonic energy results in friction, oxide layer break-up and bonding across these new contact points (in the same manner as described in the first Bond Stage) in what can be called the second Bond Stage of the process. This will be followed by another Contact Stage, and subsequently by another Bond Stage and so on. Thus ultrasonic welding involves repeated and successive occurrence of Contact and Bond Stages at every region along the weld deposit. In general, the higher the number of these stage repetitions during ultrasonic welding, the better the bonding between the mating surfaces. If the material is prone to work hardening under these conditions, a threshold can be reached, above which the bonding between the mating surfaces will begin to degrade.

Macroscopically, the bonding process at a given region along the weld deposit begins as the traveling sonotrode approaches that region and completes as the sonotrode travels

past that region after a very brief resident time. The number of stage repetitions that occur during the bonding process depends on process parameters, in particular the welding speed employed. For example, slower welding speeds (i.e., longer sonotrode resident times) allow more stage repetitions and hence, can help produce UC deposits with high weld density levels. This is illustrated in Figure A.2, which shows the microstructures of two ultrasonically consolidated Al alloy 3003 deposits, produced at different welding speeds. The deposit shown in Figure A.2a was produced using a welding speed of 28 mm/s, whereas the deposit shown in Figure A.2b was produced at a lower welding speed of 12 mm/s (other parameters being the same in both cases as listed in Table A.2). The dark regions seen along the layer interfaces are the unbonded regions. These unbonded regions arise due to lack of bonding between the mating surfaces due to surface roughness. As can be seen, use of a lower welding speed resulted in significantly fewer and smaller unbonded regions and thus a higher linear weld density in the deposit (98% for 12 mm/s welding speed versus 90% for 28 mm/s welding speed). This is attributed to a longer sonotrode resident time allowing more number of Contact and Bond Stage repetitions during the bonding process. Alternatively, if one can increase the number of contact points along the mating surfaces by reducing surface roughness, it may be possible to achieve high weld density levels even

(a)   (b)
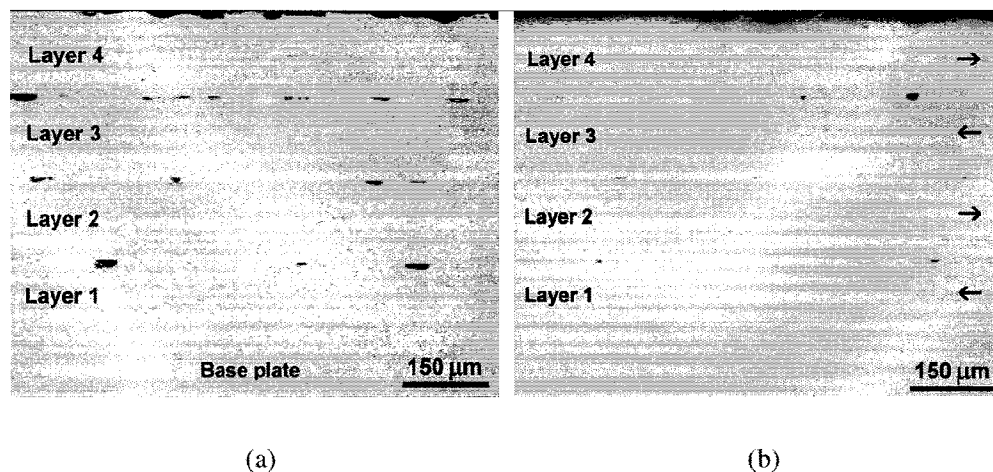
Fig. A.2: Optical microstructures of Al alloy 3003 UC deposits: (a) 28 mm/s welding speed (90% linear weld density), and (b) 12 mm/s welding speed (98% linear weld density)

at relatively high welding speeds.This idea has been demonstrated in another work by the authors (Janaki Ram *et al.*, 2006). It should be noted that other process parameters, such as oscillation amplitude, and build height also exert a strong influence on linear weld density (Janaki Ram *et al.*, 2006; Robinson *et al.*, 2006).

As can be seen, plastic deformation is a crucial player in both Contact and Bond Stages of the ultrasonic welding process. In the Contact Stage, plastic deformation of the bonded regions not only serves to generate more contact points, but also helps in the survival of already formed bonds. If the bonded regions are incapable of repeated deformation, continued ultrasonic oscillations will result in breakage of bonds. Although repeated breakage and rebonding can occur under specific processing conditions (e.g., too high an oscillation amplitude), we believe that bonded regions likely do not break in most cases, but experience plastic deformation. In essence, we believe that plastic deformation at the interface plays a crucial role in metal ultrasonic welding in four ways: i) it helps break up surface oxides and remove the broken oxide scales away from the bonding region, ii) it helps in establishing intimate nascent metal contact, and iii) it generates new contact points across which bonding can occur.

With this background, it may be expected that successful fabrication of multi-material structures using UC requires that at least one of the materials involved in a dissimilar combination should be capable of plastic deformation. Secondly, oxide layers on both the mating metal surfaces should be amenable for removal during the bonding process. The ease with which an oxide layer is removed is a function of its hardness in relation to the nascent metal hardness. In fact, the ratio of oxide layer hardness to nascent metal hardness is regarded as a good rule of thumb for determining the ultrasonic weldability of metallic materials (O'Brien, 1991). The higher the difference in the hardness levels of the oxide and nascent metal, the easier it is to break up the oxide layer and therefore, the better the ultrasonic weldability.

Preliminary microstructural results pertaining to each of the dissimilar combinations examined in the present work are discussed below under separate headings.

A.3.2 Al 3003/Al 2024

Al 3003/Al 2024 deposits were made using both the direct and the indirect welding methods detailed in Section A.2.2. Figure A.3

shows the optical microstructures of these deposits. These pictures show that Al 3003 can be very well bonded to Al 2024 and vice versa. It is interesting to note that Al 2024 was well bonded to Al 3003, even not directly welded (Figure A.3b). Further, Al 3003/Al 2024 bonding appeared to be as good as that of Al 3003/Al 3003. Thus the current work shows that multi-material parts can be successfully fabricated out of Al-Mn and Al-Cu alloys employing the UC process, allowing one to take advantage of the superior strength characteristics of Al-Cu alloys and the superior corrosion resistance of Al-Mn alloys. It is expected that various other Al alloys can be similarly combined for multi-material part fabrication using the UC process.

Al 2024 to Al 2024 bonding was not examined in the current work. In an earlier study Kong *et al.* (2003) reported inferior weld quality in ultrasonically consolidated Al-Mg alloy 6061, which was attributed to difficulties in oxide layer removal due to the presence of MgO in the oxide layer of alloy 6061. Alloy 2024 also contains a considerable amount of Mg (1.5 wt.%). Therefore, Mg might present similar difficulties during ultrasonic welding of alloy 2024 to itself. The presence of Mg, however, did not result in any problems during ultrasonic welding of alloy 2024 to alloy 3003, which contained very little Mg (0.05 wt.% max.).

A.3.3 Al 3003/SiC

Figure A.4 shows the SEM microstructures of Al 3003/SiC deposits. The SiC fiber used in this study has a tungsten core (about 10 μm dia). For successful embedment of fibers, there must be adequate plastic flow of the matrix material to close the gaps that were created by placing the fiber between the layers. As can be seen in Figure A.4, there is extensive plastic flow around the fiber, evidenced by flow lines in a circular pattern around the fiber (Figure A.4b), resulting in excellent fiber embedment. Similar success was reported by Kong *et al.* (2005) with shape memory alloy fibers in Al 3003 matrix. Kong,

(a)   (b)
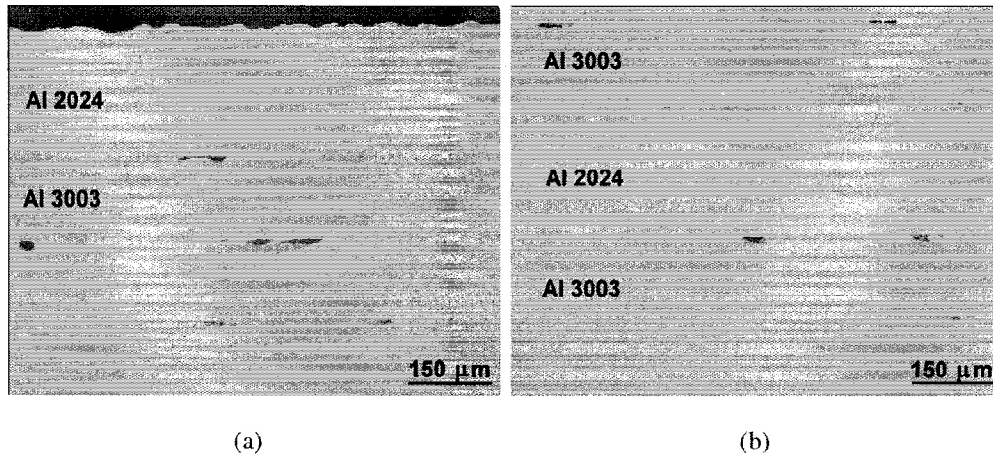
Fig. A.3: Optical microstructures of Al 3003/Al 2024 deposits: (a) Al 2024 layer directly welded to Al 3003, (b) Al 2024 layer sand witched between Al 3003 layers (indirectly welded).

(a)   (b)
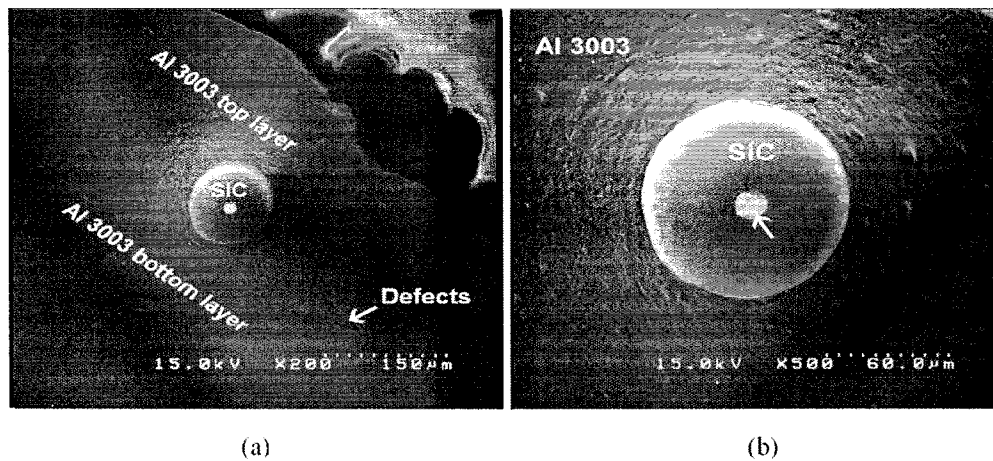
Fig. A.4: SEM microstructures of Al 3003/SiC: (a) SiC fiber embedded between Al 3003 layers, (b) SiC fiber at a higher magnification showing metal flow lines in a circular pattern. Arrow shows tungsten core.

through detailed elemental mapping studies, concluded that the matrix and the embedded fiber were not chemically or metallurgically bonded. Similarly in the present case, bonding between SiC fiber and Al 3003 matrix is expected to be physical/mechanical, rather than chemical/metallurgical.

Studies thus show that SiC fibers can be successfully embedded in an Al 3003 matrix, making UC a viable process for fabrication of intricate parts out of continuous fiber reinforced metal matrix composites.

A.3.4   Al 3003/MetPreg

Figure A.5 shows the SEM microstructures of directly welded Al 3003/MetPreg deposits. As mentioned earlier, MetPreg is a commercially available Al2O3 short fiber reinforced aluminum matrix composite. As can be seen, the MetPreg layer was very well bonded to the Al 3003 substrate with a featureless interface. On the other hand, when the MetPreg layer was indirectly welded, the Al 3003 top layer was bonded well with the MetPreg layer, but the MetPreg layer was not well bonded to the Al 3003 bottom layer. These observations are shown in Figure A.6.

The discrepancy can be explained as follows. When the ultrasonic sonotrode is passed over the Al 3003 top layer during indirect welding, much of the available ultrasonic energy acts at the Al 3003 top layer/MetPreg interface (therefore producing good bonding), as it is located directly beneath the sonotrode. Compared to this, the amount of ultrasonic energy that reaches or acts at the MetPreg /Al 3003 bottom layer interface would be much less. This makes oxide layer removal and/or plastic deformation difficult at the MetPreg /Al 3003 bottom layer interface, leading to poor bonding. In this context, one might argue that the same should be the case with indirectly welded Al 3003/Al 2024. However, indirect welding did not result in poor bonding at the Al 2024/Al 3003 bottom layer interface (Figure A.3b). This is understandable when we consider that: i) Al 2024 foil (225 μm) is considerably thinner than the MetPreg foil (325 μm), and ii) MetPreg is significantly stronger than Al 2024. Further, the composite nature of the MetPreg , which contained hard and stiff Al2O3 fibers in a soft Al matrix, can result in greater absorption or attenuation of the input

(a) (b)
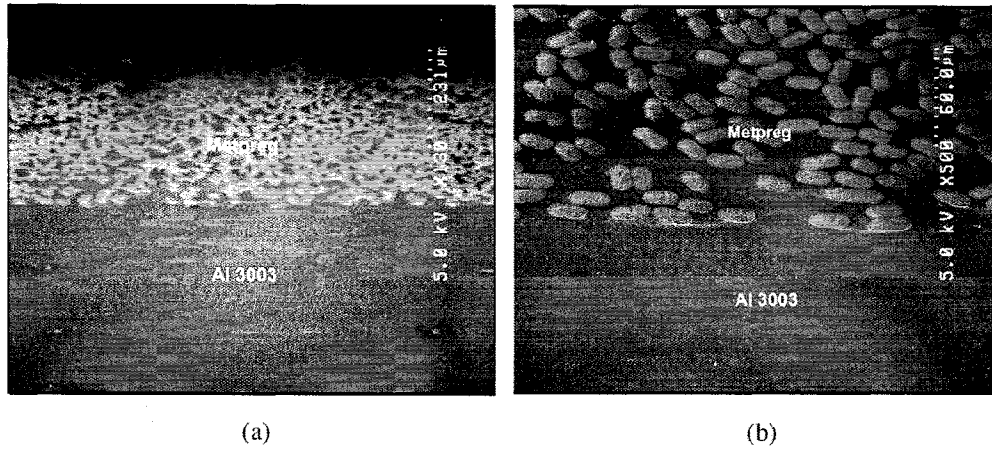
Fig. A.5: SEM microstructures of directly welded Al 3003/MetPreg : (a) MetPreg layer bonded to Al 3003 substrate, (b) Al 3003/MetPreg interface at a higher magnification.

(a) (b)
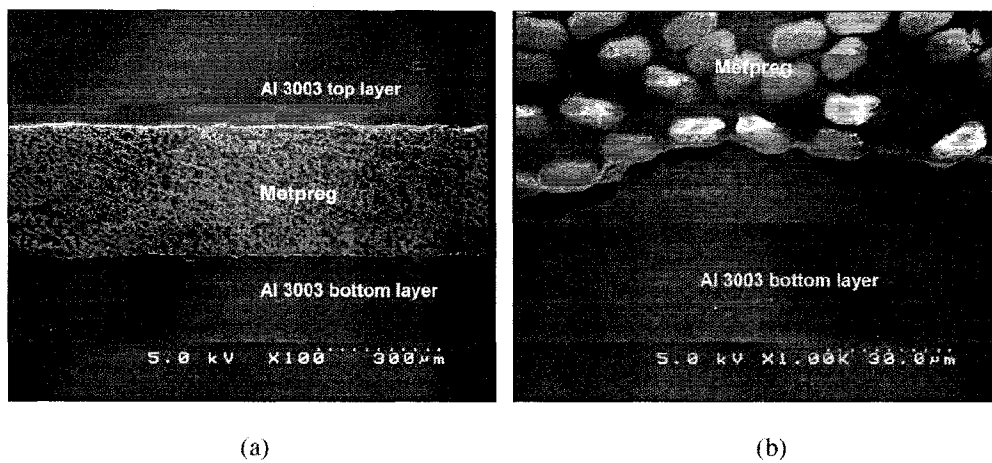
Fig. A.6: SEM microstructures of indirectly welded Al 3003/MetPreg : (a) MetPreg layer sandwiched between Al 3003, (b) Al 3003 bottom layer/MetPreg interface at a higher magnification.

ultrasonic energy.

The present work thus shows that it is possible to ultrasonically consolidate Al metal matrix composite layers and Al 3003 layers in any combination with excellent interface characteristics adopting the direct welding methodology. This capability can be utilized in many ways. For example, lighter, stronger, and stiffer Al parts can be produced by embedding metal matrix composite laminates. Further, fabrication of functionally graded Al matrix composite parts is a possibility. Fabrication of composite parts using metal matrix composite tapes is yet another possibility. Although bonding between MetPreg /MetPreg was not examined in the current work, it is expected that this material combination can be ultrasonically welded, at least up to a certain volume fraction of the reinforcing phase. Plastic deformation due to ultrasonic excitation of the softer Al matrix of the mating composite surfaces is expected to result in necessary readjustments at the interface, producing sound matrix/matrix metallurgical bonding.

A.3.5   Al 3003/IN 600

The interface microstructure of the directly welded Al 3003/IN 600 deposit is shown in Figure A.7. As can be seen, IN 600 was well bonded to Al 3003, without any physical discontinuities at the interface. The indirect welding method also produced good bonding between an Al 3003 top layer/IN 600 (Figure A.8a). The interface microstructure is quite similar to that shown in Figure A.7. However, numerous unbonded regions were observed at the IN 600 /Al 3003 bottom layer interface (Figure A.8b). As explained in Section A.3.4, insufficient ultrasonic energy is the reason for this, rather than intrinsic difficulties in bond formation.

While IN 600 appears to be well bonded to Al 3003, it is necessary to examine the interface in greater detail since Ni and Al can form an nickel aluminide intermetallic, which can affect the deposit properties. Nevertheless, the current work shows that IN 600 can be ultrasonically bonded to Al 3003 and vice versa, proving the combination viable for multi-material part fabrication using ultrasonic consolidation. It is expected that other Ni-based alloys can be similarly combined with Al 3003 for multi-material part fabrication.
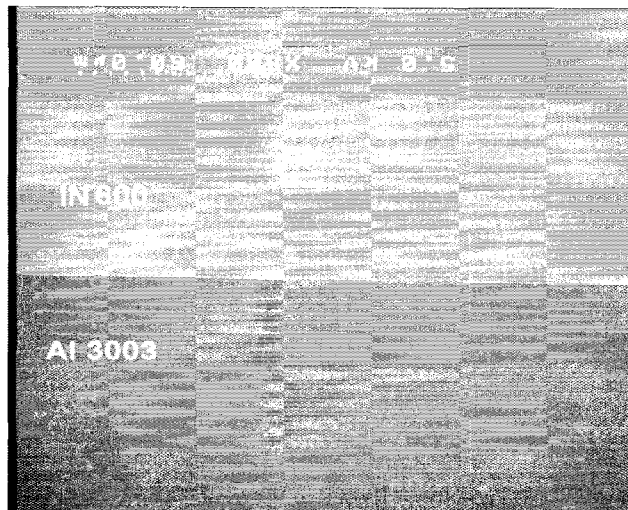
Fig. A.7: SEM microstructure of directly welded Al 3003/IN 600 .
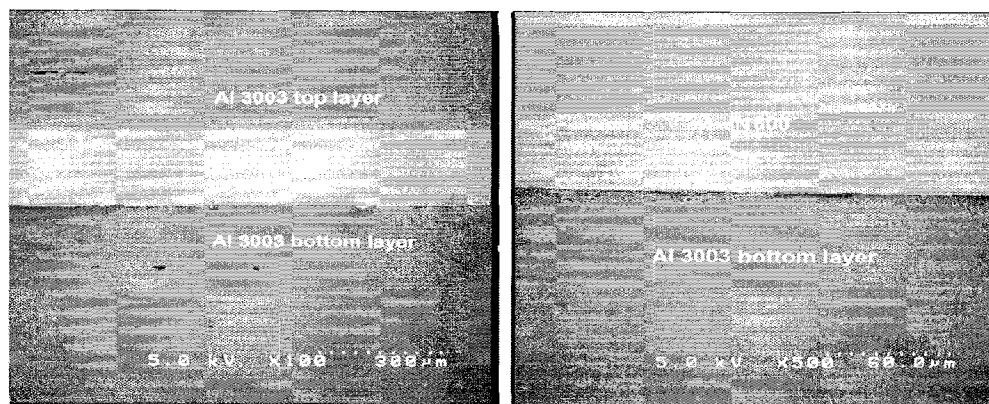
(a)   (b)

Fig. A.8: SEM microstructures of indirectly welded Al 3003/IN 600 : (a) IN 600 layer sandwiched between Al 3003 layers, (b) Al 3003 bottom layer/IN 600 interface at a higher magnification showing the interfacial defects.

A.3.6 Al 3003/Brass

Experiments with Al 3003/brass combinations were conducted using both the direct and the indirect welding methods. The interface microstructures of the indirectly welded Al 3003/brass deposit are shown in Figure A.9. As can be seen, the brass layer was not well bonded to the Al 3003 layers. The Al 3003 top layer/brass interface (Figure A.9b) looked better compared to the brass/Al 3003 bottom layer interface (Figure A.9c), although both interfaces were not tight and contained numerous interfacial defects. In another method, a brass layer was initially directly welded to Al 3003. Following this, two more brass layers

(a)   (b)

(c)
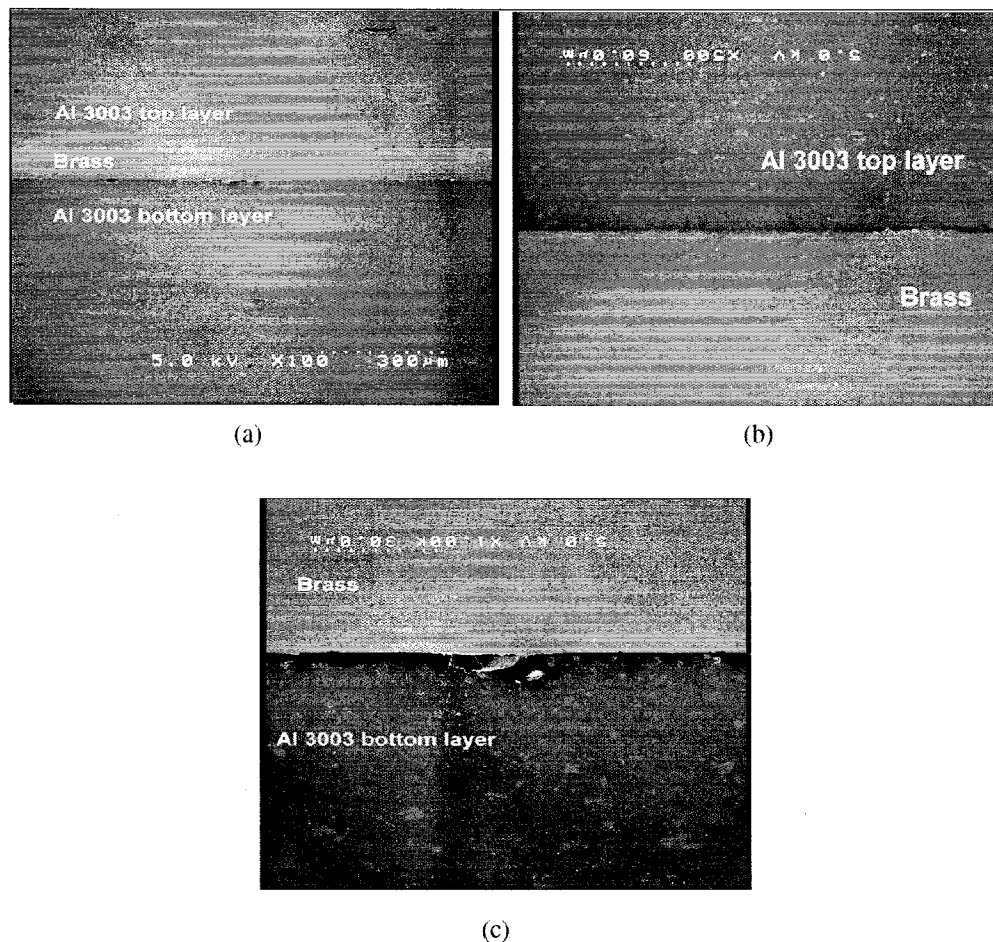
Fig. A.9: SEM microstructures of Al 3003/brass: (a) Brass layer sandwiched (indirectly welded) between Al 3003 layers, (b) Al 3003 top layer/brass interfaces at a higher magnification, (c) Brass/Al 3003 bottom layer interfaces at a higher magnification.

were deposited with each of them being directly welded to a previously deposited brass layer. The microstructures of this deposit are shown in Figure A.10. Again, the brass layer was not well-bonded to the Al 3003 substrate (Figure A.10b). However, there was reasonable bonding between the brass layers, as can be seen in Figure A.10.

It may be noted that both Cu and Zn, the main constituent elements in brass, were reported to be ultrasonically weldable to Al (Daniels, 1965; O'Brien, 1991). Therefore, one might expect that brass can be ultrasonically weldable to alloy 3003. The current work, however, indicates that brass is not easily weldable to Al 3003, although it is not clear whether the lack of bonding is due to improper process parameters or due to intrinsic difficulties in bonding. Thus the Al 3003/brass combination requires further examination using careful process parameter optimization in order to more clearly assess the situation. On another note, the current work shows that brass can be ultrasonically welded very well to itself, and therefore it can be used for part fabrication using the UC process.

A.3.7   Al 3003/SS 347

Figure A.11 shows the interface microstructures of indirectly welded Al 3003/SS 347 deposit. The Al 3003 top layer/SS 347 interface (Figure A.11b) appeared tight without

(a)   (b)
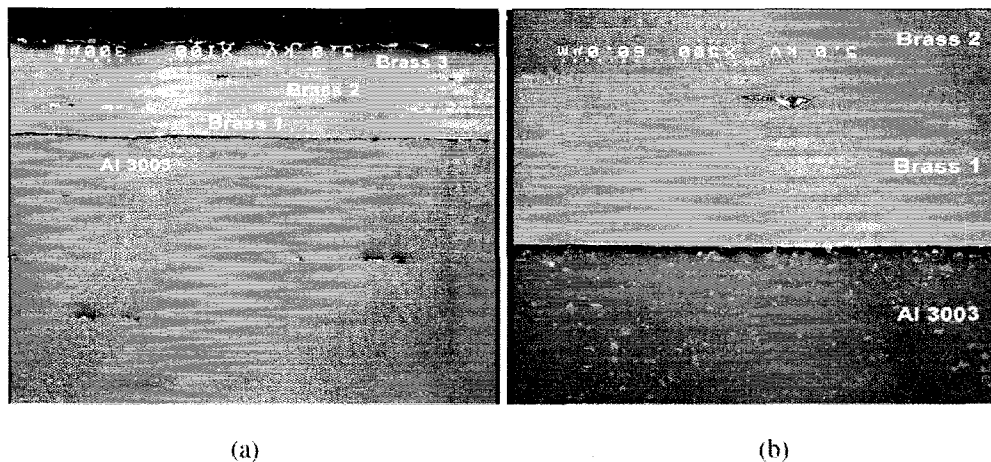
Fig. A.10: SEM microstructures of directly welded Al 3003/brass: (a) Three layers of brass over Al 3003, (b) Al 3003/brass interface at a higher magnification.
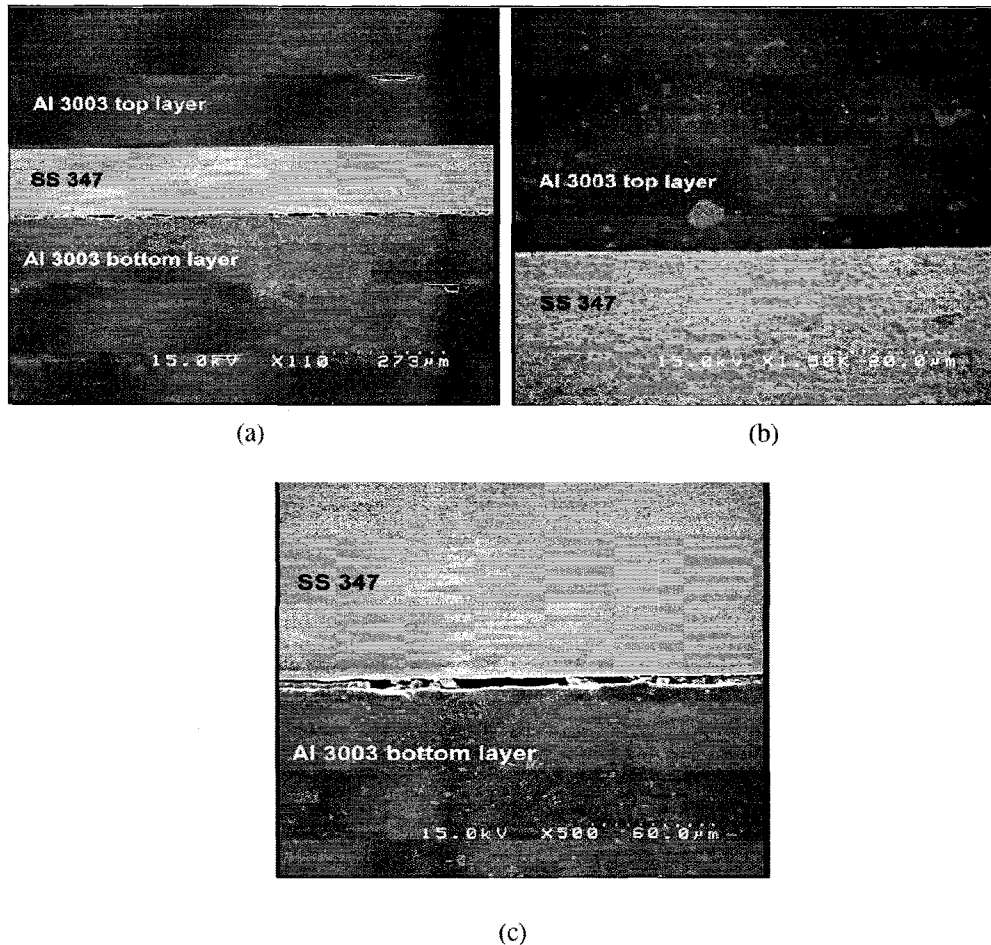
Fig. A.11: SEM microstructures of indirectly welded Al 3003/SS 347: (a) SS 347 layer sandwiched between Al 3003 layers, (b) Al 3003 top layer/SS 347 interface at a higher magnification, and (c) SS 347/Al 3003 bottom layer interface at a higher magnification.

any large physical discontinuities; however, further microstructural studies are required to assess the bond quality. In contrast, the SS 347/Al 3003 bottom layer interface (Figure A.11c) showed wide gaps and a total absence of bonding, which is attributable again to a lack of sufficient ultrasonic energy at the interface. In another method, a layer of SS 347 was initially directly welded to Al 3003. Following this, two more SS 347 layers were deposited with each of them being directly welded to previously deposited SS 347 layer. The first SS 347 layer appeared to bond well to the Al 3003 substrate, but subsequent microstructural examination showed that these materials did not bond quite satisfactorily (Figure A.12)
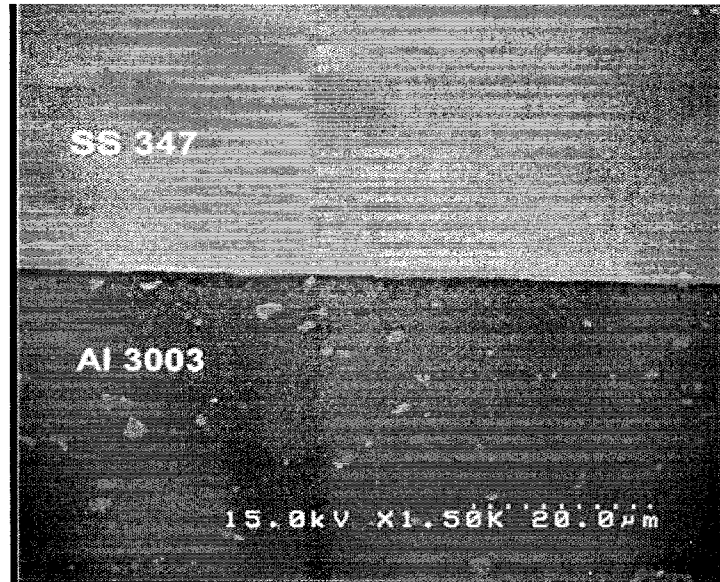
Fig. A.12: SEM microstructure at the interface of directly welded SS 347(first layer)/Al 3003.

but merely deformed to produce relatively intimate contact. The top two SS 347 layers completely came off the deposit indicating inadequate bonding between the SS 347 layers.

While Fe-base alloys were reported to be ultrasonically weldable to themselves and to Al alloys (O'Brien, 1991), the current study indicates that the bonding achievable between SS 347 and Al 3003 is not good enough for fabrication of functional multi-material parts. Further, fabrication of SS 347 parts using ultrasonic consolidation looks even more challenging considering the lack of bonding between SS 347 layers. Further deposition experiments after careful process parameter optimization and detailed microstructural studies are necessary to assess the bonding potential between SS 347 to itself and to Al 3003.

A.3.8 Al 3003/SS Mesh

Experiments with Al 3003/SS mesh combination were conducted using the direct welding method. The method consisted of depositing a few layers of Al alloy 3003 and then placing a layer of SS mesh on the Al 3003 deposit, and running the ultrasonic head directly over the SS mesh. Following this, a layer of Al 3003 was deposited on the SS mesh. The

SEM microstructures of the deposit thus made are shown in Figure A.13. As in the case for fiber embedment, plastic flow of the matrix material is critical for successful embedment of the mesh. Microstructural observation revealed excellent metal flow into the gaps of the SS mesh between the Al 3003 layers, resulting in good physical/mechanical bonding between the Al 3003 matrix and SS mesh. Also, passage of the ultrasonic head over the mesh even at a relatively high normal force level (1750 N) did not damage the original wire weaving arrangement of the mesh (Figure A.13a). However, the SS mesh was not metallurgically bonded to the Al 3003 matrix, as evidenced by a clearly discernible narrow physical gap that existed between Al 3003 and the SS mesh (shown by white arrows in Figure A.13b.

It was observed that the wire elements of the mesh became metallurgically bonded to their neighbors during the deposition process. This can be seen in Figure A.13b (black arrows), where the circular wire cross-sections present a featureless interface with the sine wave-like horizontal wire. This indicates that SS 304 can be ultrasonically bonded to itself, making it a candidate material for part fabrication using ultrasonic consolidation. Further deposition experiments using SS 304 foils are necessary to confirm this.

(a) (b)
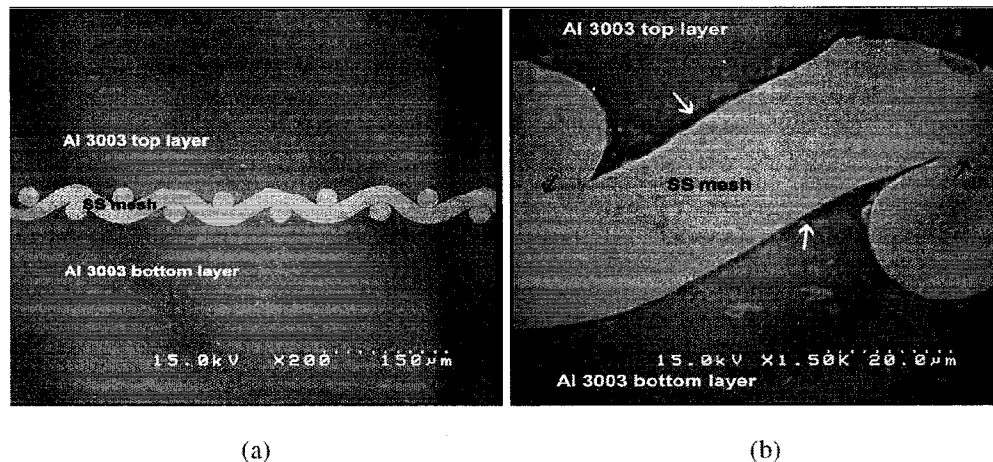
Fig. A.13: SEM microstructures of Al 3003/SS mesh: (a) SS mesh embedded between Al 3003 layers, (b) Al 3003/SS mesh interface at a higher magnification. The featureless interface between SS 304 wire elements is shown by black arrows, and the interfacial defects between Al 3003/SS mesh are shown by white arrows.

A.3.9 Multi-material ultrasonic consolidation

Although further work is considered necessary, the deposition and characterization procedures adopted in this study are appropriate enough for a preliminary assessment of the potential for multi-material part fabrication. Of the dissimilar material combinations studied, only two, Al 3003/brass and Al 3003/SS 347, appeared to be problematic. The lack of bonding in these cases is not entirely understood, but may be improved through more effective deposition techniques. Further, more detailed microstructural and microchemical characterization of the interfaces is necessary for comprehensively assessing the bond quality in most cases.

Another important aspect for future work is process parameter optimization. In the current work, process parameters were not fine-tuned to maximize bonding between Al 3003 and the second materials. Each material combination requires a unique set of process parameters for achieving optimal bonding because of the varying physical, chemical and mechanical characteristics of the materials and their surface oxides. Determination of such process parameter combinations necessitates rigorous experimentation with parameter variations, which is a time-consuming task. When the right combination of process parameters is chosen for each material combination, it may be possible to achieve better results than the ones presented in this work.

The current work amply demonstrates that multi-material parts, including fiber-reinforced metal matrix composites, can be successfully fabricated using the UC process. It shows that the process can be successfully extended to a wide range of engineering materials. This flexibility in terms of part material in combination with the multi-material capabilities opens tremendous opportunities for the UC process. While this is so, the current commercially available UC machines need to be modified to facilitate fully automated fabrication of multi-material structures. For example, a suitable mechanism for simultaneous automated tape feeding of multiple materials must be in place. In addition, further developments in the areas of computer aided design and data representation methods are necessary for efficiently handling multi-material situations in UC as well as in other additive manufacturing

processes (Liu *et al.*, 2004).

A.4 Summary

Fabrication of multi-material parts presents a significant challenge. In this context, the UC process, by virtue of its inherent process characteristics, is quite promising. The current work examines the capacities of the process for fabrication of multi-material parts. A number of engineering materials have been utilized in combination with Al alloy 3003, used as the bulk part material. Studies show that Al-Cu alloys, Al matrix composites, and Ni-based alloys can be ultrasonically welded to Al alloy 3003 and vice versa with excellent interfacial characteristics. Successful embedment of SiC fibers and a stainless steel wire mesh in Al alloy 3003 matrix was also demonstrated. AISI 347 stainless steel and brass did not weld well to Al alloy 3003 using the parameters chosen for this study. However, better results may be possible with the right process parameters. Overall, the current work shows that multi-material part fabrication out of materials with widely differing physical, chemical and mechanical characteristics is more than a mere possibility with UC.

Acknowledgments

References

Daniels, H.P.C. (1965), "Ultrasonic welding", Ultrasonics, pp. 190-196.

Doumanidis, C. and Gao, Y. (2004), "Mechanical modeling of ultrasonic welding", Welding Journal, Vol.83, No.4, pp. 140-146.

Hu, Y., Fadel, G.M., Blouin, V.Y. and White, D.R. (2006), "Optimal design for additive manufacturing of heterogeneous objects using ultrasonic consolidation", Virtual and Physical Prototyping, Vol.1, No.1, pp. 53-62.

Janaki Ram, G.D., Yang, Y., George, J., Robinson, C. and Stucker, B.E. (2006), "Improving linear weld density in ultrasonically consolidated parts", Proceedings of the 17th Solid Freeform Fabrication Symposium, Austin, Texas, USA, August 2006.

Kong, C.Y., Soar, R.C. and Dickens, P.M. (2003), "Characterization of aluminium alloy 6061 for the ultrasonic consolidation process", Materials Science and Engineering A, Vol. A363, pp. 99-106.

Kong, C.Y., Soar, R.C. and Dickens, P.M. (2004), "Optimum process parameters for ultrasonic consolidation of 3003 aluminium", Journal of Materials Processing Technology, Vol. 146, pp. 181-187.

Kong, C.Y., Soar, R.C. and Dickens, P.M. (2005), "Ultrasonic consolidation for embedding SMA fibers within aluminium matrices", Composite Structures, Vol. 66, pp. 421-427.

Liu, H. et al. (2004) "Methods for feature-based design of heterogeneous solids", Computer-Aided Design, Vol. 36, pp. 1141.

O'Brien, R.L. (1991), Welding Processes, Welding Handbook, Vol. 2, 8th edition, American Welding Society, Miami, FL.

Robinson, C.J., Zhang, C., Janaki Ram, G.D., Siggard, E.J., Stucker, B. and Li, L. (2006), "Maximum height to width ratio of freestanding structures built using ultrasonic

consolidation", Proceedings of the 17th Solid Freeform Fabrication Symposium, Austin, Texas, USA, August 2006.

Siggard, E.J., Madhusoodanan, A.S., Stucker, B. and Eames, B. (2006) "Structurally embedded electrical systems using ultrasonic consolidation (UC)", Proceedings of the 17th Solid Freeform Fabrication Symposium, Austin, Texas, USA, August 2006.

White, D.R. (2003), "Ultrasonic consolidation of aluminium tooling", Advanced Materials and Processes, Vol.161, pp. 64-65.

Wohlers, T. (2003), Wohlers Report 2003: Rapid Prototyping and Tooling State of the Industry Annual Worldwide Progress Report, Fort Collins, CO, Wohlers Associates, Inc.

Yang, Y., Janaki Ram, G.D. and Stucker, B. (2006), "Process parameters optimization for ultrasonically consolidated fiber-reinforced metal matrix composites", Proceedings of the 17th Solid Freeform Fabrication Symposium, Austin, Texas, USA, August 2006.

Autobiographical Notes

G.D. Janaki Ram is a post-doctoral researcher in the Department of Mechanical and Aerospace Engineering at Utah State University. His research interests include additive manufacturing, welding and aerospace materials. He can be reached at durgagabbita@cc.usu.edu

C. Robinson is a graduate student in the Department of Mechanical and Aerospace Engineering, Utah State University. He is currently working on fabrication of advanced satellite thermal control and aerospace structures using ultrasonic consolidation. He can be reached at cjrobi@cc.usu.edu

Y. Yang is a graduate student in the Department of Mechanical and Aerospace Engineering at Utah State University. He is currently working on fabrication of metal matrix composites using ultrasonic consolidation. He can be reached at yanzhe@cc.usu.edu

B.E. Stucker is serving as Assistant Professor in the Department of Mechanical and Aerospace Engineering at Utah State University. He conducts research in the filed of additive manufacturing, focusing on aerospace and biomedical applications. He can be reached at brent.stucker@usu.edu

Appendix B

Permissions

This appendix includes all required permissions for publication of the papers presented as Chapters 3-6 and Appendix A of this thesis.

129

Date 03/06/2007

Name   Chris Robinson
Address   1162 E. Stadium Way
            Logan, UT 84341
Phone   (435) 797-2562

Dear Amit Lopes:

I am in the process of preparing my thesis in the Department of Mechanical and
Aerospace Engineering at Utah State University. I hope to complete in the spring of
2007.

I am preparing a multiple paper thesis, which will include the papers listed below.
Because you are a co-author on these papers I am requesting your permission to include
the material just as it appeared in the paper. Please advise me of any changes you
require.

Please indicate your approval of this request by signing in the space provided, and
attaching any other form or instruction necessary to confirm permission. If you have any
questions, please call me at the number above.

Thank you for your cooperation,

Chris Robinson

I hereby give permission to Christopher J. Robinson to reprint the following material in
his thesis.

Robinson, C., B. Stucker, K.C. Branch, J. Palmer, B. Strassner, R. Bugos, M. Navarrette,
A. Lopes, E. MacDonald, F. Medina, and R. Wicker, "Fabrication of a mini-SAR
Antenna Array Using Ultrasonic Consolidation and Direct-write." *Rapid Manufacturing
Conference*, July, 2007, U.K.

Robinson, C.J., B. Stucker, A.J. Lopes, R. Wicker, and J.A. Palmer, "Integration of
Direct-Write (DW) and Ultrasonic Consolidation (UC) Technologies to Create Advanced
Structures with Embedded Electrical Circuitry." *Solid Freeform Fabrication Symposium
Proceedings*, Austin, Texas, August 2007.

Signed_____

130

Date 03/06/2007

Name   Chris Robinson
Address   1162 E. Stadium Way
            Logan, UT 84341
Phone   (435) 797-2562

Dear Berndie Strassner:

I am in the process of preparing my thesis in the Department of Mechanical and
Aerospace Engineering at Utah State University. I hope to complete in the spring of
2007.

I am preparing a multiple paper thesis, which will include the paper listed below.
Because you are a co-author on this paper I am requesting your permission to include the
material just as it appeared in the paper. Please advise me of any changes you require.

Please indicate your approval of this request by signing in the space provided, and
attaching any other form or instruction necessary to confirm permission. If you have any
questions, please call me at the number above.

Thank you for your cooperation,

Chris Robinson
_____

I hereby give permission to Christopher J. Robinson to reprint the following material in
his thesis.

Robinson, C., B. Stucker, K.C. Branch, J. Palmer, B. Strassner, R. Bugos, M. Navarrette,
A. Lopes, E. MacDonald, F. Medina, and R. Wicker, "Fabrication of a mini-SAR
Antenna Array Using Ultrasonic Consolidation and Direct-write." *Rapid Manufacturing
Conference*, July, 2007, U.K.

Signed_____

Date   03/06/2007

Name   Chris Robinson
Address   1162 E. Stadium Way
              Logan, UT 84341
Phone   (435) 797-2562

Dear Dr. Ryan Wicker:

I am in the process of preparing my thesis in the Department of Mechanical and
Aerospace Engineering at Utah State University. I hope to complete in the spring of
2007.

I am preparing a multiple paper thesis, which will include the papers listed below.
Because you are a co-author on these papers I am requesting your permission to include
the material just as it appeared in the paper. Please advise me of any changes you
require.

Please indicate your approval of this request by signing in the space provided, and
attaching any other form or instruction necessary to confirm permission. If you have any
questions, please call me at the number above.

Thank you for your cooperation,

Chris Robinson

I hereby give permission to Christopher J. Robinson to reprint the following material in
his thesis.

Robinson, C., B. Stucker, K.C. Branch, J. Palmer, B. Strassner, R. Bugos, M. Navarrette,
A. Lopes, E. MacDonald, F. Medina, and R. Wicker, "Fabrication of a mini-SAR
Antenna Array Using Ultrasonic Consolidation and Direct-write." *Rapid Manufacturing
Conference*, July, 2007, U.K.

Robinson, C.J., B. Stucker, A.J. Lopes, R. Wicker, and J.A. Palmer, "Integration of
Direct-Write (DW) and Ultrasonic Consolidation (UC) Technologies to Create Advanced
Structures with Embedded Electrical Circuitry." *Solid Freeform Fabrication Symposium
Proceedings*, Austin, Texas, August 2007.

Signed _____ 3-8-07

Date 03/06/2007

Name   Chris Robinson
Address   1162 E. Stadium Way
            Logan, UT 84341
Phone   (435) 797-2562

Dear Dr. Eric MacDonald:

I am in the process of preparing my thesis in the Department of Mechanical and
Aerospace Engineering at Utah State University. I hope to complete in the spring of
2007.

I am preparing a multiple paper thesis, which will include the paper listed below.
Because you are a co-author on this paper I am requesting your permission to include the
material just as it appeared in the paper. Please advise me of any changes you require.

Please indicate your approval of this request by signing in the space provided, and
attaching any other form or instruction necessary to confirm permission. If you have any
questions, please call me at the number above.

Thank you for your cooperation,

Chris Robinson

I hereby give permission to Christopher J. Robinson to reprint the following material in
his thesis.

Robinson, C., B. Stucker, K.C. Branch, J. Palmer, B. Strassner, R. Bugos, M. Navarrette,
A. Lopes, E. MacDonald, F. Medina, and R. Wicker, "Fabrication of a mini-SAR
Antenna Array Using Ultrasonic Consolidation and Direct-write." *Rapid Manufacturing
Conference*, July, 2007, U.K.

Signed _____ 3-10-2007 _____

Date 03/06/2007

Name	Chris Robinson
Address	1162 E. Stadium Way
	Logan, UT 84341
Phone	(435) 797-2562

Dear Francisco Medina:

I am in the process of preparing my thesis in the Department of Mechanical and Aerospace Engineering at Utah State University. I hope to complete in the spring of 2007.

I am preparing a multiple paper thesis, which will include the paper listed below. Because you are a co-author on this paper I am requesting your permission to include the material just as it appeared in the paper. Please advise me of any changes you require.

Please indicate your approval of this request by signing in the space provided, and attaching any other form or instruction necessary to confirm permission. If you have any questions, please call me at the number above.

Thank you for your cooperation,

Chris Robinson

I hereby give permission to Christopher J. Robinson to reprint the following material in his thesis.

Robinson, C., B. Stucker, K.C. Branch, J. Palmer, B. Strassner, R. Bugos, M. Navarrette, A. Lopes, E. MacDonald, F. Medina, and R. Wicker, "Fabrication of a mini-SAR Antenna Array Using Ultrasonic Consolidation and Direct-write." *Rapid Manufacturing Conference*, July, 2007, U.K.

Signed _____

Date 03/06/2007

Name   Chris Robinson
Address   1162 E. Stadium Way
             Logan, UT 84341
Phone   (435) 797-2562

Dear Yanzhe Yang:

I am in the process of preparing my thesis in the Department of Mechanical and
Aerospace Engineering at Utah State University. I hope to complete in the spring of
2007.

I am preparing a multiple paper thesis, which will include the paper listed below.
Because you are a co-author on this paper I am requesting your permission to include the
material just as it appeared in the paper. Please advise me of any changes you require.

Please indicate your approval of this request by signing in the space provided, and
attaching any other form or instruction necessary to confirm permission. If you have any
questions, please call me at the number above.
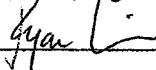
Thank you for your cooperation,

Chris Robinson

I hereby give permission to Christopher J. Robinson to reprint the following material in
his thesis.

Ram, G.D., C. Robinson, Y. Yang, and B.E. Stucker, "Use of ultrasonic consolidation for
fabrication of multi-material structures." *Rapid Prototyping Journal*

Signed_____ 03/19/2007

Date 03/06/2007

Name   Chris Robinson
Address   1162 E. Stadium Way
            Logan, UT 84341
Phone   (435) 797-2562

Dear Jared Clements:

I am in the process of preparing my thesis in the Department of Mechanical and
Aerospace Engineering at Utah State University. I hope to complete in the spring of
2007.

I am preparing a multiple paper thesis, which will include the paper listed below.
Because you are a co-author on this paper I am requesting your permission to include the
material just as it appeared in the paper. Please advise me of any changes you require.

Please indicate your approval of this request by signing in the space provided, and
attaching any other form or instruction necessary to confirm permission. If you have any
questions, please call me at the number above.

Thank you for your cooperation,

Chris Robinson
_____

I hereby give permission to Christopher J. Robinson to reprint the following material in
his thesis.

Robinson, C.J., J.W. Clements, B.E. Stucker, and E.J. Siggard, "Using Ultrasonic
Consolidation to Rapidly Manufacture Advanced Structures with Embedded Thermal
Management Devices." *International Conference on Manufacturing Automation*, May,
2007, Singapore.

Signed _____

03/06/2007

Name   Chris Robinson
Address   1162 E. Stadium Way
           Logan, UT 84341
Phone   (435) 797-2562

Dear Jeremy Palmer:

I am in the process of preparing my thesis in the Department of Mechanical and
Aerospace Engineering at Utah State University. I hope to complete in the spring of
2007.

I am preparing a multiple paper thesis, which will include the papers listed below.
Because you are a co-author on these papers I am requesting your permission to include
the material just as it appeared in the paper. Please advise me of any changes you
require.

Please indicate your approval of this request by signing in the space provided, and
attaching any other form or instruction necessary to confirm permission. If you have any
questions, please call me at the number above.

Thank you for your cooperation.

Chris Robinson

I hereby give permission to Christopher J. Robinson to reprint the following material in
his thesis.

Robinson, C., B. Stucker, K.C. Branch, J. Palmer, B. Strassner, R. Bugos, M. Navarrette,
A. Lopes, E. MacDonald, F. Medina, and R. Wicker, "Fabrication of a mini-SAR
Antenna Array Using Ultrasonic Consolidation and Direct-write." *Rapid Manufacturing
Conference*, July, 2007, U.K.

Robinson, C.J., B. Stucker, A.J. Lopes, R. Wicker, and J.A. Palmer, "Integration of
Direct-Write (DW) and Ultrasonic Consolidation (UC) Technologies to Create Advanced
Structures with Embedded Electrical Circuitry." *Solid Freeform Fabrication Symposium
Proceedings*, Austin, Texas, August 2007

Signed _____

137

Date 03/06/2007

Name   Chris Robinson
Address   1162 E. Stadium Way
              Logan, UT 84341
Phone   (435) 797-2562

Dear Karen Branch:

I am in the process of preparing my thesis in the Department of Mechanical and
Aerospace Engineering at Utah State University. I hope to complete in the spring of
2007.

I am preparing a multiple paper thesis, which will include the papers listed below.
Because you are a co-author on this paper I am requesting your permission to include the
material just as it appeared in the paper. Please advise me of any changes you require.
                    This is important!
Please indicate your approval of this request by signing in the space provided, and
attaching any other form or instruction necessary to confirm permission. If you have any
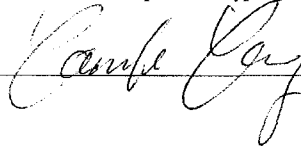questions, please call me at the number above.

Thank you for your cooperation,

  Chris Robinson

I hereby give permission to Christopher J. Robinson to reprint the following material in
his thesis.

Robinson, C., B. Stucker, K.C. Branch, J. Palmer, B. Strassner, R. Bugos, M. Navarrette,
A. Lopes, E. MacDonald, F. Medina, and R. Wicker, "Fabrication of a mini-SAR
Antenna Array Using Ultrasonic Consolidation and Direct-write." *Rapid Manufacturing
Conference*, July, 2007, U.K.

Signed _Karen Coprich Branch_

Date 03/06/2007

Name   Chris Robinson
Address   1162 E. Stadium Way
            Logan, UT 84341
Phone   (435) 797-2562

Dear Misael Navarrette:

I am in the process of preparing my thesis in the Department of Mechanical and
Aerospace Engineering at Utah State University. I hope to complete in the spring of
2007.

I am preparing a multiple paper thesis, which will include the paper listed below.
Because you are a co-author on this paper I am requesting your permission to include the
material just as it appeared in the paper. Please advise me of any changes you require.

Please indicate your approval of this request by signing in the space provided, and
attaching any other form or instruction necessary to confirm permission. If you have any
questions, please call me at the number above.

Thank you for your cooperation,
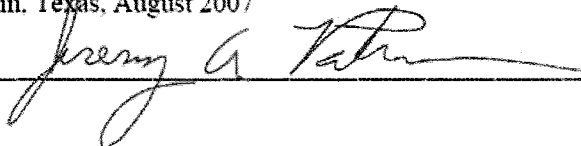

Chris Robinson

I hereby give permission to Christopher J. Robinson to reprint the following material in
his thesis.

Robinson, C., B. Stucker, K.C. Branch, J. Palmer, B. Strassner, R. Bugos, M. Navarrette,
A. Lopes, E. MacDonald, F. Medina, and R. Wicker, "Fabrication of a mini-SAR
Antenna Array Using Ultrasonic Consolidation and Direct-write." *Rapid Manufacturing
Conference*, July, 2007, U.K.

Robinson, C.J., B. Stucker, A.J. Lopes, R. Wicker, and J.A. Palmer, "Integration of
Direct-Write (DW) and Ultrasonic Consolidation (UC) Technologies to Create Advanced
Structures with Embedded Electrical Circuitry." *Solid Freeform Fabrication Symposium
Proceedings*, Austin, Texas, August 2007

Signed _____

139

Date 03/06/2007

Name   Chris Robinson
Address   1162 E. Stadium Way
          Logan, UT 84341
Phone   (435) 797-2562

Dear Erik Siggard:

I am in the process of preparing my thesis in the Department of Mechanical and
Aerospace Engineering at Utah State University. I hope to complete in the spring of
2007.

I am preparing a multiple paper thesis, which will include the papers listed below.
Because you are a co-author on these papers I am requesting your permission to include
the material just as it appeared in the paper. Please advise me of any changes you
require.

Please indicate your approval of this request by signing in the space provided, and
attaching any other form or instruction necessary to confirm permission. If you have any
questions, please call me at the number above.

Thank you for your cooperation,

Chris Robinson

_____

I hereby give permission to Christopher J. Robinson to reprint the following material in
his thesis.

Robinson, C.J., C. Zhang, G.D. Janaki Ram, E.J. Siggard, B. Stucker, and L. Li,
"Experimental and Analytical Analysis of Freestanding Rib Structures Built Using
Ultrasonic Consolidation."

Robinson, C.J., J.W. Clements, B.E. Stucker, and E.J. Siggard, "Using Ultrasonic
Consolidation to Rapidly Manufacture Advanced Structures with Embedded Thermal
Management Devices." *International Conference on Manufacturing Automation*, May,
2007, Singapore.

Signed _____   21 March 2007

Date 03/29/2007

Name   Chris Robinson
Address   1162 E. Stadium Way
            Logan, UT 84341
Phone   (435) 797-2562

Dear Chunbo Zhang:

I am in the process of preparing my thesis in the Department of Mechanical and Aerospace Engineering at Utah State University. I hope to complete in the spring of 2007.

I am preparing a multiple paper thesis, which will include the paper listed below. Because you are a co-author on this paper I am requesting your permission to include the material just as it appeared in the paper. Please advise me of any changes you require.

Please indicate your approval of this request by signing in the space provided, and attaching any other form or instruction necessary to confirm permission. If you have any questions, please call me at the number above.

Thank you for your cooperation,

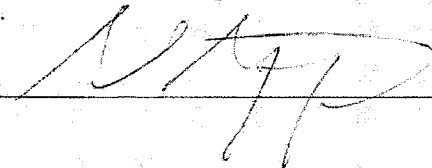Chris Robinson

---

I hereby give permission to Christopher J. Robinson to reprint the following material in his thesis.

Robinson, C.J., C. Zhang, G.D. Janaki Ram, E.J. Siggard, B. Stucker, and L. Li, Maximum Height to Width Ratio of Freestanding Structures Built Using Ultrasonic Consolidation. Solid Freeform Fabrication Symposium Proceedings, Austin, Texas, August 2007.

Signed _Chunbo Zhang_____

Date 03/29/2007

Name   Chris Robinson
Address   1162 E. Stadium Way
            Logan, UT 84341
Phone   (435) 797-2562

Dear G.D. Janaki Ram:

I am in the process of preparing my thesis in the Department of Mechanical and
Aerospace Engineering at Utah State University. I hope to complete in the spring of
2007.

I am preparing a multiple paper thesis, which will include the papers listed below.
Because you are a co-author on these papers I am requesting your permission to include
the material just as it appeared in the paper. Please advise me of any changes you
require.

Please indicate your approval of this request by signing in the space provided, and
attaching any other form or instruction necessary to confirm permission. If you have any
questions, please call me at the number above.

Thank you for your cooperation,

Chris Robinson

I hereby give permission to Christopher J. Robinson to reprint the following material in
his thesis.

Janaki Ram, G.D., C. Robinson, Y. Yang, and B.E. Stucker, "Use of ultrasonic
consolidation for fabrication of multi-material structures." *Rapid Prototyping Journal*

Robinson, C.J., C. Zhang, G.D. Janaki Ram, E.J. Siggard, B. Stucker, and L. Li,
Maximum Height to Width Ratio of Freestanding Structures Built Using Ultrasonic
Consolidation. Solid Freeform Fabrication Symposium Proceedings, Austin, Texas,
August 2007.

        Signed

Date 03/06/2007

Name   Chris Robinson
Address   1162 E. Stadium Way
          Logan, UT 84341
Phone   (435) 797-2562

Dear Robert Bugos:

I am in the process of preparing my thesis in the Department of Mechanical and
Aerospace Engineering at Utah State University. I hope to complete n the spring of
2007.

I am preparing a multiple paper thesis, which will include the paper l sted below.
Because you are a co-author on this paper I am requesting your perm ssion to include the
material just as it appeared in the paper. Please advise me of any changes you require.

Please indicate your approval of this request by signing in the space ¡ rovided, and
attaching any other form or instruction necessary to confirm permissi n. If you have any
questions, please call me at the number above.

Thank you for your cooperation,

Chris Robinson

I hereby give permission to Christopher J. Robinson to reprint the following material in
his thesis.

Robinson, C., B. Stucker, K.C. Branch, J. Palmer, B. Strassner, R. Bu gos, M. Navarrette,
A. Lopes, E. MacDonald, F. Medina, and R. Wicker, "Fabrication of ι mini-SAR
Antenna Array Using Ultrasonic Consolidation and Direct-write." *Ra pid Manufacturing
Conference*, July, 2007, U.K.

Signed _____

Appendix C

UC Guidebook

1. *Trimming Defects*: When trimming almost any part there will be defects from the trimming process in the edges of the part that can propagate to cause bad effects. It can sometimes be beneficial to trim fewer times than the defaults suggest.

2. *Final Dimensions*: Dimensions of parts that are not enclosed cavities are trimmed to 0.004 inches larger than final dimensions and then the finish toolpaths remove the final 0.004 inches of material. On enclosed cavities the dimensions created are final dimensions.

3. *Seams*: Seams are not good for tall structures. In building walls or ribs or other enclosures it is advisable to orient and position parts in a way that it will minimize the number of seams along a wall. The tapes do not always lie perfectly next to each other and this creates either a gap, which can decrease the stiffness, or the tapes will overlay and cause a bump. If a bump occurs it can either cause the machine to fault or wobble the sonotrode so that a solid bond is not formed in the subsequent layers.

4. *Cutting Fluid at Room Temperature*: When building at low temperatures, care should be taken to ensure that the cutting fluid does not cause delamination problems. Because the isopropanol does not evaporate immediately at room temperature the fluid may ramain in gaps and then act as a lubricant, which will limit the plastic deformation. The trapped cutting fluid can also cause problems as the part is heated and the isopropanol expands, often causes delamination.

5. *Heigth to Width Ratio (H/W) of 1:1*: If a freestanding rib is to be built from 3003 Aluminum using the optimal parameters determined at Utah State University, which

are Amplitude =160 tenths of a micrometer, Feedrate = 28 inches per minute, Force = 1750 Newtons, and a build temperature of 300 degrees Fahrenheit, the height dimension must not exceed the width dimension for bonding to occur. For different materials and parameters this maximum value will likely either go up or down.

6. *Longitudinal Ribs*: Walls that are built in the direction of the movement of the sonotrode (i.e. the longitudinal direction) have the least resistance to deflections caused by vibration. When creating patterns of ribs, sections in the longitudinal direction should be avoided. One example is with a six sided honeycomb cell, orient it so that two segments are in the lateral direction and the other four are all at an angle between the lateral and longitudinal directions.

7. *Lateral Ribs*: When a rib is oriented in the lateral direction, or direction where the long axis is perpendicular to the tape lay direction, there is a difficulty with having a small surface area of bonded material. Whether there is a large area or a small area the machining stresses are the same along the edge and with a smaller surface area any discontinuities can propagate to the center of the rib more quickly, creating more voids than in a ribs with a large surface area. Therefore, ribs should be oriented in a way that will maximize the bonded area of each tape on the rib. It is recommended that this consideration be secondary to avoiding longitudinal ribs, if conflict arises.

8. *45 Degree Ribs*: The weld density and H/W ratio are higher in ribs built at an angle of 45 degrees to the direction of sonotrode motion. When it is possible it is wise to orient ribs in this orientation. However, care must be taken to consider the amount of total energy that is supplied to the weld in areas where the sonotrode will only be touching a small corner of a part. In RPCAM this is controlled by the "w" parameter and can be viewed in the machine code. This parameter is intended to adjust for the total surface area where the sonotrode comes into contact with the part. When there is little area then the "w" parameter will have a low value, which applies a lower force value to try to match the pressure at all times. In general this works well, but in the

case of a very small and sharp corner there is essentially no bonding. With a rib or wall this will cause a point defect on every tape that is not bonded well. These same points will then have high machining forces because they are points and so peeling will often occur at the edges of the tapes in this orientation. Machine tools that cut well are critical and it was observed that there will be an optimal feedrate speed for each tool. This is generally lower than the default feedrate for a trim, but not less than 40 percent of the default.

9. *Bonding Over a Cavity*: UC will not bond the first layer over a cavity or an overhanging support because there is no material to cause any plastic deformation. In general the stiffness of the part even as it builds up is not sufficient over these areas to allow bond formation for a significant number of layers. Each layer experiences a very small amount of bonding over the empty space and so gradually the bonding will occur.

10. *Filler Materials*: A very stiff filler material will likely assist in recovery over an open pocket. However, in order to really be effective the material needs to have a high enough stiffness to create significant support at temperatures around 400 degrees Fahrenheit.

11. *H/W Over a Cavity*: If a tall structure is to be built over a cavity or channel, the stiffness of the ribs will generally decrease because the deposited material does not generally recover to a full bond over the cavity for a number of layers. The dimensions of the void have a very large effect upon the rate of recovery. If there is unconsolidated material below a tall structure the H/W of 1:1 is probably optimistic. However, if a support structure were used there is a possibility of being able to support the cavity area and thereby allow bonding to occur.

12. *Building Beyond a 1:1 H/W*: To build structures that have a H/W of greater than 1:1 there are a number of possibilities, some of which are listed below:

    (a) Adjusting the parameters at certain levels of the build that will alter the resonance and the damping of the vibrational waves in the ribs. Although this has

not been tested the first parameter to change would likely be the amplitude of vibration since the frequency is set and not adjustable.

(b) Various materials could be strategically placed into the rib that would cause a disruption in the propagation of the vibrational waves and thereby possibly improve the differential motion between the substrate and the new deposition.

(c) Where possible a very feasible way to obtain a H/W of greater than 1:1 is to generate a rib that is wider than the final dimensions and then after the rib or wall has been built to the desired height remove the excess material around the edges using the CNC milling capability. This can be done by simply creating two sets of machine code where one set builds the part with the enlarged dimensions and the other simply removes material to expose the desired structure.

(d) Where geometry permits, a support material can be used to support a free-standing structure. In general most polymers have not worked well as a support material because when the material is leveled using the machine tool it smears the polymer across other areas of the plate creating a type of lubricant that can cause the friction between the substrate and the deposition to drop below critical levels for bond formation. Metals with a low melting temperature are a very good prospect for this because the structure could be heated to the boiling temperature of the filler material, which would be much less than the aluminum.

(e) Where possible and feasible, transverse support ribs can be included to support the rib against vibration and thereby increase the stiffness to a level where the maximum H/W will likely increase.

(f) Patterns of ribs such as honeycomb are desirable if possible. The support that comes from the surrounding walls has proven to support the ultrasonic consolidation of ribs in a honeycomb structure with a H/W of greater than 10:1.

13. *Secondary Cavities*: The weld density and therefore the height of a rib or wall that is built over a cavity or channel will improve if the material is consolidated as a solid and

then the channel is included later as much as possible. This can be accomplished by building up a large amount of material and then doing numerous machining operations consecutively to remove the material. Post processing is also an option in locations where it is possible.

14. *Thin Walls*: When building patterns of ribs such as honeycomb, the minimum wall thickness should be determined according to buckling failure. The wall thickness must never approach the minimum thickness and even with a much thicker wall, there will likely be some amount of deformation in the upper portions of the honeycomb walls when a skin is applied. For parts that have a critical Z height value this should be tested and considered in the model.

15. *Honeycomb Cell Size*: If a face sheet is applied to tall honeycomb structures, the cell size has a very large effect on the flatness of the upper surface. For a large cell size (greater than 0.47 inches) the sonotrode will dip as it deforms the walls and the aluminum covering the sheets will then wrinkle and often times crack. The unbonded regions over the honeycomb cells usually sag if a cell is large. Smaller cell sizes allow the sonotrode to impact more walls at any given time, but in order to achieve the same mass reduction as with a larger cell the wall thickness must be reduced so there can then be greater deformation in the walls. A cell size of approximately 0.45 inches is likely to give the best results in general, but this must be considered case by case.

16. *Covering Cavities and Rib Patterns*: When enclosing a large cavity or consolidating material onto the top of a large honeycomb type area it is often critical to leave a solid rim of material around the outer edges. This will allow the new deposition of material to consolidate well during the tacking stage before it is welded into position. Sometimes without a rim the tape will not tack and then you must hand lay the tape for tacking, but this will often lead to misaligned tapes. This excess rim of material can be removed during a final machining operation after completion of the build.

17. *Overhanging Supports*: A very stiff support can be created by making a type of stair step with each layer that can start with a very small overhang (0.005 to 0.010 inches) and then the next layer can hang over the previous layer by a small amount repeatedly until the desired overhang is completed. If this process is utilized care must be taken to check the machine path to ensure that the stairsteps are being fabricated appropriately. Even without a stairstep a small stiff overhanging support can be fabricated by applying a number of layers before trimming the tapes.

18. *Internal Steps*: Geometry that hangs over the previous layers, even with sufficient support, cannot be created with a smooth surface, it will always have a stairstep effect. For instance if a complete spherical cavity was to be created internally in a part the bottom half of the sphere would be very good and smooth and the upper surface would have edges that are at best jagged from the overlay of the tapes.

19. *Hollow Supports*: For creating hollow supports, such as honeycomb or truss structures, it is possible to accomplish a much taller support with low mass by first consolidating material for as much of the support as possible out of solid metal and then creating the geometry with machining procedures. This can be done by simply delaying the machining operations in the program and reordering them at a specific point in the program where you want the machining to start. As you do this remember your tools in the machine and the cutting depth of the tool and do not mill deeper than the tool can handle. Also check the skim height of the tool paths to make sure there will not be any interference.

20. *Upper Profile*: For internal cavities, the software currently recognizes only the profile from looking from the very top of the part and the upper portions of cavities. Therefore if there is an upper layer that has a cross-section that extends into the cavity further than the cross-section at a lower level, the lower level will not be machined properly. The software will only create tool paths for the features it can see from the top of the cavity. If it is necessary to have these types of features it may be necessary

to create numerous versions of the model and generate code with the features included at different levels. With upgrades to current software this issue may be resolved.

21. *Flush Embedding*: When embedding a component that can be pressed into its pocket it may be tempting to leave the component a little above the rest of the material to ensure an intimate contact, but depending upon the compressibility of the material this can cause the material to not bond. If you need to ensure intimate contact make the component flush or within no more than 0.003 inches of flush. The sonotrode will be pushed up over this area and it will propagate an unbonded area further into the part. If the component is soft it may press in but if it is incompressible or close to, then as it deforms under the sonotrode, other areas will become elevated causing a lack of bonding to occur.

22. *Sealing of Channels*: When building channels that will contain a fluid it is important to observe that there will be porosity that can allow the fluid to seep into the part and diminish the supply of fluid. Sealants can be used prior to filling the channel to prevent leakage.

23. *Layering Features*: A feature such as a channel that needs to be sealed well should not be placed directly above another feature as there will likely be unbonded material that will cause significant porosity. When possible, all features on different levels should be staggered so that walls and ribs do not occur directly over a cavity. Also cavities should be placed to allow recovery as much as possible.

24. *Bonding Methods*: There are at least two ways of creating a multi-material part that have been proven. The first (direct method) is to just introduce the dissimilar material in an interrupted build and secure it in place through the use of Very High Bond (VHB) tape or another adhesive. Then run the welding program to consolidate the material to the substrate. The second method (indirect method) is to build to the point where the dissimilar material will be introduced and then secure the dissimilar material and then skip one layer of machine code and continue the build with the next level of

aluminum being tacked directly to the top of the dissimilar material. The second option is much better for preserving the life of the sonotrode, but depending upon the material thickness and the material properties of the dissimilar material the energy from the sonotrode may not effectively reach the lower interface of the dissimilar material, which will result in little or no bond formation. In general it appears to be more effective to directly embed the dissimilar material.

25. *Parameter Adjustment*: Although some materials will bond to the base material of 3003 aluminum with the optimal parameters for aluminum consolidation, many materials will require varied parameter settings to create an effective bond. Some considerations for materials that will likely bond well are those with a face centered cubic structure and those materials that have uniform grain boundaries. Materials with a very thick or very stiff oxide layer are very difficult to bond to. The specific alloys as well as heat treatments can greatly affect the bondability of materials.

26. *Material Behavior*: When attempting to determine the best parameters for a specific multi-material structure, the material behavior should be considered. For instance some materials will harden significantly with plastic deformations and other materials could soften while others may experience little effect. Copper is a material that experiences significant hardening and therefore requires a very large amount of energy to create a good bond. Copper and other such materials will also wear the surface finish from the sonotrode more quickly than aluminum.

27. *Material Stiffness*: The stiffness of a material seems to have a major effect on how well the material can be bonded to aluminum. Generally, stiffer materials seem to not bond as well when using the optimal aluminum parameters, while less stiff metals seem to do okay.

28. *Oxidation*: Materials will oxidize at different temperatures so when building a multi-material part it is important to determine the temperature at which thick oxide layers will form and attempt to stay below that temperature. As the temperature is lowered

below 300 degrees Fahrenheit, the bond quality goes down, so care should be taken to not go to a temperature below that which is necessary to minimize oxide formation.

29. *Energy Dissipation*: If a dissimilar material is consolidated the thicknesses of the materials are often times not exact, this is usually okay as far as the machine is concerned because it can compensate for small variations in the height of a part. If you can get the height of the actual layer and the layer in the code to within 0.003 inches there will be no problems. However depending upon the stiffness of and damping properties of the material, consolidation may be difficult on the bottom side of the dissimilar material. For instance Metpreg, which is aluminum oxide fibers in a pure aluminum matrix, will absorb the ultrasonic energy and not allow a large amount of deformation or bonding to occur on the bottom side of the strip of material.

30. *Embedding Stiff Filaments*: When a small diameter filament with a stiffness much greater than that of the aluminum or other base material is consolidated between two pieces of aluminum the aluminum will flow around the stiff element and create a very tight mechanical bond between the two materials. This has been demonstrated with fibers as well as stainless steel mesh.

31. *Fiber Yarn Embedment*: When embedding numerous fibers, especially those with a high stiffness, it is important to make sure that the fibers are not lying on top of each other. It is very common to obtain high modulus carbon fiber in a yarn configuration, but if this material is placed between layers of aluminum the fibers themselves rub against other fibers. With the brittleness of these very stiff fibers, the result is carbon dust and at best a chopped fiber embedment. It has been demonstrated that carbon fibers with a nickel coating can be embedded in aluminum, but only with a very small mass fraction.

32. *Conductivity of Multi-material Parts*: Various materials may be introduced into a structure to enhance properties such as electrical conductivity, but before the application is made consideration should be taken for the fact that often time a multi-

material bond is not a fully dense bond and so the conductivity could actually be reduced instead of increased. The lack of bonding could also cause adverse effects in regards to vibration and stiffening.

33. *Electrical Insulating*: When putting DW ink into a UC structure it is important to remember that the aluminum will conduct electricity so you must ensure that the conductive ink does not come into contact with the aluminum. An insulator material can be applied and channels can then be milled into the insulator material. The conductive ink can then be applied and covered with more insulator material. After milling the top of the insulator material flat, aluminum can be consolidated over the insulator material without causing adverse effects to the electrical conductivity.

34. *DW Ink Cure Temperature*: There are many DW conductive inks that have a cure temperature that is close to or below the standard building temperature (300 degrees Fahrenheit). If these materials are used, the curing can either be performed on the UC heat plate or can be enhanced on the heat plate. If the material should not be heated longer, the aluminum can be consolidated at temperatures lower than the cure temperature.

35. *Mechanical Strength of DW ink*: In relation to mechanical strength DW has the tensile strength about 1/50 to 1/40 of the tensile strength of standard solder. Any connections should be observed to determine if the DW will have sufficient strength to withstand the vibrations that may be experienced. In many cases solder is greater than 100 times as strong as it needs to be, so DW ink would also be okay.